N O T I C E

THIS DOCUMENT HAS BEEN REPRODUCED FROM MICROFICHE. ALTHOUGH IT IS RECOGNIZED THAT CERTAIN PORTIONS ARE ILLEGIBLE, IT IS BEING RELEASED IN THE INTEREST OF MAKING AVAILABLE AS MUCH INFORMATION AS POSSIBLE

DRL No. 131
DRD Line Item 7

JPL NO. 9950-593 DOE/JPL 954796-81/13
Distribution Category UC-63, List of 02/23/81

(NASA-CR-164867) ANALYSIS AND EVALUATION IN THE PRODUCTION PROCESS AND EQUIPMENT AREA OF THE LOW-COST SOLAR ARRAY PROJECT Final Report (Pennsylvania Univ.) 319 p HC A14/MF A01 CSCL 10A G3/44

N81-33607

Unclas 27648

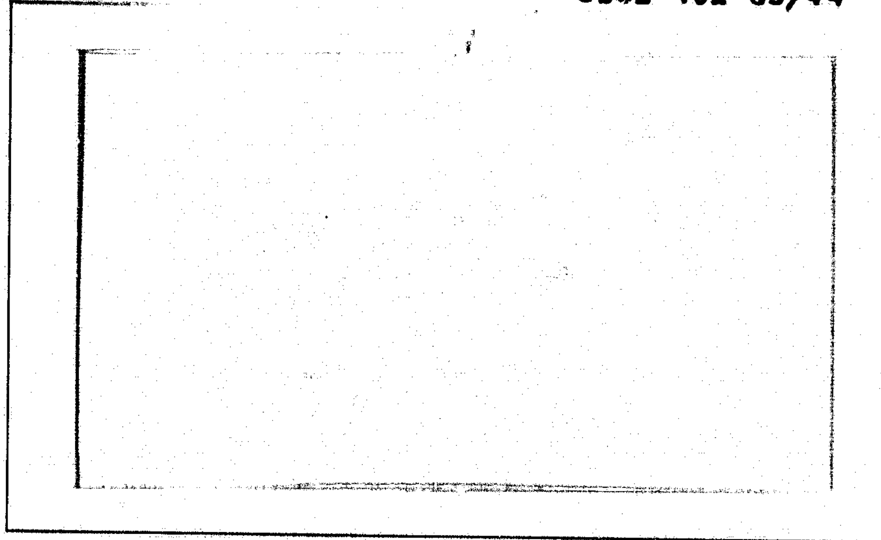

Contract 954976
Final Report

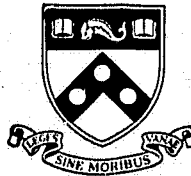

UNIVERSITY of PENNSYLVANIA

PHILADELPHIA, PENNSYLVANIA 19104

DRL No. 131
DRD Line Item 7

DOE/JPL-954976-81-13
Distribution Category UC-63, List of 02/23/81

ANALYSIS AND EVALUATION
IN THE PRODUCTION PROCESS
AND EQUIPMENT AREA
OF THE
LOW-COST SOLAR ARRAY PROJECT

Contract JPL-954976
Final Report (Draft)

April 1981

M. Wolf and H. Goldman

The JPL Low-Cost Silicon Solar Array Project is sponsored by the U.S. Department of Energy and forms part of the Solar Photovoltaic Conversion Program to initiate a major effort toward the development of low-cost solar arrays. This work was performed for the Jet Propulsion Laboratory, California Institute of Technology by agreement between NASA and DOE.

This report was prepared as an account of work sponsored by the United States Government. Neither the United States nor the United States Department of Energy, nor any of their employees, nor any of their contractors, subcontractors, or their employees, makes any warranty, express or implied, or assumes any legal liability or responsibility for the accuracy, completeness or usefulness of any information, apparatus, product or process disclosed, or represents that its use would not infringe privately owned rights.

Summary

The solar cell metallization processes show a wide range of technical limitations, which influence solar cell performance. These limitations interact with the metallization pattern design. A detailed analysis carried out over the last year has led to the following conclusions:

1. Attention to the metallization structure becomes particularly important, as the solar cell size increases. The voltage drop in a conducting element, such as a grid line, and consequently the power loss, is proportional to the square of the length of the current path in the element. Consequently, grid line lengths significantly above 2.5 cm should be avoided. As a result, large area - square or round - cells will need a periodic grid line structure with multiple bus lines.

2. The sheet resistance for each level in the hierarchy of elements for the current paths (front layer, grid line, bus line) needs to be considerably below that of the preceding level, in order to be effective. Thus, the bus lines in large area cells have to be of substantially greater thickness than obtainable by metal deposition processes, if shading is to be kept within reasonable bounds. Thus, the reinforcement of the bus lines by interconnectors or wires is a logical answer.

3. The power output losses due both to the voltage drop from series resistance and to the shadowing by the front metallization, can be held to acceptably low levels. This

level can be 5% of the maximum power output for all of these losses combined for a 10 cm x 10 cm cell. This requires a relatively fine grid line system of, for instance, 1.54 mm spacing (65 grid lines) and 25 μm line width. This is well within the capabilities of several types of current metallization processes.

4. When it is not possible to apply bus lines of substantially lower sheet resistance than the grid lines, a pattern with grid lines only (no bus lines) will give a better performance (less shading for equal voltage drop. However, the total series resistance connected losses are then at least 11.5% for a 10 cm x 10 cm cell.

5. The end point voltage drops on metallization lines of constant width and on tapered lines ending in zero width are identical, if the total area shaded by these lines is equal. However, the effective voltage drop for the power dissipation, is 2/3 of the end point voltage drop for the constant width grid lines, and only 1/2 for the tapered grid lines.

6. Grid lines arranged normal to the bus lines give better performance than obliquely arranged grid lines.

7. The energy dissipated in the series resistance elements themselves is by far the dominant energy loss resulting from series resistance. A rematching of the load to reduce the current from that giving maximum power in the "ideal" cell without series resistance, can result in a slightly greater power output than would correspond to the maximum power output

of the ideal cell minus the energy dissipated in the series resistance.

8. While in general an optimum value exists only for the grid line and bus line shading ratios, with monotonously decreasing losses as grid and bus line spacings tend towards zero (with the shading ratios maintained at their optimum values), this rule does not hold, when the bus line is a round or square wire, or the choice of grid line width is limited by technological requirements. In these cases, optimum values can be found for the bus line spacing and wire diameter separately, or for the grid line spacing in dependence on the minimum practical line width.

9. The analysis of the solar cell performance implications of the front metallization design for large area solar cells has led to a set of definitive Design Rules, contained in this report.

10. Some of the metallization processes used in solar cell production are not capable of yielding low losses. Worst seem to be the print-on thick film processes, which are limited to line widths of 127 μm or greater, and which yield only a fraction of the bulk conductance of the deposited metal.

11. Several metallization process sequences will lead to adequate metallization for large area, high performance solar cells at a metallization add-on price in the range of 6.- to 12.-/m^2, or 4 to 8¢/W(peak), assuming 15% efficiency.

12. Conduction layer formation by thick film silver or by

tin or tin/lead solder leads to metallization add-on prices significantly above the \$6.- to 12.-/m^2 range.

13. The wet chemical processes of electroless and electrolytic plating for strike/barrier layer and conduction layer formation, respectively, seem to be most cost-effective.

14. Vacuum deposition of the strike/barrier layer may be competitive with electroless plating.

15. The final selection of a process sequence may hinge on small, but important effects connected with masking, such as underspray under shadow masks, overplating of the edges of the barrier layer, registration problems, etc.

16. The use of the AR coating as the metallization mask may be even more attractive as it may avoid some of the problems mentioned in point 15).

17. Some further development effort should be expected to be needed after carefully observed pilot line operations may reveal problems of process controllability, yield, or like those mentioned in point 15 which may influence initial solar cell performance or cause long term degradation.

TABLE OF CONTENTS

		PAGE
	Summary	iii
	Table of Contents	vii
	List of Tables	ix
	List of Figures	x
I.	Introduction	1
II.	The Impacts of Metallization Pattern Design in 10 cm x 10 cm Solar Cells: Illustrative Examples	7
III.	The Influence of Series Resistance on Solar Cell Performance	25
	1. A single lumped series resistance	25
	2. The effect of different solar cell elements operating at differing voltages	33
IV.	The Voltage Drop in Uniform Width or Tapered Grid Lines	43
V.	The General Tapered Grid Line Problem	49
VI.	Oblique versus Normal Grid Lines	57
VII.	Grid and Bus Line Pattern Optimization	69
VIII.	Design Rules	89
IX.	Brief Description of the Metallization Options	93
	A. General	93
	B. Chemical Deposition Processes	93
	1. Immersion Plating	93
	2. Electroless Plating	96
	3. Electrolytic Plating	98
	C. Physical Deposition Processes	101
	1. Vacuum Deposition, incl. Sputtering	101
	2. Thick Film Screen Printing	102
X.	Comparative Evaluation of the Metal Deposition Options	109
	A. General	109
	B. Chemical Deposition Process	115
	1. Electroless Plating	115
	2. Electrolytic Plating	124
	C. Thick Film Screen Printing	129
	D. Physical Vapor Deposition	137
XI.	The Principal Metallization Process Options	145
XII.	Selection of Metals for the Conduction Layer	161

TABLE OF CONTENTS (continued)

		PAGE
XIII.	Metal Utilization in the Various Deposition Processes	165
XIV.	Comparative Economic Evaluation	171
XV.	Preparation of SAMIC Format A Input Information from the UPPC Forms	187
XVI.	Potential Metallization Process Sequences	195
XVII.	Conclusions	199
XVIII.	References	203
	Appendix I: Detail Data For 6 Generic Metallization Processes	
	Appendix II: SAMIC Format A for the Six Generic Metallization Processes	
	Appendix III: Sample Set of Forms for the University of Pennsylvania Process Characterization (UPPC)	

LIST OF TABLES

		PAGE
Table I	The Physical Parameters of the Seven Metallization Cases Used as Illustrative Examples	8
Table II	The Voltage Drops and Front Area Shading by Metal for the Seven Cases of Table I	14
Table III	Output Power (Efficiency) and Solar Cell Values for the Seven Metallization Cases of Table I	20
Table IV	Losses, cell efficiencies, and cell values associated with several metallization design variations	84
Table V	Design Rules for Front Metallization for Large Area Solar Cells	90-91
Table VIA	Metallization Process Options	112-113
Table VIB	Metallization Process Options	130
Table VIC	Metallization Process Options	136
Table VII	Principal Metallization Process Options	144
Table VIII	A. Plating	146
	B. Thick Film Processes (Screen-Printing)	149
	C. Photoresist Type Processes	150
	D. Vacuum Metal Deposition and Plating	151
Table IX	Comparison of the Compositions of the Inks Used by RCA	154
Table X	Physical and Cost Data of Various Metals of Interest for Solar Cell Metallization	162
Table XI	Comparative Tabulation of Direct Material Consumption and Cost for the Principal Metallization Options	176
Table XII	Comparison of Indirect Material Consumption For The Principal Metallization Options	178
Table XIII	Comparison of Labor Requirements For The Principal Metallization Options	180
Table XIV	Comparison of Capital Requirements For The Principal Metallization Options	182
Table XV	Cost Summary For The 6 Principal Metallization Options	184
Table XVI	Potential Process Sequences (Add-on prices in $\$/m^2$)	194

LIST OF FIGURES

		PAGE
FIG. 1	Four Types of Front Contact Pattern Investigated.	6
FIG. 2	Two Backside Metallization Patterns Considered.	10
FIG. 3	Solar Cell (and Module) Value as Function of Module Efficiency, Based on the 1986 LSA Goals.	22
FIG. 4	Simplified Lumped-Constant Equivalent Circuit of the Solar Cell.	24
FIG. 5	Current - Voltage Characteristics of the Solar Cell Without and With Series Resistance (a), and of the Output Power Without Series Resistance (b).	26
FIG. 6	Parallel Arrangement of three Identical Solar Cells with Different Series Resistances.	34
FIG. 7	Grid Line Configurations.	42
FIG. 8	Voltage drop along a uniform-width and a tapered grid line, respectively. Note that the end-point ($\ell=W$) voltage drops are equal, when both grid lines cover identical areas ($T_{GL} \cdot W$).	46
FIG. 9	Explanation of nomenclature used in the analysis of the general tapered grid line.	48
FIG. 10	The values of the voltage drop multipliers G(f) and H(f) as function of f.	52
FIG. 11	Oblique grid line arrangement on half of a unit field around a bus line. The grid line inclination angle is α, the bus line length $L-W \cdot \tan\alpha$.	56
FIG. 12	Illustration of the 4 end triangles on the unit field which contain the grid lines of less than full length.	58
FIG. 13	Sketch of one of the two triangles at the far end of the bus line, with explanation of the geometric relationships.	60
FIG. 14	Sketch of one of the two triangles at the near end of the bus line, with explanation of the geometric relationships.	64
FIG. 15	Illustration of the nomenclature used in the analysis of the front metallization pattern.	74

I. INTRODUCTION

The manufacturing methods for photovoltaic solar energy utilization systems consist, in complete generality, of a sequence of individual processes. This process sequence has been, for convenience, logically segmented into five major "work areas": reduction and purification of the semiconductor material, sheet or film generation, device generation, module assembly and encapsulation, and system completion, including installation of the array and the other subsystems. For silicon solar arrays, each work area has been divided into 10 generalized "processes" in which certain required modifications of the work-in-process are performed. In general, more than one method is known by which such modifications can be carried out. The various methods for each individual process are identified as process "options". This system of processes and options forms a two-dimensional array, which is here called the "process matrix".

In the search to achieve improved process sequences for producing silicon solar cell modules, numerous options have been proposed and/or developed, and will still be proposed and developed in the future. It is a near necessity to be able to evaluate such proposals for the technical merits relative to other known approaches, for their economic benefits, and for other techno-economic attributes such as energy consumption, generation and disposal of waste by-products, etc. Such evaluations have to be as objective as possible in light

of the available information, or the lack thereof, and have to be periodically updated as development progresses and new information becomes available. Since each individual process option has to fit into a process sequence, technical interfaces between consecutive processes must be compatible. This places emphasis on the specifications for the work-in-process entering into and emanating from a particular process option.

The objective of this project is to accumulate the necessary information as input for such evaluations, to develop appropriate methodologies for the performance of such techno-economic analyses, and to perform such evaluations at various levels.

The reduction of quartzite to metallurgical grade silicon was examined first, followed by comparative evaluations of advanced Czochralski techniques for growing single crystal, cylindrical ingots, and of various slicing process options to produce single crystal silicon wafers. The next "work area" for producing solar arrays is the fabrication of the silicon wafers to solar cells. This process involves many steps, one of which is the front junction formation. Of the major junction forming processes currently employed, diffusion from gaseous sources was examined in detail as a baseline process. It was then compared to alternate options, including modified diffusion processes and ion implantation, to determine their potential for mass production processes of lower cost.

After junction formation, the next major step in cell fabrication is metallization. The metal pattern is needed to collect and deliver the current from the photovoltaically active parts of the solar cell to a terminal where the load can be conveniently connected. To facilitate the techno-economic evaluation, the input work-in-process specifications, procedures, attributes, technical readiness, and costs for current and proposed major metallization processes, as well as the requirements for ancillary processes, such as masking, sintering, etc., were examined. The basic processes applicable to metallization are: wet chemical plating which includes immersion, electroless, and electrolytic plating; physical vapor deposition where the metal is vaporized by thermal energy, by an electron beam, or by sputtering with Argon ions; and thick film screen printing of noble and base metals with and without the presence of frits. An example of their application is the formation of strike and sensitizing layers by immersion or electroless plating, or alternately by vacuum evaporation. A variation of vacuum evaporation is ion plating, where the vaporized metal atoms are ionized either by an Argon plasma or by an RF field. Variations to the state-of-the-art thick film screen printing process are also under development, such as the Midfilm process which combines some aspects of the photoresist process with the thick film methods.

It is not only necessary to establish low resistance

contacts and an adequate conduction layer, but it is important to define a metal pattern on the front of the solar cell which combines minimum series resistance losses and area coverage.

Consequently, a part of this report deals with the metallization pattern design, often called "grid line design". It is more readily open for analysis than other aspects of the metallization process/performance relationship. Nevertheless, a lot of misunderstanding of the metallization pattern/performance relationship seems to have existed.

The various processes applicable to metal deposition and pattern generation impose differing limits to the design options available, and consequently to the solar cell performance achievable. Thus, the limitations of the various processes with respect to pattern design enter critically into the techno-economic evaluations. It is also to be observed that, in general, the metallization pattern design is much more sensitive in large area solar cells than in small cells. While small cells are quite forgiving to mistakes in grid structure design - very small cells do not even need any grid-patterned contact system - careless design of the contact geometry in large cells can lead to serious performance loss.

The later part of this report concentrates on the process options for applying the metal to the silicon surface. The ancillary processes for pattern definition have not yet

been examined equally intensively. In some cases, these processes are connected with AR-coating formation, in others, they are an integral part of the metallization procedure, as in thick film screen printing.

As in the preceding studies of processes, the evaluations were started with the current methods of metallization for which a large amount of the needed information is normally available. Nevertheless, substantial gaps or uncertainties were found in important information required for both technical and economic evaluation of the currently practiced processes. In proceeding to the evaluation of processes which are still in the developmental or even conceptual stage, the gaps in needed information become even larger. In these cases, it is necessary to fill the gaps more extensively with estimates based on extrapolations or analogies.

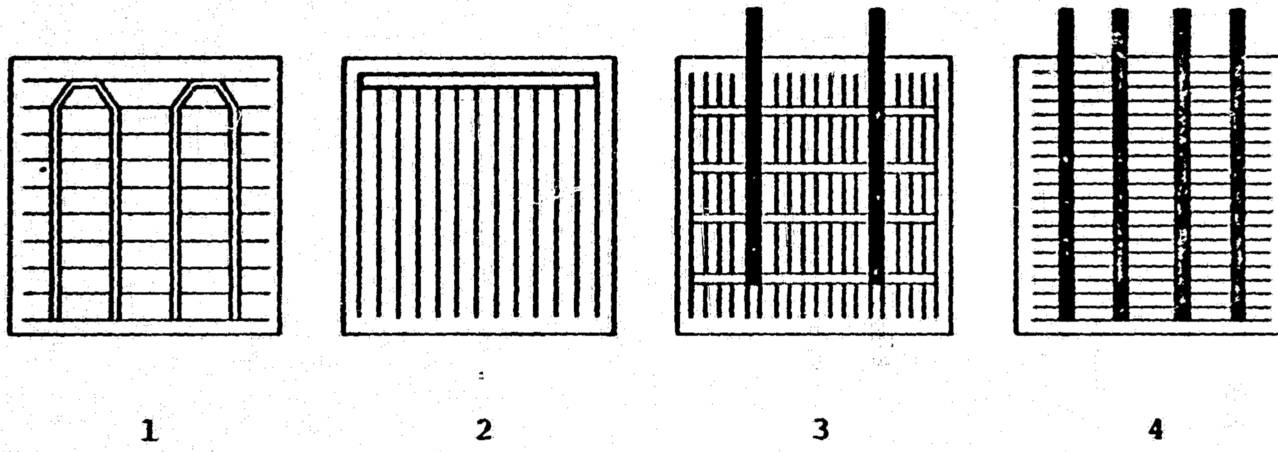

FIG. 1 Four Types of Front Contact Pattern Investigated.

II. The Impacts of Metallization Pattern Design in 10 cm 10 cm Solar Cells: Illustrative Examples.

To illustrate the impacts of metallization design on efficiency and process cost-effectiveness, seven metallization systems, including four different patterns, were evaluated for the resistive voltage drop and the area coverage. In the remaining three variants, the influence of the metal sheet resistance, as it would result from different process-parameters or process options, was considered. For this purpose, the thickness of the metallization, assumed to be copper of bulk conductivity, was varied from 5 μm thickness to 10 μm, simultaneously for both the front and the back metallization. In the final variant, the most favorable pattern geometry has also been evaluated with a metal layer as it would result from screen printing and sintering a silver paste, resulting in 10 μm thickness after firing. The study was based on the 10 cm x 10 cm cell size which seems to emerge as a standard size for large area cells. The differences in the 4 types of grid line patterns are illustrated in Fig. 1.

Pattern Type 1 uses 4 busses with equal spacing (2.5 cm centerline spacing), placed normal to the grid pattern of parallel lines, and parallel to one of the sides of the 10 cm x 10 cm square cells. The width of the bus lines is 1 mm (40 mil). Each pair of adjacent busses is joined near one edge of the cell to form two attachment ponts for interconnectors to an adjacent cell in the module. The busses are assumed to be formed simultaneously with the grid line metallization, and consequently

Table I.

The Physical Parameters of the Seven Metallization Cases Used as Illustrative Examples.

CASE (COLUMN #)	1	2	3	4	5	6	7
PATTERN TYPE (Fig. 1)	1	2	2	3	3	4	4
BASE: BULK:							
RESISTIVITY (Ωcm)	3	→	1	→	→	→	→
THICKNESS (μm)	300	→	200	→	→	→	→
CONTACT:							
METAL THICKNESS (μm)	5	→	10	→	→	→	→
PICK-UP POINTS	1	→	2	→	→	4	→
FRONT: DIFFUSED LAYER							
SHEET RESISTANCE (Ω)	35	→	→	→	→	→	→
METAL:	Cu	→	→	→	→	→	PRINTED Ag
THICKNESS (μm)	5	→	10	→	→	→	10(FIRED)
GRID LINE							
SPACING (mm)	4		2	→	→	→	→
WIDTH (μm)	127	→	75	→	→	→	127
BUS LINES							
NUMBER	4	1	→	4	→	→	→
WIDTH (mm)	1	→	→	0.25	→	0.64	→
PICK-UP WIRES							
NUMBER	-	→	→	2	8	4	→
GAUGE	-	→	→	26	→	22	→
DIAMETER (mm)	-	→	→	0.405	→	0.644	→

to be of the same material and the same thickness as these (5 μm). The center-to-center spacing of the grid lines is 4 mm (160 mil), their width 127 μm (5 mil)(Table I). The back of the cell has been assumed to be fully metallized, with one attachment point for an interconnector to the next cell located in the center of the cell. This general cell configuration is similar to some now on the market.

Once the geometry is defined, the voltage drops can be determined which result from the various series-resistance components in the cell. The first concerns the base region itself. Its resistance is given by:

$$R_B = \rho \frac{d_B}{A} \; ; \; [\Omega] \qquad (2)$$

With a semiconductor resistivity ρ of 3 Ωcm, and a base region thickness, d_B, of 300 μm, the resistance is $9 \cdot 10^{-2}$ Ω cm^2 for the unit cell area. For the entire cell of area A = 100 cm^2, R_B is $9 \cdot 10^{-4}$ Ω. The corresponding voltage drop at a maximum power point current of 3 A for the whole device will then be 2.7 mV, or approximately 0.5 percent of the expected maximum power point voltage.

For the back surface metallization with copper of bulk resistivity and 5 μm thickness, the sheet resistance R_{sh} is 3.2 mΩ. With uniform injection of the current over the entire back surface, the effective current flow within the metal layer is only one half of the total current extracted from the back contact. This could also be expressed as an effective resistance of the back contact metallization of 1.7 mΩ. However, the current is usually extracted from a small area to which an interconnector

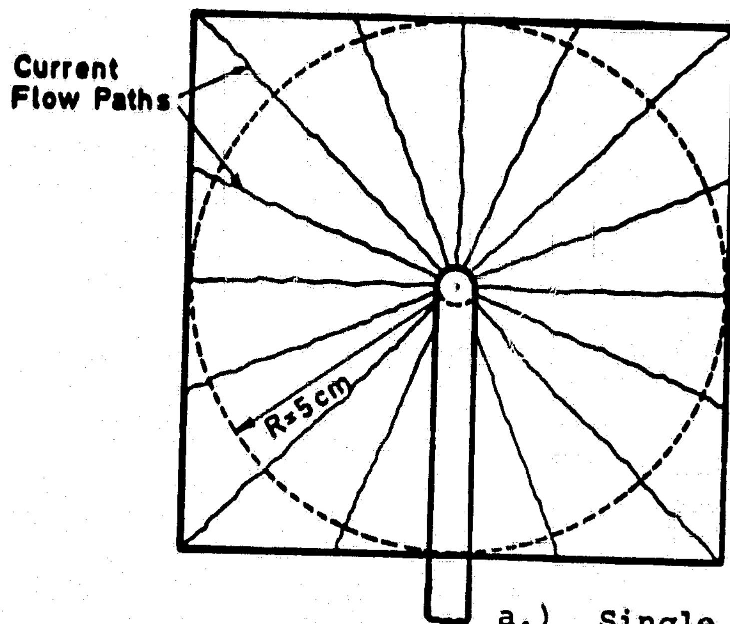

a.) Single Point Interconnector Attachment in Center of Cell

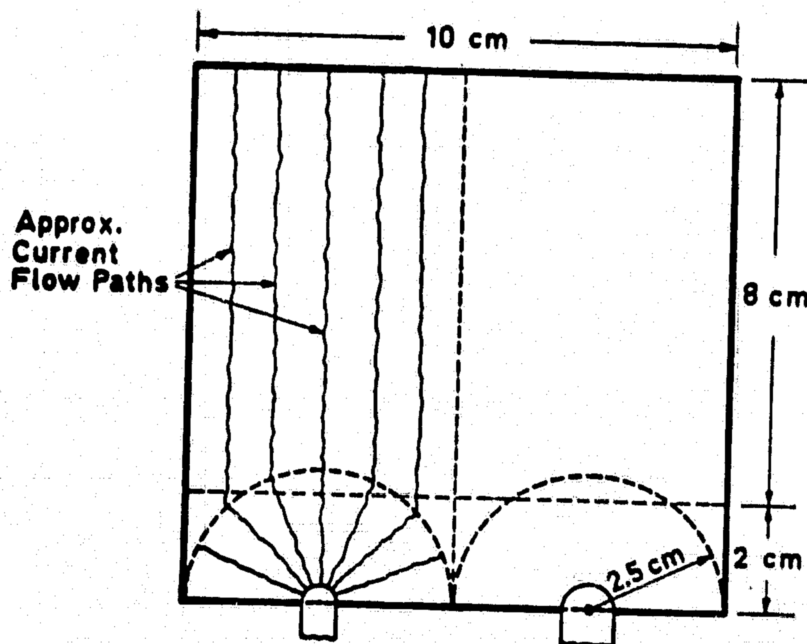

b.) Two Interconnector Attachments near Edge of Cell.

FIG. 2 Two Backside Metallization Patterns considered.

to the adjacent cell is attached, rather than from a strip pick up uniformly attached along the entire length of one of the sides of the cell. The effective resistance value discussed would be appropriate for this latter arrangement. For the small area pick-up mentioned first, the spreading resistance has to be taken into account. Its value is given by:

$$R_{sp} = \frac{R_{sh}}{\pi} \cdot \left\{ \frac{\ln \frac{r}{a}}{1 - \left(\frac{a}{r}\right)^2} - \frac{1}{2} \right\} , \qquad (3)$$

Assuming the interconnector to be attached in the center of the wafer with a circular joint of radius a=1.5 mm, the spreading resistance would be 3.3 mΩ (Fig. 2a). This spreading resistance value leads to a voltage drop of approximately 5 mV.

The sheet resistance of the front layer $R_{sh,FL}$ is assumed to be 35 Ω, the value generally used in modern silicon solar cells. With the current path to the nearest grid line extending over half the spacing S between adjacent grid lines, and with uniform current injection into the layer occuring over this distance resulting in another factor of 2, the effective resistance R_{FL} of the front layer itself attains the value given by:

$$R_{FL} = \frac{R_{sh,FL}}{4} \frac{S}{W} , \qquad (4)$$

In this relationship, W is the total length of the grid line to the nearest bus line, or half the clear spacing between adjacent bus lines. The voltage drop in the front sheet is then given by the product of the resistance value given by equation (4)

and the current contributed from half of the space between adjacent grid lines, that is the area $\frac{S}{2} \cdot W$:

$$\Delta V_{FL} = j \cdot R_{sh,FL} \cdot \frac{1}{8} S^2 \; ; \tag{5}$$

It may be noted that the voltage drop is proportional to the square of the total length of the current path in the given sheet. This is characteristic for all current flow in sheet structures in the cell, and it emphasizes the need to keep the length of each of the current paths adequately small.

Designating the width of the grid lines as T_{GL}, the effective resistance R_{GL} of the grid line itself is similarly given by:

$$R_{GL} = R_{sh,GL} \cdot \frac{W}{2} \cdot \frac{1}{T_{GL}} \; ; \tag{6}$$

and the voltage drop in the grid line due to the current collected from an area equal to $S \cdot W$ is given by:

$$\Delta V_{GL} = j \cdot R_{sh,\,GL} \frac{1}{2} \frac{S}{T_{GL}} W^2 \; ; \tag{7}$$

The 4 mm line spacing of the Type 1 grid pattern thus results in a voltage drop of 21 mV within the diffused layer. Using bulk resistivity of copper, 5 µm grid line thickness, and 127 µm line width, a 2.5 mV drop is found for the grid lines themselves.

Relationships corresponding to those for the grid lines (eq. (6) and (7)) apply for the bus lines, with the effective bus line resistance R_{BL} given by (T_{BL} = width of the bus lines):

$$R_{BL} = R_{sh,BL} \cdot \frac{L}{2} \cdot \frac{1}{T_{BL}} \; ; \tag{8}$$

and the voltage drop in the bus line, with current collected from an area equal to 2W·L, being expressed by:

$$\Delta V_{BL} = j\, R_{sh,BL} \frac{W}{T_{BL}} L^2 \; ; \qquad (9)$$

In equations (8) and (9), L expresses the length of the side of the solar cell, which is parallel to the bus line, assuming the bus line length to equal the length of this side. With the 5 μm thickness of the bus lines and their 1 mm width, the resistance of the bus lines is considerable, resulting in a voltage drop of 129 mV for the current flow of 0.75 A per bus line of pattern Type 1.

The voltage drops discusses here for the front layer and the metallization are the maximum voltages, appearing, for a grid line as an example, between the connection point to the bus line and the farthest point of the given grid line. The "effective voltage drop" which constitutes a weighted average, depends on the shape of the grid line, as will be discussed in section IV. For lines of uniform width, as well as the front layer itself and the back metallization, in the case of full coverage, the factor of 2/3 is to be applied to the maximum voltage drop. For uniformly tapered lines reaching zero width at the farthest point, the factor is 1/2. For pattern type I with uniform width grid and bus lines, the sum of all effective voltage drops, including those in the base region and the back contact, is 108 mV, or approximately 21% of the maximum power point voltage of the ideal cell with zero resistance.

Table II.

The Voltage Drops and Front Area Shading by Metal for the Seven Cases of Table I.

CASE (COLUMN #)	1	2	3	4	5	6	7
PATTERN TYPE	1	2	2	3	3	4	4
VOLTAGE DROP (mV)							
BASE: CONTACT	5 →	→	2.9 →	→	→	→	→
BULK	2.7 →	→	0.6 →	→	→	→	→
FRONT: DIFFUSED LAYER	21	11.1	4.9 →	→	→	→	→
GRID LINES	2.5	106.9	61	1.0 →	→	→	1.65
BUS LINES	129	15.1	15.1	15.6	0.97	0.96	0.95
WIRE	0 →	→	→	8.6	2.8	0 →	→
TOTAL EFFECTIVE: (mV)	108	95	56.5	22.7	8.9	7.1	7.5
AS % OF V_{MAX}, IDEAL	21	18.3	10.9	4.3	1.7	1.4	1.5
AREA COVERAGE (cm^2 = %)							
GRID LINES	3.18	4.02	3.6 →	→	→	→	6.1
BUS LINES	4.0	0.97	0.98 →	→	→	2.5	2.5
WIRES	0 →	→	→	0.7	2.8	0	
TOTAL	7.2	5.0	4.6	5.3	7.4	6.1	8.6

This value is clearly untolerably high. In addition, the grid lines and the bus lines cover 3.2 and 4.0 percent, respectively, of the frontal area of the cell. For the cell with metallization design Type I, the combined series resistance related power loss, including the front area coverage, thus amounts to approximately 28% of the potential power output (Table II).

As equations (6) and (8) show, the maximum voltage drop is proportional to the square of the path-length of the current in the respective conductor. In order to limit a given voltage drop, it is therefore important to limit the path length for the current. Since in the first metallization pattern, Type 1, the main voltage drop occurred in the bus lines, the remedy would be shortening their length. This consideration leads to the pattern design Type 2, where there is only one bus line, running along one edge of the cell (Fig. 1). The number of pick-up points, two, on the front has been maintained from Type I, so that the average path length in this main bus line is now reduced from 10 cm to 2½ cm, with a resulting decrease of the voltage drop in this element from 129 mV to 15 mV. Simultaneously, the grid line spacing has been reduced from 4 mm to 3 mm (Table I). The back metallization has been maintained as before. As a consequence of the reduced grid line spacing, the voltage drop in the front layer itself has been reduced from 21 mV to 11 mV. Because of the increase of the length of the grid lines, however, and in spite of the reduced current flow in each one of them, their voltage drop has grown from 2.5 mV to 107 mV.

In consequence, the total effective voltage drop for the cell is 95 mV. Simultaneously, the increase in the number of grid lines has increased their area coverage from 3.2 to 4%, while the coverage by bus lines has been reduced to 1%, yielding a total area coverage of 5%. (Column 2 of Table II).

While the change in metallization pattern from Type 1 to Type 2 brought significant reductions in both voltage drop and area coverage, the series resistance power loss is still much higher than acceptable. In the next step, the Type 2 pattern has been maintained, but a number of refinements have been assumed, in order to reduce the voltage drop. All metallization has been increased in thickness from 5 to 10 μm, which is about the maximum thickness reliably obtainable by various deposition methods. The resistivity of the base material has been decreased from 3 to 1 Ωcm, and the thickness of the base region from 300 to 200 μm, in order to reduce the base voltage drop (Table I). For the same reason, the number of pick-up points on the base contact has been increased to 2. This number also corresponds to the number of pick-up points on the front of the cell, and it provides redundancy. Also, the base pick-up points have been moved from the center of the cell to one edge of the cell (nearest to the adjacent cell), and they have been shaped as semicircles of 4 mm diameter. Their effective spreading resistance is 1.1 mΩ. Outside of the spreading resistance region, the metallization sheet is effectively two times 5 cm wide and 8 cm long, each half leading to one of the contact points (Fig. 2b).

The additional resistance of this metallization sheet is 2.7 mΩ, so that the total resistance is 3.9 mΩ for each half of the back metal layer. Because of the uniformly distributed injection into the metal layer, only one half of this total resistance is effective. Since each pick-up point carries only one half of the total cell current, the back metallization voltage drop is 2.9 mV, for a total base region voltage drop of 3.5 mV.

In addition to these base region refinements, the grid line spacing has been further decreased from 3 to 2 mm, with a simultaneous decrease in the width of the grid lines from 127 to 75 μm, so as not to increase the area covered by grid lines (Table I). This reduced gridline spacing gives a voltage drop of 4.9 mV in the front layer itself. Simultaneously, the reduced current flow in each grid line, together with their increased thickness, yields a grid line voltage drop of 61 mV. Taking also account of the voltage drop in the main bus line (15 mV), a total effective voltage drop for the entire cell of 56.5 mV is now obtained, for a power loss of approximately 11%. At the same time, a small reduction of the metal coverage in front (4.6%) has been achieved as a result of the slightly decreased grid line width (Column 3 of Table II).

Since the major voltage drop is now incurred in the grid lines, the logical next step is to decrease their length. A way of accomplishing this is by distributing the bus line again to four lines, directed normal to the grid lines (Type 3 in Fig. 1). The average center-to-center spacing of these busses is 2.5 cm.

The interconnectors to the adjacent cell are now running over the top of the cell for most of its length, serving simultaneously as pick-ups from the 4 bus lines, as shown by the open and solid wide lines, respectively, in the Type 3 pattern illustration. All other metallization features have been kept constant. The grid line voltage drop has been reduced to 1 mV without additional area coverage, but an additional 8.6 mV drop is now incurred in the interconnect wires, which are assumed to be of 26 gauge (B & S) which corresponds to 0.4 mm diameter. The total effective voltage drop now is 22.7 mV, or 4.3% of the ideal maximum power point voltage. Because an additional area is covered (0.7%) by the 2 interconnect wires, the total area coverage by metal has increased to 5.3% (Column 4 of Tables I and II).

Since the largest voltage drop in the Type 3 pattern is in the bus lines, the number of pick up wires has, for a trial, been increased from 2 to 8, mindful of the L^2 rule for the bus lines. The other features of the Type 3 pattern have been maintained. This change resulted in a decrease of the bus line voltage drop from 16 mV to 1 mV, and that in the pick-up wires from 8.6 mV to 2.6 mV, with a consequent total effective voltage drop of now 8.9 mV, for a 1.7% total series resistance power loss. While this could be considered as a tolerable level, the increased number of pick-up wires now shade 2.8% of the frontal area, for a total shaded area of 7.4%, a value significantly larger than considered acceptable.

As the number of pick-up wires used in the previous trial seems excessive, their number has subsequently been again reduced to 4. Also, since there occurs some unnecessary shading by both bus lines and pick-up wires, the pattern has been rotated by 90°, so that the pick-up wires run now on top of the bus lines (Type 4 in Fig. 1). This, in effect, constitutes a reduction of the sheet resistance of the bus lines through a thickness increase. In fact, by slightly increasing the diameter of the pick-up wires to 22 gauge (0.64 mm diameter), the bus line voltage drop could be maintained at the same value as in the prior arrangement, although only half the number of pick-up wires is used. Simultaneously, the additional voltage drop in the pick-up wires is eliminated (Column 6 of Table II). Consequently, the total effective voltage drop is 7.1 mV, corresponding to 1.4% power loss. In this approach, the bus line area coverage has been increased to 2.5%, but no additional area coverage by pick-up wires is incurred. Thus, the total front area coverage by metallization is 6.1% (Column 6 of Table II).

The use of printing methods for application of the metallization pattern has recently found widespread interest because of potentially very low processing costs. For this reason, the grid and bus line pattern Type 4 which was just discussed with plated-copper metallization, has also been evaluated for a screen-printed thick film silver system. Use of this system entails two restrictions. First, the minimum line width attainable with thick film screen printing has been projected to

Table III.

Output Power (Efficiency) and Solar Cell Values for the Seven Metallization Cases of Table I.

CASE (COLUMN #)	1	2	3	4	5	6	7
PATTERN TYPE	1	2	2	3	3	4	4
APPROX. OUTPUT VOLTAGE V_{MAX} (V)	0.412	0.425	0.463	0.497	0.511	0.513	0.513
APPROX. CURRENT DENSITY J_{MAX} (mA cm^{-2})	30.64	31.36	31.50	31.27	30.57	31.00	30.19
APPROX. POWER OUTPUT P (mW cm^{-2})	12.6	13.3	17.6	15.5	15.6	15.9	15.5
CELL VALUE $/$m^2$	55	62	78	88	90	93	88
$/W	0.403	0.443	0.505	0.54	0.545	0.554	0.54

127 μm, although 254 μm is currently the minimum practical line width. In contrast, line widths of less than 75 μm are readily attainable now with various other plating methods. This necessitates larger area coverage with screen printing. The second restriction is that the sintered metal layers have a higher resistivity than the bulk metal, or plated layers. With the practically attainable maximum thickness of 10 μm for a single screen printed layer after firing, the sheet resistance becomes limited by the generally experienced conductivity of the paste-deposited and sintered silver, which is about 30% of its bulk conductivity (Column 7 of Table I). With this, the grid line voltage drop is increased to 1.65 mV for a total effective voltage drop in the cell of 7.5 mV corresponding to 1.5% power loss (Column 7 of Table II Because of the greater grid line widths, the total area coverage is increased to 8.6%. Together, this entails a power output reduction by 2.6% incurred in switching from the plated copper to the screen-printed silver metallization system.

In a solar cell idealized to zero series resistance and zero front area coverage, a maximum-power-point current of 33 mA cm^{-2} and a maximum-power-point voltage of 0.52 V would correspond to current technology, for a power output of 17.2 mW. Assuming the series resistance to effect only the output voltage by reduction from the ideal maximum-power-point voltage with the effective voltage drop, and the area coverage to affect only the maximum-power-point current in proportion to the unshaded front area, a table of power output per unit cell area for the seven different

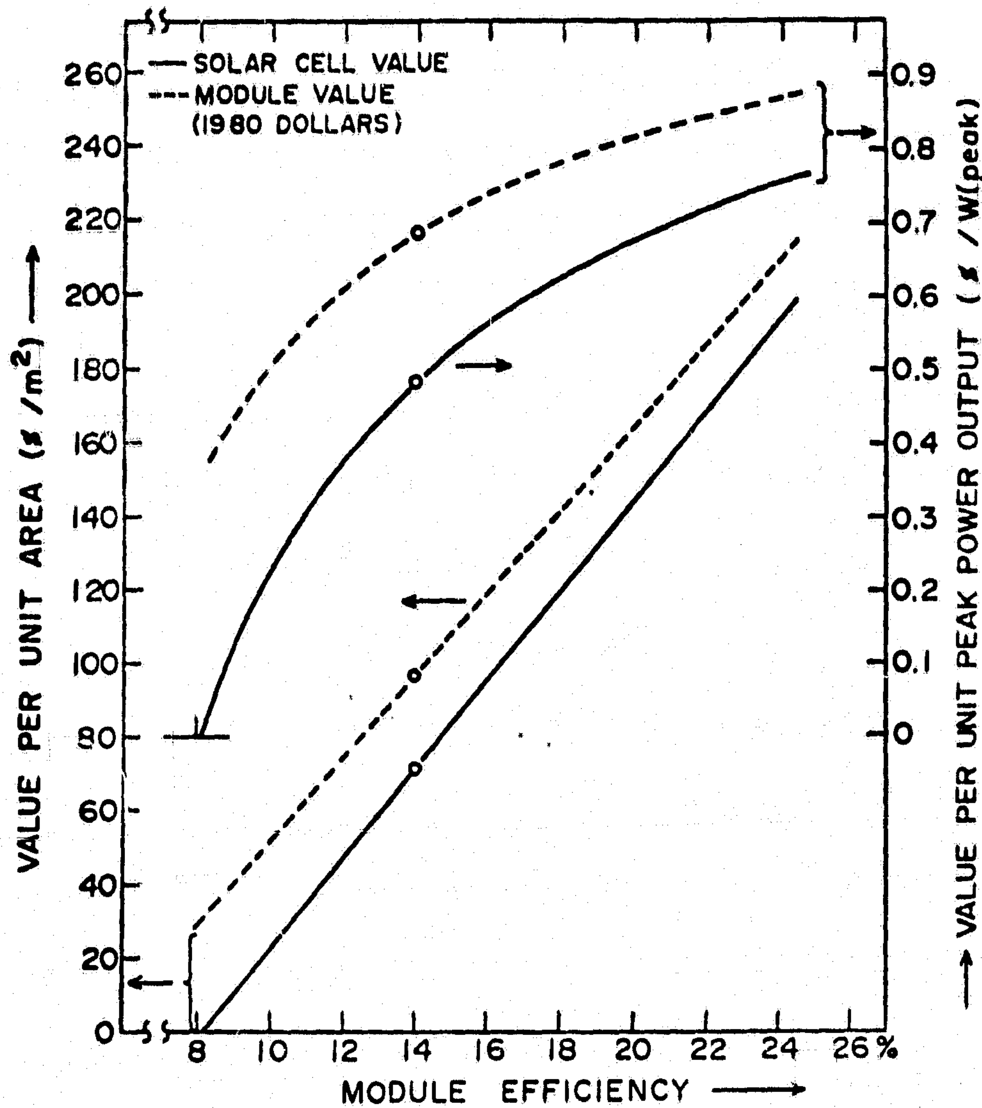

Fig. 3: Four curves representing the relationships between the value of solar cells and solar modules, respectively, and the efficiency of the modules. Both are expressed in dollars/m^2 (left hand scale) and dollars/peak Watt (right hand scale). The value is determined by the equal price of the energy delivered from the array. The reference module value is 0.683$/W(peak) at a module efficiency of 14% (circles), with an 0.201$/W(peak) encapsulation and module assembly price, using a ratio of 0.933 between module efficiency to encapsulated cell efficiency. The array installation price is 60$/$m^2$, with an array packing factor of 0.95. All these base data are DOE/JPL 1986 goals for single crystal silicon cells.

The array installation price determines the slope of the module value curves, the module encapsulation and assembly cost the differences in the pivot-point values (circles) and in the slopes between the module and cell-value curves.

metallization cases can be generated (Table III). Because of the use of 100 mW cm^{-2} peak insolation, the power output numbers represent simultaneously the efficiency numbers. Using the curve of solar cell value as function of module efficiency (Fig. 3) which was described in the Fourth Quarterly Report of this project, cell values can be assigned to the different cell metallization systems, based on their differences in module efficiency. A perhaps somewhat optimistic factor of 0.9 has been used in converting from the bare cell efficiencies to module efficiencies. As Table III shows, the cell values vary from \$93 per m^2 to below \$60 per m^2 for the less carefully designed systems. Even the \$5/m^2 difference in value between the copper plated and the silk screened metallization of Type 4 is large enough to permit use of a significantly more costly process to accomplish a metallization pattern of narrower lines than achievable by screen printing.

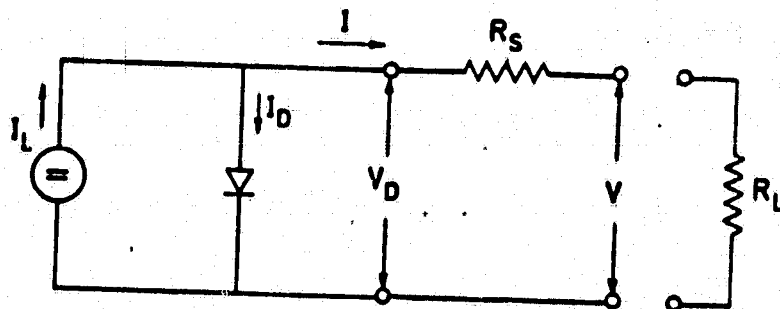

FIG. 4 Simplified Lumped-Constant Equivalent Circuit of the Solar Cell.

III. The Influence of Series Resistance on Solar Cell Performance.

1. A single lumped series resistance.

Because of the exponential I-V characteristic of the junction of the solar cell, all considerations of series resistance become complicated. Consequently, some of the effects of series resistance are not thoroughly explored, and a good deal of confusion seems to persist in the technical community. A small effort has, therefore, been spent on trying to clarify some of the simpler points. As Fig. 4 shows, the solar cell with a single lumped series resistance can generally be represented by a constant current generator which delivers the light generated current I_L, in parallel with an ideal diode which drains off part of this current as the "diode current" I_D. Consequently, the remaining current I is available for passage through the solar cell terminals to an outside circuit which is represented by the load resistance R_L in Fig. 4:

$$I = I_D - I_L \quad ; \tag{10}$$

$$I_D = I_o\left(e^{BV_D} - 1\right) \approx I_o e^{BV_D} \quad ; \tag{10a}$$

With: $B = q/kT$.

The solar cell with series resistance can be considered as an ideal solar cell without series resistance, having imaginary terminals across which the "diode voltage" V_D appears, as indicated in Fig. 4. This ideal solar cell is then connected to an external resistance R_S, which represents the single lumped series resistance of the cell, and which leads to the real solar cell

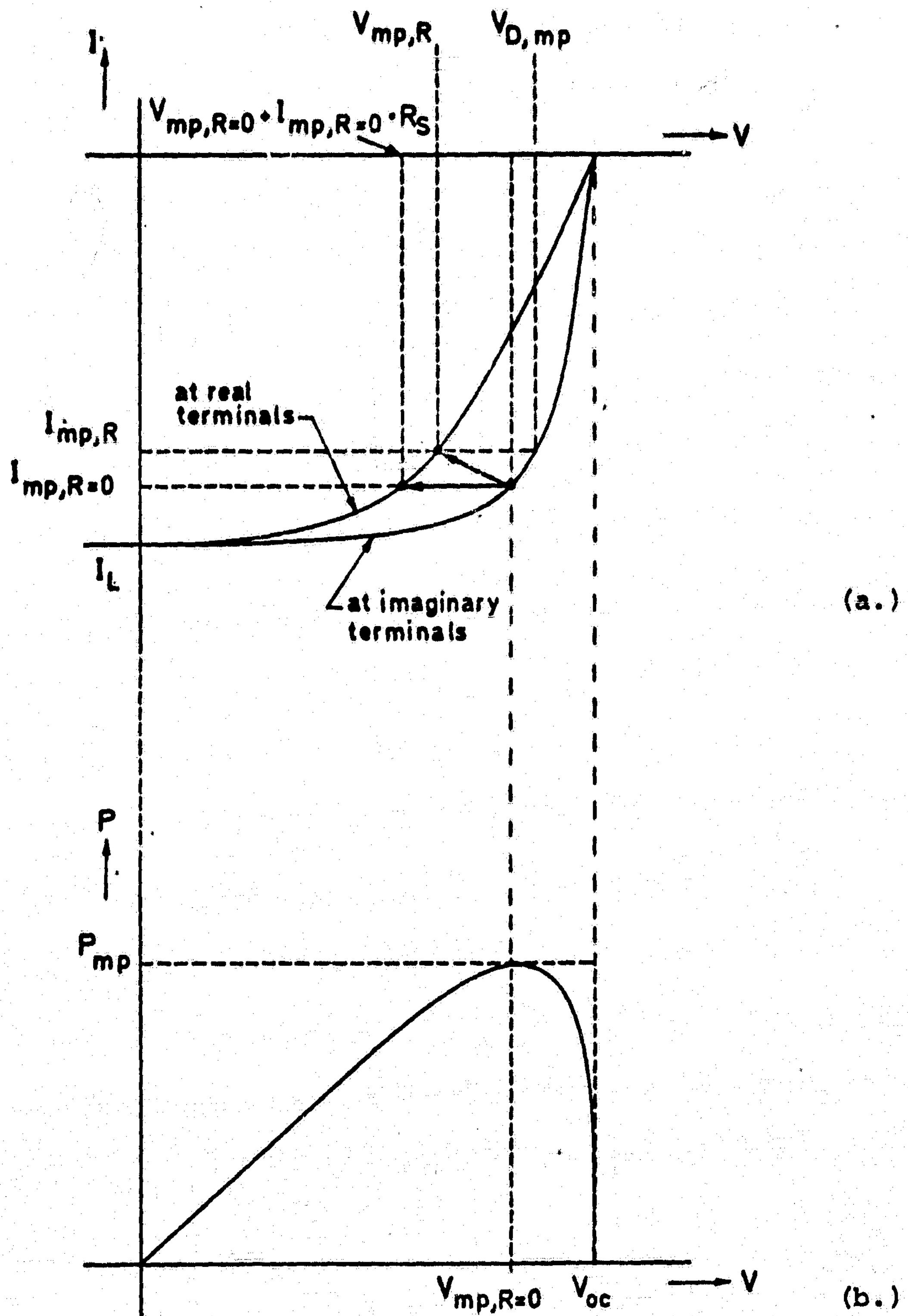

FIG. 5 Current - Voltage Characteristics of the Solar Cell Without and With Series Resistance (a), and of the Output Power Without Series Resistance (b).

terminals. The voltage V appears across these terminals, and the adjusted external load resistance R_L is connected to them. Thus, the ideal solar cell would see the combined load resistance:

$$R_L' = R_S + R_L \; ; \tag{11}$$

and its maximum power output would be $I \cdot V_D$, where the current I and the voltage V_D are designated as $I_{mp,R=0}$ and $V_{mp,\,R=0}$ in Fig. 5a. Thus, that IV characteristic in Fig. 5a on which the point $V_{mp,R=0}$, $I_{mp,R=0}$ lies, is the charateristic of the ideal solar cell without series resistance.

On the real terminals, after the series resistance R_S, that characteristic applies which is represented by the curve going through the point $V_{mp,R}$ and $I_{mp,R}$ (Fig 5a). At each current point, the voltage V_R on this characteristic is reduced from that of the ideal solar cell by the voltage drop $I \cdot R_S$ in the series resistance:

$$V_R = V_D + I\,R_s \; ; \tag{12}$$

Thus, for the maximum power point current $I_{mp,R=0}$ on the ideal diode, the voltage $V_{mp,R=0} - I_{mp,R=0} \cdot R_S$ appears at the terminals of the device after the series resistance. Note that all terminal currents I are negative according to eq. (10) and Fig. (5a).

The power output of the solar cell is given by the product of current and voltage at each point of the IV characteristic. Thus, for the device with series resistance, the power output at any terminal voltage V_R is given by:

$$P = IV_R = V_R I_o e^{BV_D} - V_R I_L \; ; \tag{13}$$

with V_D as it appears at the ideal diode terminals according to eq. (12). The power output P as function of the terminal voltage V_R has the form shown in Fig. 5b. The maximum power available from the device is indicated by P_{mp}. The derivative of the power output with respect to the terminal voltage V_R is given by:

$$\frac{dP}{dV_R} = I + V_R \frac{dI}{dV_R} = I + BV_R I_o e^{BV_D'} \; ; \qquad (14)$$

and, in order to find the maximum power point voltage V_{mp}, this derivative is set equal to 0.

The interesting part is, that introduction of relationship (12) into the left hand part of eq. (13) leads to:

$$P = IV_D + I^2 R_s \; ; \qquad (15)$$

which shows that the available power output at the terminals is the power output from the ideal solar cell reduced by the power dissipated in the series resistance. The power output according to eqs. (13) and (15) appears as a negative quantity, while the dissipated power is a positive quantity. It should also be noted that the derivative $\frac{dI}{dV}$ is a positive quantity, although I is a negative quantity in the range of interest. The current I_D which flows through the diode junction, is also positive. Thus, for the idealized solar cell with zero series resistance, the maximum output attainable is:

$$P_{mp,R=0} = I_{mp,R=0} V_{mp,R=0}$$

$$= \left(I_o e^{BV_{mp,R=0}} - I_L \right) V_{mp,R=0} \; ; \qquad (16)$$

with all concerned quantities indicated by subscript R=0.

For the real solar cell with a single lumped-constant resistant R_S, however, the maximum power output is:

$$P_{mp,R} = I_{mp,R} V_{mp,R}$$

$$= I_{mp,R} \left(V_{D,mp} + I_{mp,R} R_s \right) \quad ; \qquad (17)$$

or

$$P_{mp,R} = V_{D,mp} \left[I_o e^{BV_{D,mp}} - I_L \right] + I_{mp,R}^2 \cdot R_s \quad ; \qquad (17a)$$

Here, $V_{D,mp}$ is the voltage which appears across the idealized solar cell for maximum power out of the real terminals. The question is, whether maintaining the maximum power output from the idealized device also delivers maximum power into the properly adjusted load resistance R_L (eq.11), or whether deviating from the point at which the idealized solar cell itself supplies maximum power will actually deliver more power into the load. The latter statement means, that the power output from the ideal device would decrease less rapidly than the power dissipated in the load resistance, as this deviation from the ideal device maximum power point occurs. This can be readily tested by use of the derivative of the maximum power output from the real device with load resistance:

$$\frac{dP_{mp,R}}{dV_{D,mp}} = \frac{dP_{mp,R=0}}{dV_{D,mp}} + \frac{d}{dV_{D,mp}} \left(I_{mp,R}^2 \cdot R_s \right)$$

$$\approx 2 I_{mp,R} R_s \frac{dI_{mp,R}}{dV_{D,mp}} \quad ; \qquad (19)$$

This equation contains basically two terms according to those of eq. (17a), where the first term was derived from the maximum power point of the idealized device. Now, the maximum power output from the idealized device has been found by setting its derivative with respect to the voltage equal to zero. Thus, a deviation from the maximum power value at small changes of the voltage can only be of very small magnitude. The dissipated power, however, changes with the first derivative of the current, and will thus be much larger. As remarked above, the derivative $\frac{dI}{dV}$ is positive and is multiplied in the second term of eq. (19) with the maximum power point current itself which is a negative quantity. Thus, the change in power output from the real device terminals with a change in voltage is a negative quantity, indicating an increase in the available power output. Consequently, the optimum operating point of the solar cell with series resistance is at a voltage which is slightly greater than given by $V_{mp,R=0} - I_{mp,R=0} \cdot R_s$, and the power output thus obtainable will be slightly greater than that of the solar cell matched for a terminal voltage equal to the ideal maximum-power-point voltage minus the voltage drop in the series resistance, as indicated by the horizontal arrow in Fig. 5a. The related, commonly used way of analyzing the solar cell by considering the matched case of the idealized device and reducing the power output by the dissipation in the series resistance results in a slightly smaller than optimum power output. Since the differences in power output are small, most results obtained this way should be justifiable, but it will be good to keep in mind that these analyses actually

are worse-case approximations. In the following discussions, this same approach will also be used for reasons of simplicity.

2. The effect of different solar cell elements operating at differing voltages.

The treatment of series resistance as a single lumped constant element, as carried out in the preceding section, is quite appropriate for series resistance components through which the entire cell current flows. This is the case with the contact resistance and the bulk resistance of the base region. Other series resistance components, however, cause differing voltages to appear across various parts of the pn junction. These are the voltage drops caused in the back metallization, and in the sheet resistance of the front layer, as well as the voltage drops occurring in the grid lines and the bus lines.

When various parts of the solar cell operate at different junction voltages, one might expect that differing current contributions are made from these parts of the solar cell, according to eqs. (10). In the single lumped constant representation, the reduction in output power was shown to be at most the power dissipated in the resistive component, and influences of the exponential nature of the I-V characteristic to be slightly beneficial rather than detrimental. When parts of the cell operate at differing voltages, however, the situation is different. The losses expected in this case will be termed "mismatch losses".

In order to investigate the magnitude of such potential mismatch losses, it was assumed that the cell operates essentially

PRECEDING PAGE BLANK NOT FILMED

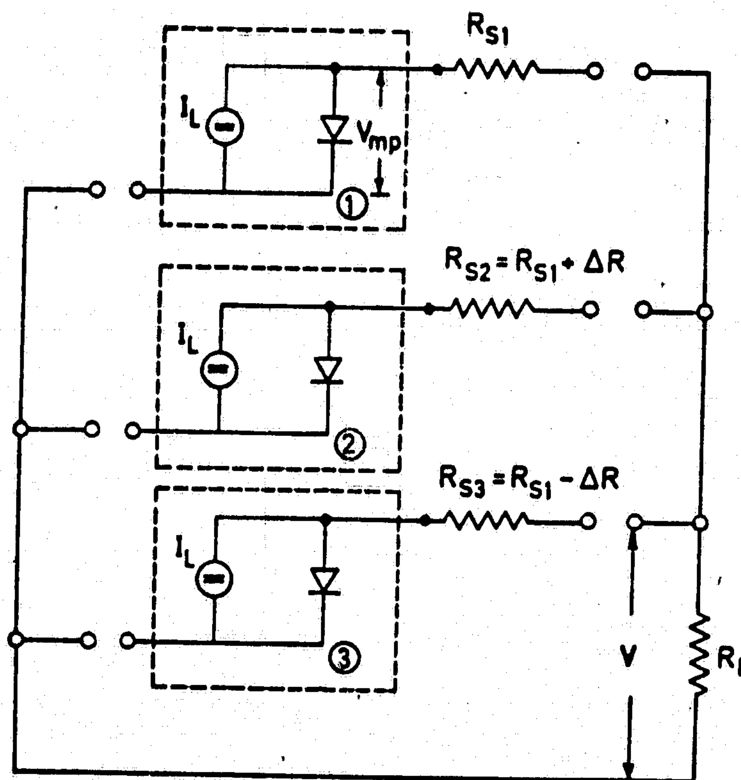

FIG. 6 Parallel Arrangement of three Identical Solar Cells with Different Series Resistances.

in the maximum power point condition at an average voltage drop across the resistive elements, and that the deviations of the junction voltage from the average at the individual parts of the solar cell will be both in the positive and negative directions. To simulate this case in a simple manner, a model was devised which consists of 3 identical solar cells, which are connected in parallel over 3 different series resistances to a common external load (Fig. 6). The series resistance of cell 1 was called R_{s1}, and those of cells 2 and 3 were considered to be larger and smaller then R_{s1} by equal amounts ΔR:

$$R_{s2} = R_{s1} + \Delta R \; ; \qquad (20a)$$

$$R_{s3} = R_{s1} - \Delta R \; ; \qquad (20b)$$

It was thought that such a symetrical arrangement might best illustrate the existence of the expected mismatch losses.

The power output of the 3 parallel connected cells can be expressed as:

$$P_{out} = (I_1+I_2+I_3)V = \left\{ \bar{I}_o \left[e^{B(V-I_1R_{s1})} + e^{B(V-I_2R_{s2})} + e^{B(V-I_3R_{s3})} \right] - 3I_L \right\} V \; ; \qquad (21)$$

with:

$$V - I_1R_{s1} = V_{mp,R=0} \; ; \qquad (22)$$

or

$$V = V_{mp,R=0} + I_1R_{s1} \; ; \qquad I_1<0. \qquad (22a)$$

In the subsequent parts of this section, $V_{mp,R=0}$ will be written simply as V_{mp}.

The I·R voltage drops across the 3 series resistances will be of unequal magnitude, as expressed by:

$$I_2R_2 > I_1R_{s1} > I_3R_{s3} ; \tag{23}$$

While the common terminal voltage for all 3 solar cells is assumed to be the maximum power point voltage V of the real cell 1, the voltage across the ideal solar cell 1, exclusive of series resistance, is its maximum power point voltage V_{mp}, as expressed in eq. (22).

Combining eqs. (21) and (22a) leads to the form:

$$P_{out} = \left[I_o e^{BV_{mp}} \left(1 + e^{B(I_1R_{s1} - I_2R_{s2})} + e^{B(I_1R_{s1} - I_3R_{s3})} \right) - 3I_L \right] V ; \tag{24}$$

which can be, for adequately small differences in the voltage drops over the 3 different series resistances, expressed by first order approximation:

$$P_{out} \simeq \left\{ I_o e^{BV_{mp}} \left[1 + 1 + B(I_1R_{s1} - I_2R_{s2}) + 1 + B(I_1R_{s1} - I_3R_{s3}) \right] - 3I_L \right\} V ; \tag{25}$$

Segregating appropriate terms leads to:

$$P_{out} = \left[3\left(I_o e^{BV_{mp}} - I_L \right) + I_o e^{BV_{mp}} B \left(I_1R_{s1} - I_2R_{s2} + I_1R_{s1} - I_3R_{s3} \right) \right] V ; \tag{25a}$$

which, after application of eq. (22a) takes the form:

$$P_{out} = 3I_{mp}V_{mp} + 3I_{mp}^2R_{s1} + B(I_1R_{s1} - I_2R_{s2} + I_1R_{s1} - I_3R_{s3}) I_o e^{BV_{mp}} V ; \tag{26}$$

In this form, the first two terms give the sum of the maximum power output of the 3 idealized solar cells, reduced by 3 times the dissipation in the average series resistance value R_{s1}. The remaining terms indicate the deviation from this simplified model.

The differences in the actual voltage drops which are expressed in the third term on the right hand side of eq. (26), can be transformed as in eq. (27a) and (27b):

$$I_1R_{s1}-I_2R_{s2}=(I_1-I_2)R_{s1}-I_2\Delta R=(I_1-I_2)(R_{s1}+\Delta R)-I_1\Delta R \;; \qquad (27a)$$

$$I_1R_{s1}-I_3R_{s3}=(I_1-I_3)R_{s1}+I_3\Delta R=(I_1-I_3)(R_{s1}-\Delta R)+I_1\Delta R \;; \qquad (27b)$$

and to:

$$I_1-I_2 \approx BI_oe^{BV}\left[-R_{s1}(I_1-I_2)+(I_2-I_1)\Delta R+I_1\Delta R\right]. \qquad (28)$$

Finally, the differences in the terminal currents of solar cells 2 and 3 against that of cell 1 can be expressed as:

$$I_1-I_2=FI_1(1-F) \;; \qquad (29a)$$

and:

$$I_1-I_3= -FI_1(1+F) \;; \qquad (29b)$$

with:

$$F = \frac{BI_D\Delta R}{1+BI_DR_{s1}} \;; \qquad (30)$$

Introducing these forms into eq. (26) permits expressing the output power in the simpler form:

$$P_{out}=3(I_1V_{mp}+I_1^2R)+2FR \left\{\frac{\Delta R}{R}-F\right\} I_1BI_oe^{BV_{mp}}(V_{mp}+I_1R) \;; \quad (31)$$

The actual dissipation in the three series resistances of differing magnitude is given by:

$$P_{Diss}=I_1^2R_{s1}+I_2^2R_{s2}+I_3^2R_{s3} \;; \quad (32)$$

By combining eq. (26), (29 a and b), (30), and (32), the expression for P_{Diss} can be transformed into one contaning only the current I_1, the average resistance R, and the difference in the series resistance values ΔR:

$$P_{Diss}=3I_1^2R+2I_1^2 \left[(3F^2+F^4)R-2F(1+F^2)\Delta R\right] \;; \quad (33)$$

The power output P_{out} actually transferred into the load resistance, as given by eq. (31), plus the power dissipated, according to eq. (33), should add up to the maximum power output available from the three "ideal devices", unless there are "mismatch losses". In the latter case, the sum of the power output plus the dissipated power would be expected to be smaller than the "ideal" maximum power output. This hypothesis shall be tested in the following.

Since the power output into the load resistance is given by the IV product, where I is a negative quantity, this power output also appears as a negative quantity. The dissipated power which is a positive quantity, thus will actually have to be subtracted from the power output to form the larger negative quantity of the ideal power, as is done for eq. (34) which combines eqs. (31) and (33):

$$P_{out}-P_{Diss}=3I_1V_{mp}+4I_1{}^2\left[F(1+F^2)\Delta R-\left(\frac{3}{2}F^2+\frac{1}{2}F^4\right)R\right]$$
$$+2F\,R\left(\frac{\Delta R}{R}-F\right)I_1BI_oe^{BV_{mp}}V_{mp}$$
$$+2F\,R\left(\frac{\Delta R}{R}-F\right)B\,I_oe^{BV_{mp}}I_1{}^2R\ ; \qquad (34)$$

and which can readily be simplified to the form:

$$P_{out}-P_{Diss}=3I_1V_{mp}+2\,F\left(\frac{\Delta R}{R}-F\right)BI_oe^{BV_{mp}}R\cdot I_1V_{mp}$$
$$+2\left\{2(F+F^3)\frac{\Delta R}{R}-3F^2-F^4+F\left(\frac{\Delta R}{R}-F\right)BI_oe^{BV_{mp}}R\right\}I_1{}^2R\ ; \qquad (35)$$

The first term on the right hand side of eq. (35) represents the expected maximum power output from the three idealized solar cells, disregarding the series resistance voltage drop. The remaining part of the right hand side of eq. (35) represents the expected potential mismatch losses. This remaining part is the only quantity of further interest. It will, from here on, be evaluated for its magnitude. Since it is attributable to the two cells #2 and 3, it shall be designated as $2\Delta P$:

$$P_{out}-P_{Diss}=3I_1V_{mp}+2\Delta P\ ; \qquad (36)$$

Combining terms, expressing the quantity V_{mp} in the exponent by the relationship (22), and approximating the exponential factor with the exponent BI_1R by the Taylor expansion broken off after the linear term, leads to the expression:

$$\Delta P = F^2 \left\{ (1 - BI_1 R) I_1 V_{mp} + \left[\frac{2}{BI_D R} - BI_1 R + \left(\frac{2}{BI_D R} + 1 \right) F^2 \right] I_1^2 R \right\} ; \qquad (37)$$

$$\text{with } F = \frac{BI_D \Delta R}{1 + BI_D R}$$

The first term in the large brackets on the right hand side of eq. (37) contains what might be expected as the "mismatch losses". This term is, however, negative, and consequently means an increase in maximum power output rather than a reduction. The second term on the right hand side, containing the square brackets, is connected with the dissipation loss, and turns out to be generally positive, which means increased dissipation. The first term in the square bracket is the dominant term by far.

Entering numbers into eq. (37), such as a series resistance R of 0.25 Ω, and a ΔR of 0.1 Ω, a terminal current $I_1 = 3 \cdot 10^{-2}$A (as for a 1 cm^2 cell), and a saturation current $I_o = 2.8 \cdot 10^{-12}$A, it turns out that the ΔP becomes 5.4% of the I^2R loss. The ΔP is negative, however, which means that the power output obtainable from the three solar cells in combination is slightly greater than that which would correspond to the maximum power output from the three ideal solar cells, reduced by the I^2R losses in the three differing series resistance.

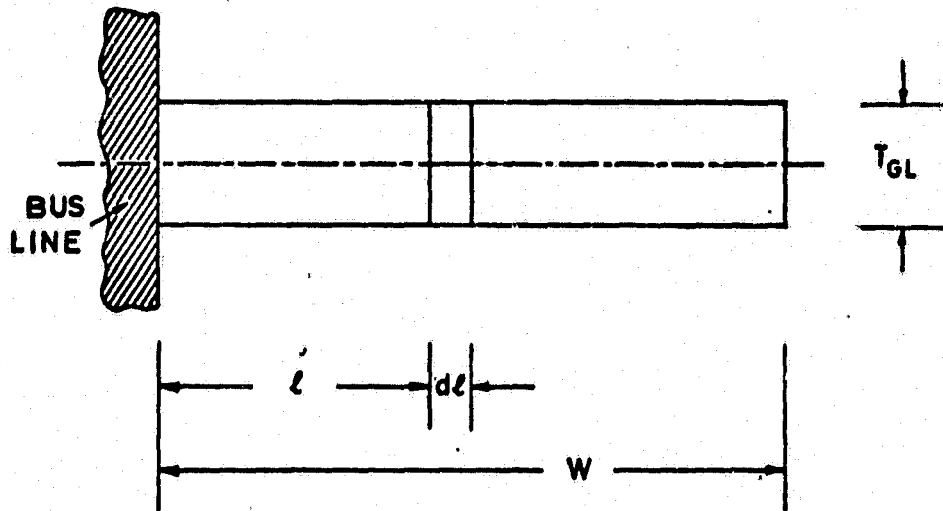

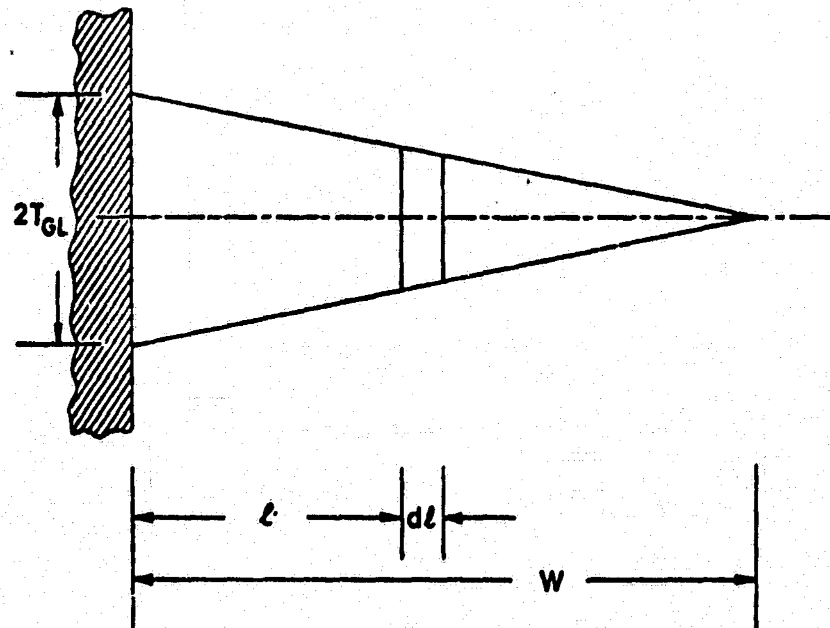

FIG. 7 Grid Line Configurations.

PRECEDING PAGE BLANK NOT FILMED

IV. The Voltage Drop in Uniform Width or Tapered Grid Lines.

The width of the grid line at the distance ℓ from its connection to the bus line is given for the grid line of uniform width by (Fig. 7a):

$$T_{PGL}(\ell)=T_{GL} \; ; \tag{38}$$

and for the tapered grid line by (Fig. 7b):

$$T_{TGL}(\ell)=2T_{GL} \frac{W-\ell}{W} \; ; \tag{39}$$

For the tapered grid line, the width at the connection to the bus line is set equal to 2 x T_{GL}, so that the total area shaded by the tapered grid line equals that shaded by the grid line of uniform width $T_{GL}W$. The voltage drop over the length element $d\ell$ of the gridline is then given by the product of the resistance of this length element and the current flowing in the grid line at this distance from the bus connection:

$$dV=R_{sh} \frac{d\ell}{T(\ell)} \cdot j_{mp}(W-\ell)S \; ; \tag{40}$$

where R_{sh} is the sheet resistance of the grid line. Substituting either eq. (38) or (39) for $T(\ell)$, and integrating eq. (40) from zero to W gives the voltage drop V(W) to the end point of the grid line:

$$V(W)=j_{mp}R_{sh} \frac{S}{2T_{GL}} W^2 \; ; \tag{41}$$

This "end point voltage drop" is the voltage drop which occurs

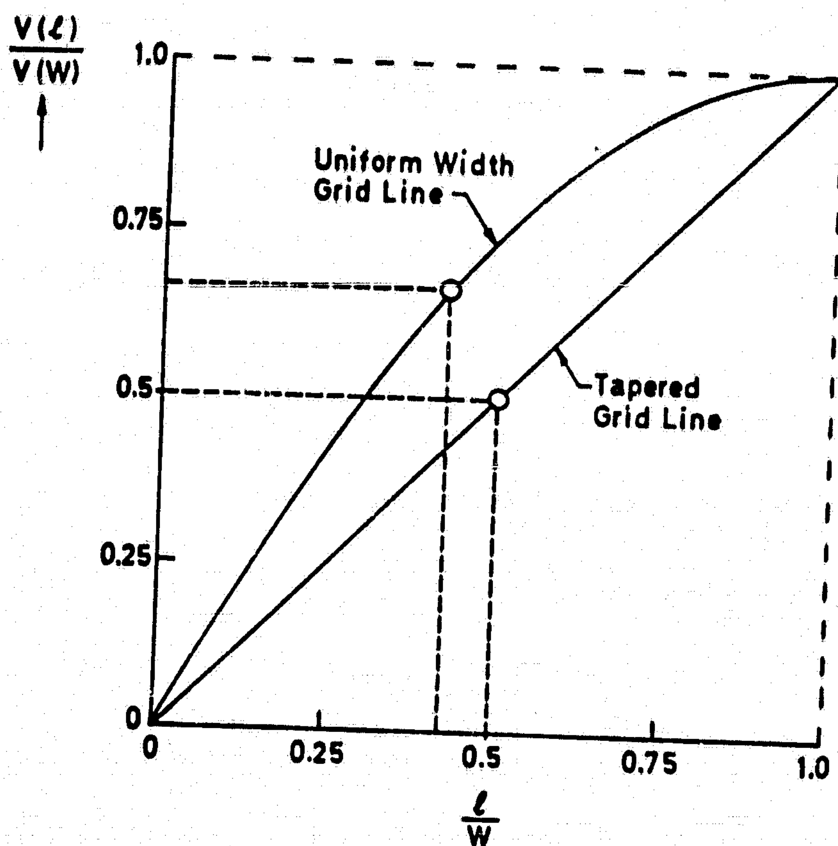

FIG. 8 Voltage Drop along a Uniform Width and a Tapered Grid Line, respectively. Note that the end-point (ℓ=W) voltage drops are equal, when both grid lines cover identical areas (T_{GL}·W).

over the entire length of the gridline. It signifies how much higher the junction voltage is at the farthest point from the bus line, than it is at the connecting point to the bus line.

Although this end point voltage drop is the same for both the tapered and the uniform width grid line, the voltage distribution along the length of the two types of grid lines varies (Fig. 8). For the uniform width grid line, the voltage drop $V(\ell)$

$$V_{PGL}(\ell) = V(W)\left[2\,\frac{\ell}{W} - \left(\frac{\ell}{W}\right)^2\right] \; ; \qquad (42)$$

increases more rapidly near the connection to the bus line than that of the tapered grid line which rises linearly over the length of the grid line:

$$V_{TGL}(\ell) = V(W)\,\frac{\ell}{W} \; ; \qquad (43)$$

In correspondence to this increasing voltage drop along the grid line, a varying voltage exists across the pn junction, and the diode current will vary accordingly. Thus, one would expect a complicated relationship for finding the effective maximum power point in a device with such varying junction voltage, considering the exponential nature of the IV characteristic. This is indeed the case, and an attempt to derive a manageable solution has so far only resulted in lengthy and non-transparent expressions.

However, in consequence of the discussions in section III-2, in which this case was modelled in a very simplified approach by 3 solar cells connected in parallel over three different series resistances, it was found adequate to evaluate the dissipation occurring in each type of grid line. Integration of the dis-

sipated power contributions along the grid line according to:

$$P_{Diss} = \int_{0}^{W} I(\ell)\, dV = \int_{0}^{W} j_{mp}(W-\ell) S \; dV \; ; \tag{44}$$

utilizing eq. (40) with either eq. (38) or (39), yields the total power dissipated in the uniform width or the tapered grid line, respectively. Equation (45) gives the result for the uniform width grid line:

$$P_{Diss,PGL} = \frac{2}{3} V(W) \cdot j_{mp} SW \; ; \tag{45}$$

showing that the power dissipation equals 2/3 times the end point voltage V(W) times the total current flow through the grid line. For the tapered grid line:

$$P_{Diss,TGL} = \frac{1}{2} V(W) \cdot j_{mp} SW \; ; \tag{46}$$

the factor 2/3 is replaced by 1/2. Thus, the "effective voltage drop" is 2/3 or 1/2 of the end-point voltage drop for the uniform width or the tapered grid line, respectively. Consequently, the tapered grid line has a slight advantage with respect to solar cell performance over the uniform width grid line.

It should be noted, however, that a truly tapered grid line, ending in a zero width end point, is practically impossible to produce. Therefore, the actually fabricated tapered grid lines are a compromise between the truly tapered and the uniform width grid line. Their effective voltage drop will thus be between 1/2 and 2/3 of the end point voltage.

A situation equivalent to that just discussed with respect to the grid lines also exists in the bus lines, in the semiconducting front layer, and in the back metallization. With the possible exception of the bus lines, they all are represented by analogues to the "uniform width grid lines" equations. The bus lines may be tapered, but where they are reinforced by an overlayed wire, they act like uniform width lines.

In the semiconducting front layer, the voltage drop occurs between the edge of the grid line and a line halfway between two adjacent grid lines. This line is at the endpoint voltage relative to the voltage existing at the nearest points on the adjacent grid lines, assuming a parallel grid system. The drops in the various components - bus lines, grid lines, front layer - thus add up to a different voltage at each portion of the junction area. However, as shown in Section III, the "effective junction voltage" can be determined from the terminal voltage by deducting the voltage drops occuring in the various resistive components present in the device.

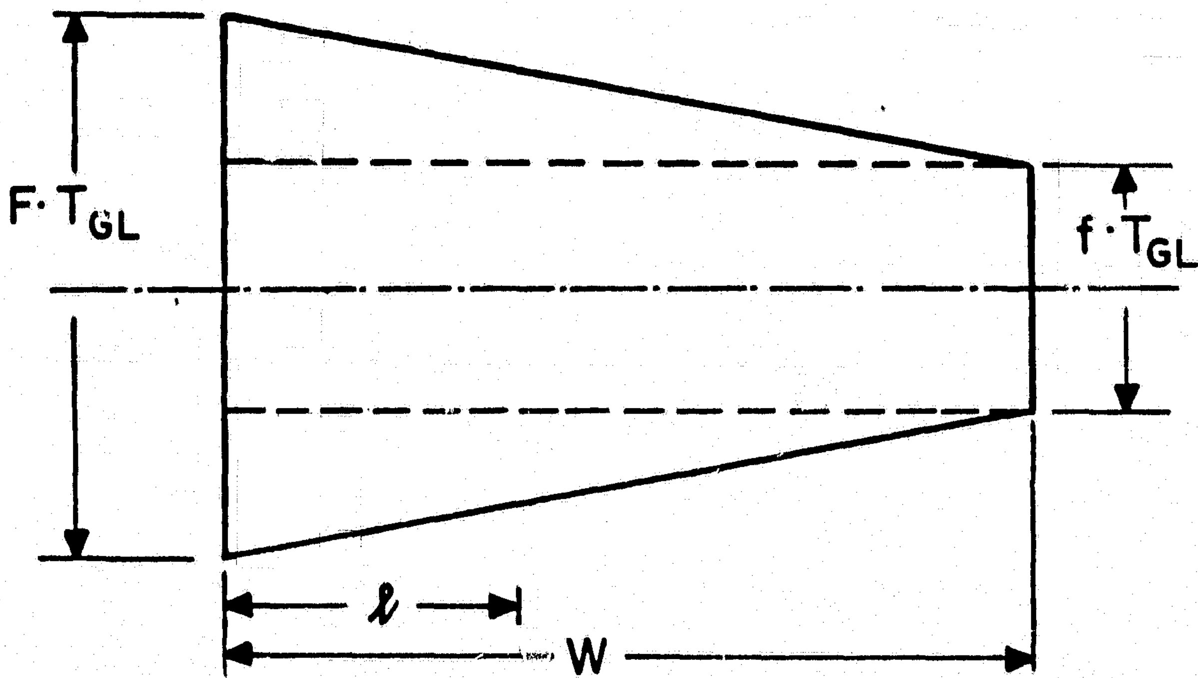

FIG. 9 Explanation of nomenclature used in the analysis of the general tapered grid line

V. The General Tapered Grid Line Problem

In our quarterly report the end point voltage drop V(W) and the effective voltage drop were investigated for uniform width and fully tapered grid lines. Since then, an integration method has been developed for partially tapered grid lines (Ref. 1). While the solutions resulting from that method appear to be singular at both end points of the range of possible tapers, which are the uniform width and the fully tapered grid line, it can be shown that the solution really is well behaved in those two cases and yields the same results as given in section IV. It seems therefore useful to generalize this approach.

Figure 9 explains the nomenclature used to describe the geometry of the general tapered grid line. The width of the base of the grid line is $F \cdot T_{GL}$, while the width of the grid line at its end is $f \cdot T_{GL}$, with the length of the grid line being given by W as before. Thus, the area covered by the grid line is given by:

$$A = \tfrac{1}{2}(F + f)\ T_{GL}W \ ; \qquad (48)$$

Since the area covered by the grid line shall be the same for all grid shapes, and equal to $T_{GL} \cdot W$, the condition:

$$\tfrac{1}{2}(F + f) = 1 \ ; \qquad (49)$$

has to be fulfilled, which means that:

$$F = 2 - f ; \tag{49a}$$

The grid line width in dependence on position along the grid line is then given by:

$$T_{GL}(\ell) = fT_{GL} + (F - f)\,\frac{W-\ell}{W}\,T_{GL} ; \tag{50}$$

or, expressing $T_{GL}(\ell)$ exclusively in terms of the taper parameter f, after making use of eq. (49a) in eq. (50):

$$T_{GL}(\ell) = T_{GL}\left[f + 2(1-f)\,\frac{W-\ell}{W}\right] ; \quad 0 \leq f \leq 1 \tag{50a}$$

$f = 1$ describes the uniform width grid line, and $f = 0$ the fully tapered grid line, ending in zero width.

The incremental voltage drop over a length element $d\ell$ at the position ℓ along the grid line is then given by:

$$dV = R_{sh}\,\frac{d\ell}{T_{GL}(\ell)} \cdot j_{mp}(W-\ell)\;S ; \tag{51}$$

where R_{sh} is the sheet resistance of the grid line, and S obtained from the center-to-center spacing $S + T_{GL}$ of the grid lines. After inserting eq. (50a), eq. (51) can be expressed as:

$$dV = R_{sh} j_{mp}\,\frac{SW}{T_{GL}}\;\frac{(W-\ell)\,d\ell}{fW + 2(1-f)(W-\ell)} ; \tag{51a}$$

Integration from the base of the grid line to its end yields the end point voltage drop V(W):

$$V(W) = R_{sh} j_{mp}\,\frac{SW}{T_{GL}} \int_0^W \frac{(W-\ell)\,d\ell}{fW + 2(1-f)(W-\ell)} ; \tag{52}$$

The integral has the solution:

$$\int_0^W \frac{(W-\ell)\ d\ell}{fW + 2(1-f)(W-\ell)} = -\frac{W-\ell}{2(1-f)} - \frac{fW}{4(1-f)^2} + \frac{fW}{4(1-f)^2}\ \ell n\left[fW + 2(1-f)(W-\ell)\right]\Bigg|_0^W ; \tag{53}$$

which yields the expression for the end point voltage drop:

$$V(W) = R_{sh} j_{mp} \frac{SW^2}{2T_{GL}} \cdot G(f) ; \tag{54}$$

where:

$$G(f) = \frac{1}{1-f}\left[1 + \frac{f}{2(1-f)}\ \ell n \left(\frac{f}{2-f}\right)\right] ; \tag{54a}$$

For $f \to 0$, $\ell n\ (\frac{f}{2-f})$ would tend towards minus infinity. However it is:

$$\frac{f}{2(1-f)}\ \ell n\left(\frac{f}{2-f}\right) = \frac{1}{2(1-f)}\ \ell n\ \left(\frac{f}{2-f}\right)^f ; \tag{55}$$

so that this relationship tends to $\frac{1}{2}\ell n\ 1 = 0$ for $f \to 0$. Consequently, the end-point voltage multiplier $G(f)$ for the fully tapered grid line becomes:

$$\lim_{f \to 0} G(f) = 1 ; \tag{56}$$

to yield the value of $V(W)$ just as obtained in the preceding report.

When f approaches 1, it is useful to substitute $f = 1 - x$, so that:

$$\frac{1}{1-f}\ \left[1 + \frac{f}{2(1-f)}\ \ell n\ \frac{f}{2-f}\right] = \frac{1}{x}\ \left[1 + \frac{1-x}{2x}\ \ell n\ \frac{1-x}{1+x}\right] ; \tag{57}$$

The logarithm can be expressed by an infinite series, so that the right hand side of eq. (57) changes to:

$$= \frac{1}{x}\ \left[1 - \frac{1-x}{2x} \cdot 2\left(x + \frac{x^3}{3} + \ldots\right)\right] \tag{57a}$$

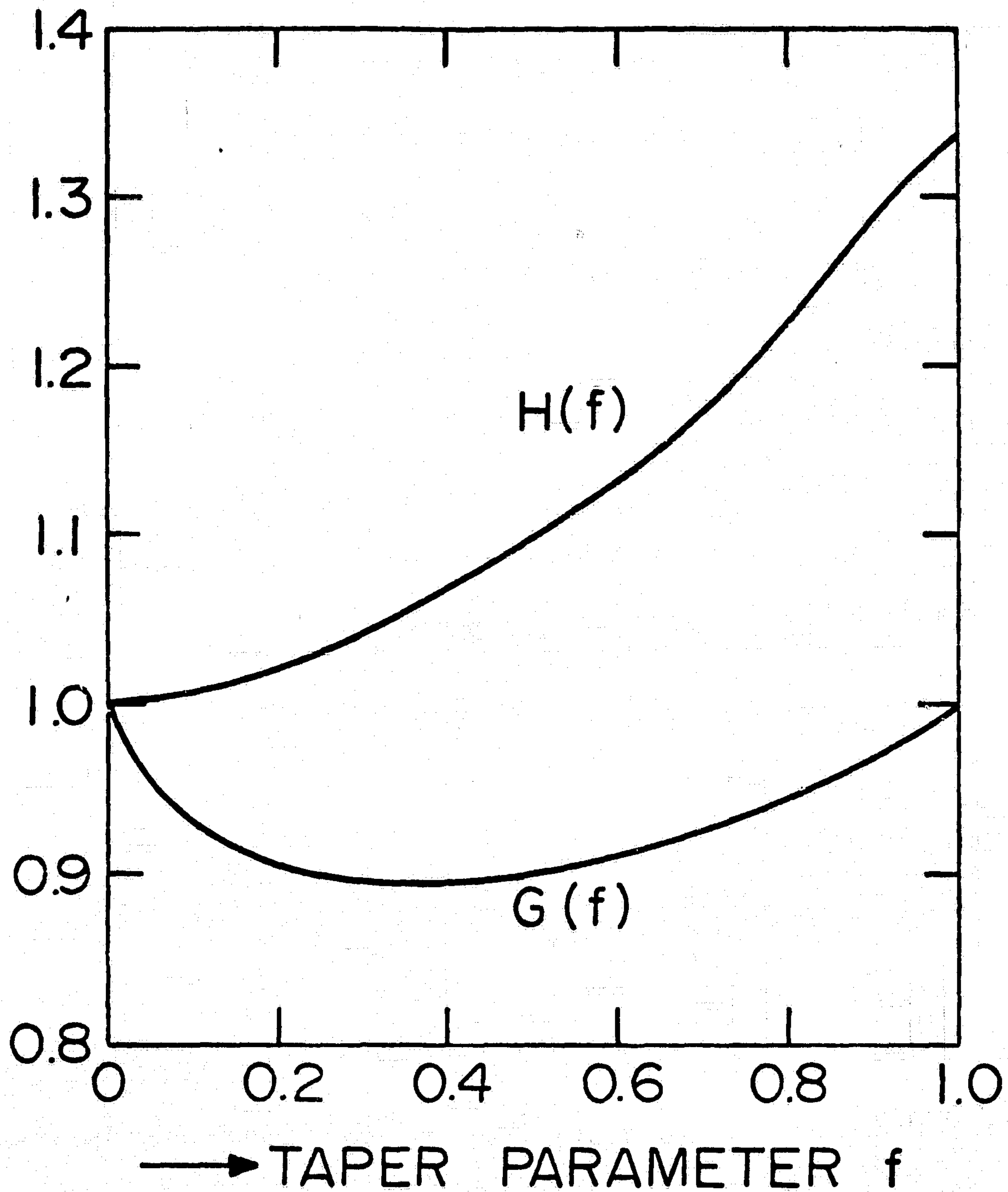

FIG. 10 The values of the voltage drop multipliers G(f) and H(f) as function of f

or:

$$= \frac{1}{x}\left[1 - 1 - \frac{x^2}{3} - \ldots + x + \frac{x^3}{3} + \ldots\right] \qquad (57b)$$

which, for $x \to 0$, becomes unity. Thus, the end-point voltage multiplier for the uniform width grid line is:

$$\lim_{f \to 1} G(f) = 1 \; ; \qquad (58)$$

The values of $G(f)$ for intermediate values of f are shown in Fig. 10.

The incremental power dissipation in the grid line length element $d\ell$, located at value ℓ of the grid line length coordinate, can in similarity to eq. (51), be expressed as:

$$dP = R_{sh} \frac{d\ell}{T_{GL}(\ell)} \left[j_{mp} (W-\ell) \; S \right]^2 \qquad (59)$$

which leads to the total power dissipated in the grid line;

$$P = R_{sh} j_{mp}^{\;2} \frac{S^2 W}{T_{GL}} \int_0^W \frac{(W-\ell)^2 \, d\ell}{fW + 2(1-f)(W-\ell)} \; ; \qquad (60)$$

The integral has the solution:

$$\int_0^W \frac{(W-\ell)^2 \, d\ell}{fW + 2(1-f)(W-\ell)} = \frac{1}{8(1-f)^3} \left[\frac{3}{2} f^2 W^2 + 2fW(1-f)(W-\ell) - 2(1-f)^2 (W-\ell)^2 - f^2 W^2 \ln \left[fW + 2(1-f)(W-\ell) \right] \right] \Bigg|_0^W \qquad (61)$$

which results in the total dissipated power in the grid line:

$$P = R_{sh} j_{mp}^{\;2} \frac{S^2 W^3}{8 T_{GL}} \frac{1}{(1-f)^3} \left[2 - 6f + 4f^2 + f^2 \ln \left(\frac{2-f}{f} \right) \right] \; ; \qquad (62)$$

Since the dissipated power can also be expressed by the product of the total current flowing out of the grid line and an "effective voltage drop" $V_{eff}(f)$:

$$P = j_{mp} \cdot SW \cdot V_{eff}(f) \quad ; \qquad (63)$$

comparing this relationship with eq. (62) leads to the expression for $V_{eff}(f)$:

$$V_{eff}(f) = R_{sh} j_{mp} \frac{SW^2}{4T_{GL}} \cdot H(f) \quad ; \qquad (64)$$

with:

$$H(f) = \frac{1}{2(1-f)^3} \left[2 - 6f + 4f^2 + f^2 \, \ell n \left(\frac{2-f}{f} \right) \right] \quad ; \qquad (64a)$$

When f goes towards zero, the third term in the bracket of eq. (64 a) approaches zero, as shown in the discussion relating to eq. (55), and the effective voltage drop multiplier becomes:

$$\lim_{f \to 0} H(f) = 1 \quad ; \qquad (65)$$

When f approaches unity, 1-x is suitably substituted for f in eq. (64a), with x>0, so that:

$$\lim_{f \to 1} H(f) = \tfrac{1}{2} \lim_{x \to 0} \frac{1}{x^3} \left[2 - 6(1-x) + 4(1-x)^2 + (1-x)^2 \, \ell n \left(\frac{1+x}{1-x} \right) \right] ; \qquad (66)$$

Consolidating the first three terms in the bracket of eq. (66), and expressing the logarithm by an infinite series, yields:

$$\lim_{f \to 1} H(f) = \tfrac{1}{2} \lim_{x \to 0} \frac{1}{x^3} \left[-2x + 4x^2 + (1-2x + x^2)\ 2(x + \frac{x^3}{3} + \frac{x^5}{5} + \ldots) \right]; \tag{67}$$

Equation (67) reduces to:

$$\lim_{f \to 1} H(f) = \tfrac{1}{2} \lim_{x \to 0} \left[\frac{8}{3} - \frac{4}{3}x + \frac{4}{5}x^2 - \frac{4}{5}x^3 + - \ldots \right] = \frac{4}{3}, \tag{68}$$

Thus, the effective voltage drop for the fully tapered grid line is $\tfrac{1}{2}$ of the end-point voltage drop, that of the uniform width grid line $\frac{2}{3}$ of the end-point voltage drop. The end-point voltage drops are equal for these two cases, and it may be remembered that the grid lines have been made to shade equal areas.

Values for the effective voltage drop multiplier $H(f)$ for intermediate values of f are presented in Fig. 10. It is seen that $H(f)$ increases monotonically from $H(0) = 1$ to $H(1) = 1.333$.

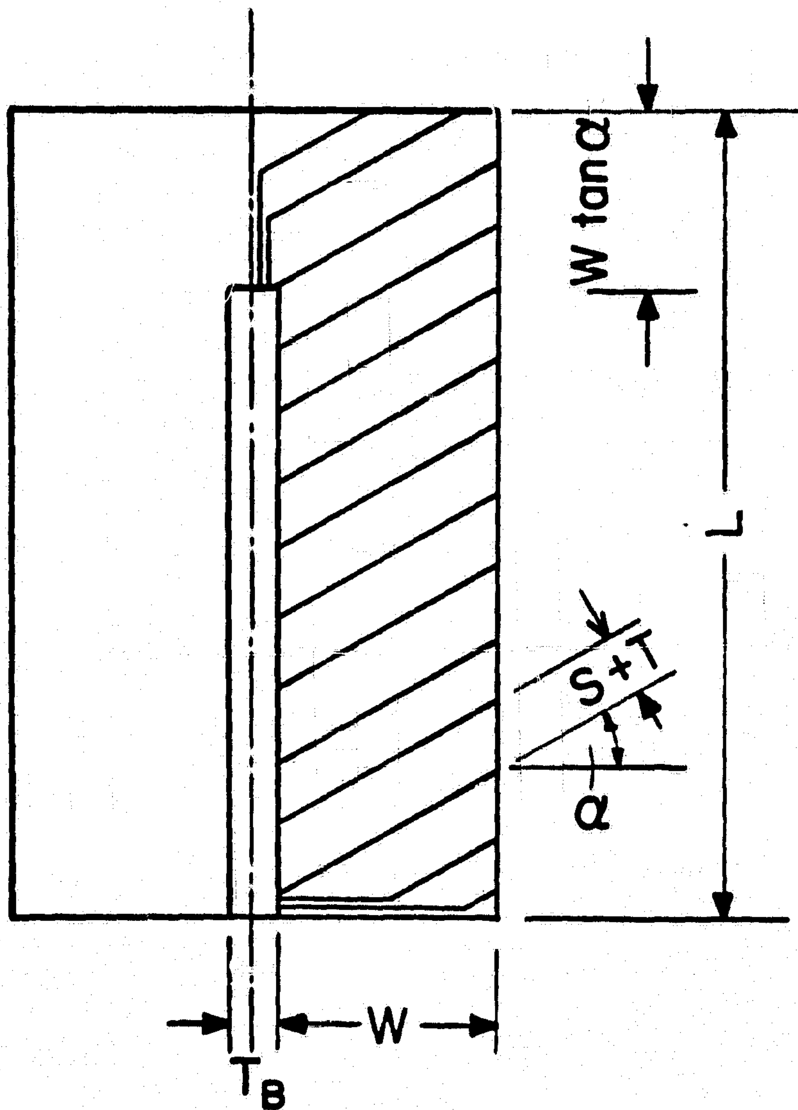

FIG. 11 Oblique grid line arrangement on half of a unit field around a bus line. The grid line inclination angle is α, the bus line length L-W tanα.

VI. Oblique versus Normal Grid Lines

A question which does not have an obvious answer concerns possible advantages which an oblique arrangement of the grid lines relative to the bus lines might have over a normal arrangement. The only way to answer this question is through an analytical evaluation. In this evaluation, the total performance losses incurred with either of the arrangements, that is the voltage drops incurred and the area covered by metal, are the quantities to be analyzed. The voltage drops of concern are those in the front layer, usually a diffused semiconductor sheet, in the grid lines, and in the bus lines.

The analysis shall be based on a unit field of the solar cell. This unit field is defined as the area of a solar cell from which current flows into a single bus line. The pattern of this unit field is repeated periodically on the cell. For the purposes of the considerations here, the size of the unit field is constant, having been determined in a separate design process. The inclination angle α of the grid lines (Fig. 11) is measured against the normal to the bus line. The voltage drop in the front layer which is caused by the charge carrier flow to the nearest grid line, is given by:

$$\Delta V_{FL} = j \cdot \frac{S}{2} \cdot W \frac{1}{\cos\alpha} \cdot \frac{1}{2} R_{sh,FL} \cdot \frac{S}{2} \cdot \frac{\cos\alpha}{W} ; \qquad (69)$$

where $R_{sh,FL}$ is the sheet resistance of the front layer, usually a semiconducting sheet generated by diffusion or ion implanation.

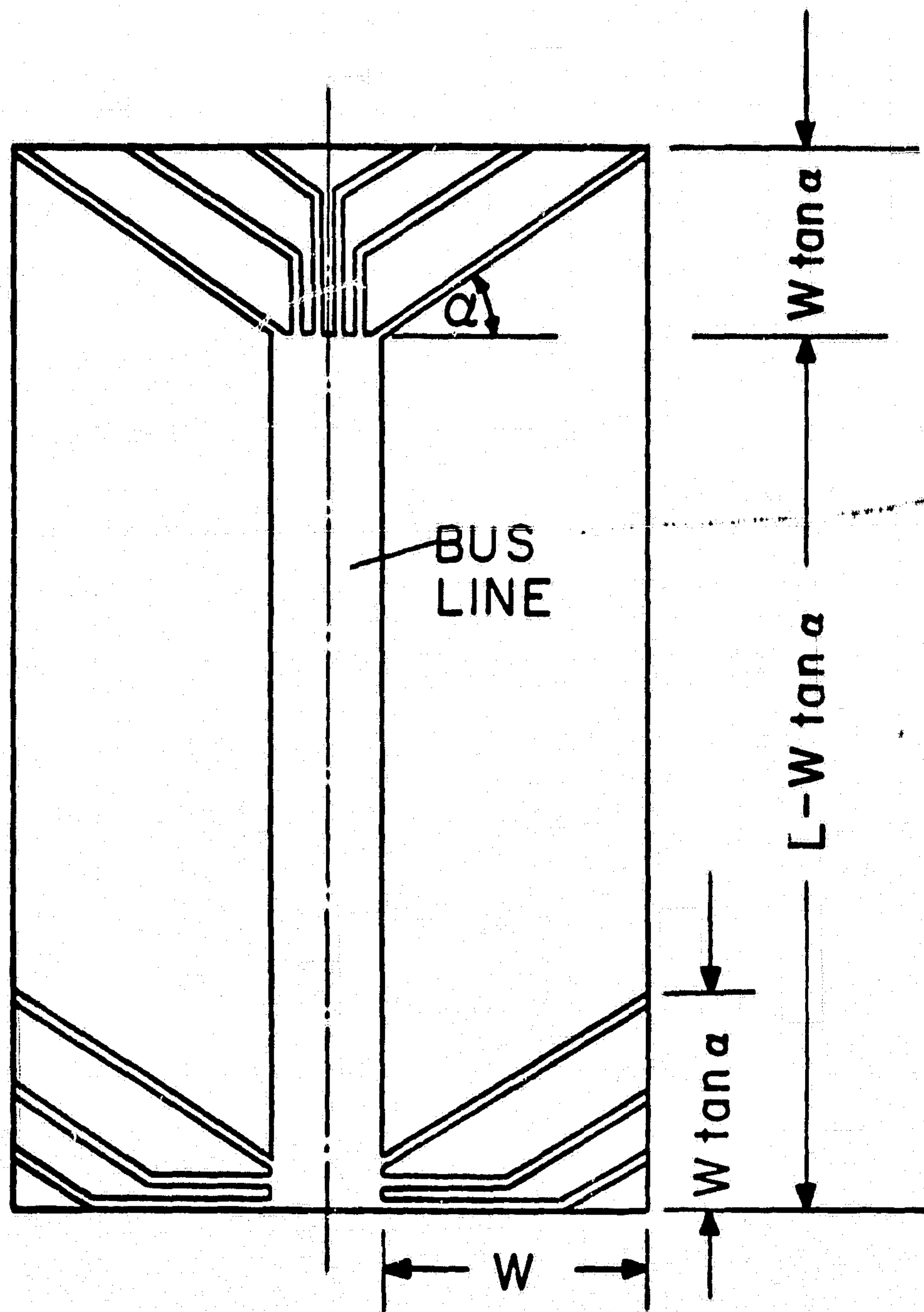

FIG. 12 Illustration of the 4 end triangles on the unit field which contain the grid lines of less than full length

As evident, the angle dependence in this relationship falls out, so that eq. (69) reduces to the front layer voltage drop for any grid line arrangement:

$$\Delta V_{FL} = \frac{1}{8} j \, R_{sh,FL} \quad S^2 \quad ; \tag{70}$$

It may be noted that eq. (70) expresses the end-point voltage drop, and that the effective voltage drop will be two thirds of the value of the end-point voltage drop, in accordance with the discussions of the preceding section.

Next to be considered is the voltage drop in the grid lines, which is given by:

$$\Delta V_{GL} = j \; S \; W \frac{1}{\cos\alpha} \frac{1}{2} R_{sh,GL} \frac{W}{\cos\alpha} \cdot \frac{1}{T_{GL}} \; ; \tag{71}$$

This relationship, again expressing the end-point voltage drop, yields an inverse proportionality of the voltage drop to the square of the cosine of the inclination angle:

$$\Delta V_{GL} = \frac{1}{2} j \; R_{sh,GL} \cdot \frac{S}{T_{GL}} \cdot \frac{W^2}{\cos^2\alpha} \; ; \tag{72}$$

Of final concern among the voltage drops is that in the bus line. Because of the oblique arrangement of the grid lines, it should not be necessary to extend the bus line over the whole length L of the cell (Fig. 12). In fact, it might be hoped that additional losses incurred by the oblique arrangement of the grid lines could be, at least in part, compensated through the reduced length of the bus line. Thus, this length is chosen so that the bus line extends just far enough to

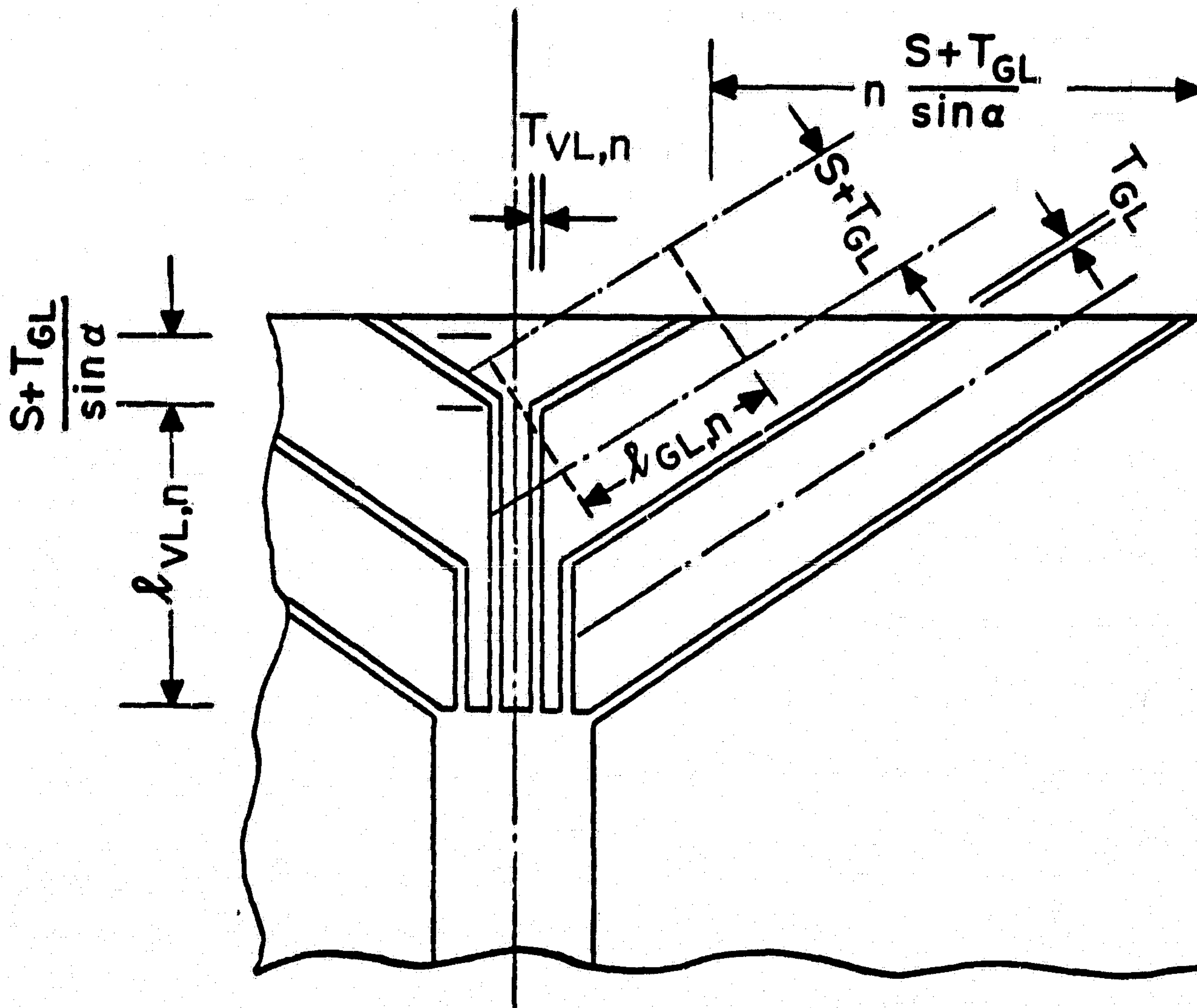

FIG. 13 Sketch of one of the two triangles at the far end of the bus line, with explanation of the geometric relationships

connect with the last full-length grid line on the unit field. A separate arrangement will be made for connecting the remaining grid lines which have less than full length. The voltage drop in the bus line is given by the definite integral:

$$\Delta V_{BL} = j \frac{R_{sh,B}}{T_{BL}} \int_{L-W\tan\alpha}^{0} (W^2 \tan\alpha + Wx)\, dx \qquad (73)$$

Solving the integral and consolidating terms leads to the form:

$$\Delta V_{BL} = \frac{1}{2} R_{sh,BL}\, j \; \frac{L\,W}{T_{BL}} \frac{S}{S + T_{GL}} \left[L - W \tan\alpha \right] ; \qquad (74)$$

For consideration of the grid lines in the triangular end portions of the unit field, only the grid lines of less than full length are of interest, which means of length less than given by $W/\cos\alpha$. Four triangles are of concern here, two each of which are symmetrically arranged around the center line of the unit field (Fig. 12). One of these pairs is located at the far end of the unit field, that is beyond the end of the bus line. The other pair is located near the base of the bus line where normally the interconnection to the next cell will be made.

For the far-end triangle, the length $\ell_{GL,n}$ of the n-th grid line is defined according to Fig. 13 as:

$$\ell_{GL,n} = (W \tan\alpha - \ell_{VL,n}) \frac{1}{\sin\alpha} ; \qquad (75)$$

with n counting from the last grid line of full length. The length $\ell_{VL,n}$ of the corresponding vertical connecting line

is given by:

$$\ell_{VL,n} = n(S + T_{GL}) \frac{1}{\cos\alpha} ; \tag{76}$$

The maximum number n_{max} of grid lines of less than full length in this triangle is then:

$$2n_{max} + 1 = 2 \frac{W \tan\alpha \cos\alpha}{S+T_{GL}} ; \tag{77}$$

This relationship, however, would truly apply only if the right hand side were an integer. The proper value for n_{max} will be obtained by truncating to the next lower integer value from that given by one half of the right hand side of eq. (77)

$$n_{max} = \frac{W \sin\alpha}{S+T_{GL}} \Big|_{\text{truncate to integer}} ; \tag{78}$$

Using this relationship, eq. (75) can be transformed into:

$$\ell_{GL,n} = (n_{max} - n) \frac{S + T_{GL}}{\sin\alpha \cos\alpha} ; \tag{79}$$

The total current contributed by each grid line is then determined by:

$$I_n = S \cdot \ell_{GL,n} \cdot j ; \tag{80}$$

which, by use of eq. (79), takes the form:

$$I_n = (n_{max} - n) \frac{S(S + T_{GL})}{\sin\alpha \cos\alpha} j ; \tag{81}$$

The grid lines of less than full length need to be connected to the bus line which ends at the distance $W \cdot \tan\alpha$ from the far end of the unit field. These connections shall be accomplished

by lines which form extensions of the bus line (running in the same direction as the bus line) and have the length $\ell_{VL,n}$ given by eq. (76), and the width $T_{VL,n}$. The voltage drop $\Delta V_{GL,FT}$ in the total grid line of the far triangle, including the inclined grid line portion and the connection to the bus line, is then given by:

$$\Delta V_{GL,FT} = j \frac{(n_{max} - n)\, S(S + T_{GL})}{\sin\alpha \cos\alpha} \left\{ \frac{1}{2} \frac{R_{sh,GL}}{T_{GL}} \ell_{GL,n} + \frac{R_{sh,GL}}{T_{VL,n}} \ell_{VL,n} \right\}; \tag{82}$$

T_{GL} refers to the width of the inclined portions of the grid lines which has been maintained constant for all grid lines on the cell. By use of eq. (75) and (76), eq. (82) can be transformed into:

$$\Delta V_{GL,FT} = j\, R_{sh,GL} \frac{S(S + T_{GL})}{\sin\alpha \cos\alpha} (n_{max} - n) \left\{ \frac{(n_{max} - n)(S + T_{GL})}{2\, T_{GL} \sin\alpha \cos\alpha} + \frac{n(S + T_{GL})}{T_{VL,n} \cos\alpha} \right\}; \tag{83}$$

Since all the grid lines of the far triangle are connected to the bus line at the same point, they shall be designed to have an identical voltage drop ΔV_{GL}, which shall be equal to that obtained from application of eq. (71). Equation (83) can then be solved for the width $T_{VL,n}$ of the connecting portion of the grid line:

$$T_{VL,n} = \frac{2T_{GL}\, n(n_{max} - n) \sin\alpha}{\dfrac{2\Delta V_{GL,FT}\, T_{GL} \sin^2\alpha \cos^2\alpha}{jR_{sh,GL}\, S(S + T_{GL})^2} - (n_{max} - n)^2}; \tag{84}$$

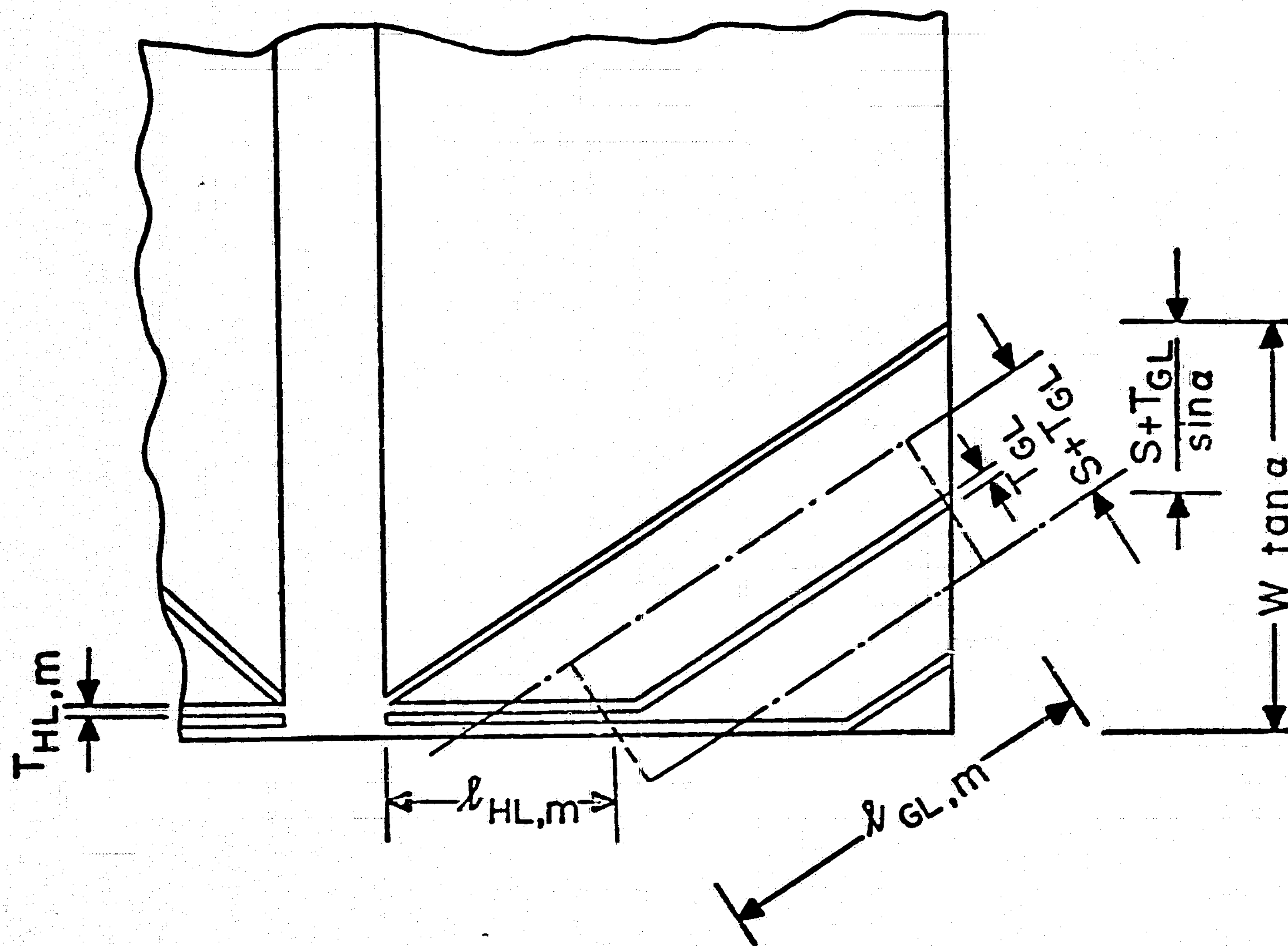

FIG. 14 Sketch of one of the two triangles at the near end of bus line, with explanations of the geometric relationships

Similar considerations are performed for the near-end triangle. In this triangle, there are $m_{max} = n_{max}$ inclined grid lines of less than full length. The length $\ell_{GL,m}$ of the m-th grid line is determined by:

$$\ell_{GL,m} = \frac{W - \ell_{HL,m}}{\cos\alpha} ; \quad (85)$$

These grid lines also do not meet the bus line, unless a special connection is made. Here, the connecting lines run normal to the bus line, along the near edge of the solar cell (Fig. 14). This connecting line has the length $\ell_{HL,m}$:

$$\ell_{HL,m} = m \frac{S + T_{GL}}{\sin\alpha} ; \quad (86)$$

Using eq. (85), (86), and (78), the grid line length can be expressed as:

$$\ell_{GL,m} = (m_{max} - m) \frac{S + T_{GL}}{\sin\alpha \cos\alpha} ; \quad (87)$$

in complete analogy to $\ell_{GL,n}$ of eq. (79). Again, a voltage drop for the grid line plus the connecting line is obtained, and again the voltage drop is considered the independent variable, from which the width $T_{HL,m}$ of the connecting line is determined. Thus, for the connecting line between the m-th grid line and the bus line, the width is:

$$T_{HL,m} = \frac{2 \, T_{GL} \, m(m_{max} - m) \cos\alpha}{\dfrac{2\Delta V_{GL,NT} \, T_{GL} \sin^2\alpha \cos^2\alpha}{j \, R_{sh,GL} \, S(S + T_{GL})^2} - (m_{max} - m)^2} ; \quad (88)$$

It should be noted, that the ΔV_{GL} values used in eq. (84) and (88) are the end-point voltage drops, which are obtainable from the desired effective voltage drops through the shape multiplier discussed in the preceding section.

With all the line dimensions determined, the question of the area coverage by metal can now be attacked. The total number k_{GL} of grid lines to be used, that is full-length lines and partial length lines added together to make full length, is:

$$k_{GL} = \frac{L}{(S + T_{GL})/\cos\alpha} ; \qquad (89)$$

and the area of each of these k_{GL} grid lines is given by:

$$A_{GL,k} = T_{GL} \cdot \ell_{GL} = \frac{T_{GL}\ W}{\cos\alpha} ; \qquad (90)$$

Thus, the total area covered by all grid lines is:

$$A_{GL} = \frac{2\ L\ W\ T_{GL}}{(S + T_{GL})} ; \qquad (91)$$

Equation (91) shows that the area covered is independent of the angle of the grid lines, as long as their width T_{GL} and their normal spacing S are maintained constant. However, constant width T_{GL}, independent of the grid line inclination angle α, results in a varying voltage drop according to eq. (71).

The area covered by the bus wire is expressed by:

$$A_{BL} = (L - W \tan\alpha)\ T_{BL} ; \qquad (92)$$

and the total area covered by the connecting lines in the triangles is determined by:

$$A_{CL} = \sum_{n=1}^{n_{max}} \left(T_{VL,n} \; n \frac{S + T_{GL}}{\cos\alpha} \right) + \sum_{m=1}^{m_{max}} \left(T_{HL,m} \; m \frac{S + T_{GL}}{\sin\alpha} \right); \quad (93)$$

A numerical example shall be used to demonstrate the application of the relationships developed, and to illustrate the impact of oblique arrangements of the grid lines. The unit field shall have the width $W = 2$ cm, and may be a part of a square solar cell of dimension $L = 10$ cm. The grid line spacing shall be $S = 1.96$ mm, and the grid line width $T_{GL}=40$ μm, so that the area coverage by grid lines is 0.80 cm^2. The sheet resistance $R_{sh,FL}$ of the front layer shall be 35 Ω. and that of the grid lines $R_{sh,GL} = 1.7 \cdot 10^{-3}$Ω, corresponding to 10 μm thick copper conductors. The current density shall be $j = 0.03$ A cm^{-2}. Applying eq. (70), the end-point voltage drop obtained for the front layer is 5.04 mV. Using eq. (72) yields an end-point voltage drop of 5 mV over the grid lines arranged normal to the bus line. For a grid line inclination angle of 30°, the grid line voltage drop would be 33% greater, or 6.67 mV. To maintain the voltage drop equal to that of the normal grid line case, the width of the grid lines could be corrected to $T_{GL} = 53.3$ μm, for an area coverage of 1.066 cm^2.

The bus line voltage drop is obtained from eq. (74). In order to make this end-point voltage drop also 5 mV, a bus line width T_{BL} of 0.36 mm is obtained for the case of normally arranged grid lines, assuming that the bus line is a copper wire of circular cross section. The bus line area coverage is 0.36 cm^2. To obtain the same voltage drop for the slightly shorter bus line to be used with the grid lines

of 30° inclination angle, the bus wire diameter needs to be only $T_{BL} = 0.34$ mm, and the area coverage 0.30 cm^2. Still needed is the determination of the lines in the triangles for the case of 30° inclination of the grid lines. Equation (91) includes the area coverage by the grid lines of less than full length, and application of eq. (76), (84), (86), (91), and (93) yields an area coverage of $0.88 \cdot 10^{-2}$ cm^2 and $2.66 \cdot 10^{-2}$ cm^{-2} for the connecting lines in the far and near triangles, respectively. Summing up the area coverage contributions for the normally arranged grid lines, the total area covered by metal is found to be 1.16 cm^2, or 2.9% of the unit-field area. In contrast, for the grid lines inclined under a 30° angle to the bus line, the total area covered by metal amounts to 1.40 cm^2, or 3.5% of the unit-field area, for the condition of equal total voltage drop from all contributions. This area coverage is 20% greater than that in the case of normally arranged grid lines. This additional area coverage amounts to a loss of 0.60% of the power output of the solar cell, or about one tenth of a percentage point in efficiency, incurred solely from the inclined arrangement of the grid lines.

The preceding result thus leads to the clear conclusion that normally arranged grid lines are to be used, if the power output from the solar cell is to be optimized. On the other hand, the loss of power output is not large for small inclination angles.

VII. Grid and Bus Line Pattern Optimization

The task of a grid and bus line pattern optimization is to minimize the power loss connected with the various series resistance elements of the front region (usually the diffused layer) and the front contact structure. These losses consist of the series resistance voltage drops as well as the partial shading of the front surface of the solar cell by metal which is used to reduce these series resistance losses. As was shown in Section III, the power output of a real solar cell, with series resistance, can be well approximated by the power output of the ideal cell without series resistance, minus the power dissipated in the various resistive elements. It has also been shown that a higher power output can be obtained by rematching the cell to a slightly lower maximum power point current than found for the ideal cell, but that the improvement in power output is, for most practical purposes, negligibly small.

The power output for the ideal solar cell of total area A_{tot} and of light-sensitive area A_{eff} can be approximately described by:

$$P = j\ A_{tot}\ V_d = j_o\ A_{tot}\ (e^{\frac{qV_d}{kT}} - 1)\ V_d - j_L A_{eff}\ V_d\ ; \qquad (94)$$

where V_d refers to the voltage appearing across the pn-junction itself ("diode voltage"!). The maximum power output available can be found from setting the derivative of the power output with respect to the junction voltage, equal to zero:

$$\frac{dP}{dV_d} = 0 = j\ B e^{BV_{d,mp}}\ V_{d,mp} + j_o\ (e^{BV_{d,mp}} - 1) - j_L \frac{A_{eff}}{A_{tot}}\ ; \tag{95}$$

where as before:

$$\frac{q}{kT} = B \tag{95a}$$

Equation (95) can be transformed into an expression for the exponential term as function of the light generated current j_L, the saturation current j_o, and the maximum power point voltage across the pn-junction $V_{d,mp}$:

$$e^{BV_{d,mp}} = \frac{j_L \frac{A_{eff}}{A_{tot}} + j_o}{j_o} \quad \frac{1}{BV_{d,mp} + 1}\ ; \tag{96}$$

The maximum power point current j_{mp} can be approximately described by the commonly used solar cell equation:

$$j_{mp}\ A_{tot} = j_o\ A_{tot}\ (e^{BV_{d,mp}} - 1) - j_L\ A_{eff}\ ; \tag{97}$$

Equation (97) with the same approximation discussed in connection with eq. (94) gives the current which flows out of the solar cell when the voltage $V_{d,mp}$ appears across the pn-junction.

Equations (94) and (97) represent an idealized current-voltage characteristic which, however, adequately describes the real characteristics near the maximum power point in very well designed and fabricated solar cells in normal solar cell operation. For cells of lower quality, a second exponential term should be included to describe the depletion region recombination current. In addition, current flow through a shunt

resistance is often observed, and there can be other spurious current components, which all represent unnecessary losses. They are, however, usually omitted from maximum power calculations. In addition, under high-level injection conditions, deviations from the simple exponential characteristics of eq. (94) and (97) can occur.

Using eq. (96), eq. (97) can be transformed to:

$$j_{mp} = (j_L \frac{A_{eff}}{A_{tot}} + j_o) \frac{1}{BV_{d,mp} + 1} - j_o - j_L \frac{A_{eff}}{A_{tot}} ; \qquad (98)$$

which can be simplified to the form:

$$j_{mp} = - \frac{V_{d,mp}}{V_{d,mp} + \frac{1}{B}} (j_L \frac{A_{eff}}{A_{tot}} + j_o) ; \qquad (99)$$

Since the saturation current density j_0 is usually many orders of magnitude smaller than the light generated current density j_L, eq. (99) can be well approximated by:

$$j_{mp} \simeq - \frac{V_{d,mp}}{V_{d,mp} + \frac{1}{B}} j_L \frac{A_{eff}}{A_{tot}} ; \qquad (99a)$$

Using eq. (99), the maximum power output of the solar cell with zero series resistance can be written as:

$$P_{d,mp} = V_{d,mp} j_{mp} A_{tot} = - V_{d,mp} \cdot \frac{V_{d,mp}}{V_{d,mp} + \frac{1}{B}} \cdot j_L \left(\frac{A_{eff}}{A_{tot}} + \frac{j_o}{j_L} \right) A_{tot} ; \qquad (100)$$

which can be approximated by:

$$P_{d,mp} \simeq - j_L \frac{V_{d,mp}}{V_{d,mp} + \frac{1}{B}} A_{eff} ; \qquad (100a)$$

In a real solar cell which experiences voltage drops

due to finite resistance components, the terminal voltage V_t will differ from the voltage across the junction V_d by the total voltage drop ΔV_R:

$$V_t = V_d + \Delta V_R; \tag{101}$$

Rewriting this relationship for the maximum power point voltage yields:

$$V_{t,mp} = V_{d,mp} + \Delta V_{R,mp}; \tag{102}$$

The voltage drop $\Delta V_{R,mp}$ consists of a number of individual voltage drops across the various series resistance components which occur in the path of the current flow through the solar cell. In the ideal case, these voltage drops can be expressed according to Ohm's law by an equivalent series resistance value for each individual effect, multiplied by the total current flowing through the device:

$$\Delta V_{R,mp} = \sum_{i=1}^{N_R} \Delta V_{i,mp} = I_{mp} \sum_{i=1}^{N_R} R_{s,i} ; \tag{103}$$

The maximum power output $V_{t,mp}$ from the terminals of the real solar cell with finite series resistance can then be expressed as:

$$P_{t,mp} = V_{t,mp} \cdot j_{mp} \cdot A_{tot}; \tag{104}$$

and, after inserting eq. (100) and (102) as:

$$P_{t,mp} = -(V_{d,mp} + V_{R,mp}) \frac{V_{d,mp}}{V_{d,mp} + \frac{1}{B}} j_L \left(\frac{A_{eff}}{A_{tot}} + \frac{j_o}{j_L} \right) A_{tot}; \tag{105}$$

Expressing the light-exposed area through the total area and the area covered by metal (shaded area) A_{shade} according to:

$$A_{eff} = A_{tot} - A_{shade} ; \quad (106)$$

permits writing eq. (105) as:

$$P_{t,mp} = P_{d,mp,id} + \frac{V_{d,mp}^2}{V_{d,mp} + \frac{I}{B}} j_L A_{shade} + \Delta V_{R,mp} j_{mp} A_{eff} ; \quad (107)$$

where $P_{d,mp,id}$ stands for the ideal maximum power output with $A_{eff} = A_{tot}$.

Equation (107) represents the form:

$$P_{t,mp} = P_{d,mp,id} + \Delta P_R = P_{d,mp,id} \left(1 + \frac{\Delta P_R}{P_{d,mp,id}}\right) ; \quad (108)$$

It may be noted that $P_{t,mp}$, $P_{d,mp,id}$, and $\Delta V_{R,mp}$ are negative quantities in solar cell operation, according to eq. (99) (100), (103), and (104). Equation (105) thus describes the power output of the real solar cell by the power output of the ideal solar cell reduced by the power losses related to series resistance, ΔP_R. Only the relative power loss $\frac{\Delta P_R}{P_{d,mp}}$ is of interest for the further discussions, which therefore concentrate on minimizing this relative power loss. This relative power loss is represented by:

$$\frac{\Delta P_R}{P_{d,mp,id}} = \frac{A_{shade}}{A_{tot}} \frac{1}{1 + \frac{j_o}{j_L}} - \frac{\Delta V_{R,mp}}{V_{d,mp}} \frac{\frac{A_{eff}}{A_{tot}} + \frac{j_o}{j_L}}{1 + \frac{j_o}{j_L}} ; \quad (109)$$

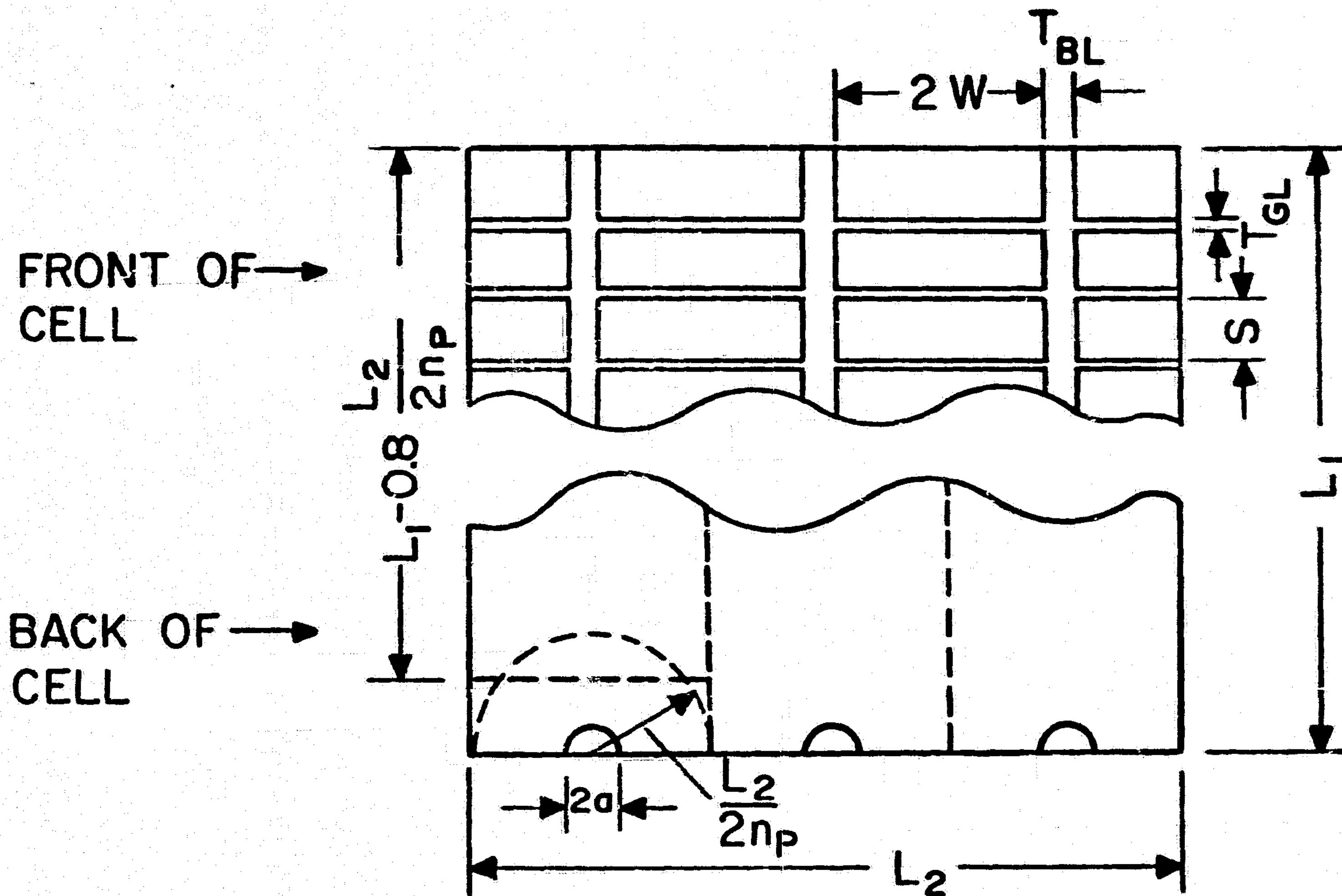

FIG. 15 Illustration of the nomenclature used in the analysis of the front metallization pattern

which is derived from eq. (107) by use of eq. (100). Neglecting second or higher order terms in the small quantities, eq. (109) is readily re-expressed as:

$$\frac{\Delta P_R}{P_{d,mp,id}} \simeq \frac{A_{shade}}{A_{tot}} - \frac{\Delta V_{R,mp}}{V_{d,mp}} ; \tag{110}$$

which contains one term each representing the relative voltage loss and the relative area loss.

Following the nomenclature of Fig. 15, the total area can be expressed as:

$$A_{tot} = L_1 L_2 ; \tag{111}$$

and the shaded area as:

$$A_{shade} = n_{GL} \, T_{GL} \, W \cdot 2n_{BL} + n_{BL} \, T_{BL} \, L_1 ; \tag{112}$$

where the number of grid lines n_{GL} is given by:

$$n_{GL} = \frac{L_1}{S + T_{GL}} ; \tag{113}$$

and the number of bus lines n_{BL} by:

$$n_{BL} = \frac{L_2}{2W + T_{BL}} ; \tag{114}$$

Thus, the shaded area according to eq. (112) can be expressed as:

$$A_{shade} = L_1 L_2 \frac{2W}{2W + T_{BL}} \left(\frac{S}{S + T_{GL}} \; \frac{T_{GL}}{S} + \frac{T_{BL}}{2W} \right) ; \tag{115}$$

Since, for a well designed solar cell, the effective area differs from the total area only by a few percent, the second

order terms in eq. (115) can be neglected, as they have been in eq. (109), so that the shaded area can be approximated by:

$$A_{shade} \approx L_1 L_2 \left(\frac{T_{GL}}{S} + \frac{T_{BL}}{2W} \right) ; \qquad (115a)$$

The contribution $\Delta V_{R,mp,F}$ of the front layer and the front contact structure to the $\Delta V_{R,mp}$ consists of the effective voltage drops (see section "Oblique versus normal grid lines" of this report) in the three major elements through which the current flows:

$$\Delta V_{R,mp,F} = j_{mp} \Big\{ \underbrace{R_{sh,FL} \frac{\frac{S}{2}}{W} \frac{1}{2} \frac{S}{2} W \cdot G_{FL}(f) \frac{1}{2} H_{FL}(f)}_{\text{Front Layer}}$$

$$+ \underbrace{R_{sh,GL} \cdot \frac{W}{T_{GL}} \cdot \frac{1}{2} \cdot SW \cdot G_{GL}(f) \frac{1}{2} H_{GL}(f)}_{\text{Grid Line}}$$

$$+ \underbrace{R_{sh,BL} \cdot \frac{L_1}{T_{BL}} \cdot \frac{1}{2} \cdot 2n_{GL} \cdot SW \cdot G_{BL}(f) \frac{1}{2} H_{BL}(f)}_{\text{Bus Line}} \Big\} \qquad (116)$$

As the front layer is, for all parallel-grid line systems, of uniform width, it is practical to express $\Delta V_{R,mp,F}$ relative to uniform width elements by use of a "shape factor" δ. This factor is unity for uniform width elements and decreases monotonically to $\frac{3}{4}$ for increasingly tapered elements covering equal area. δ is thus defined as:

$$\delta = \frac{G(f)\ H(f)}{G(1)\ H(1)} = \frac{3}{4} G(f)\ H(f) ; \qquad (117)$$

Equation (116) then reduces to:

$$\Delta V_{R,mp,F} = \frac{1}{3} j_{mp} \left\{ R_{sh,FL} \left(\frac{S}{2}\right)^2 \delta_{FL} + R_{sh,GL} \frac{S}{T_{GL}} W^2 \delta_{GL} + R_{sh,BL} \frac{S}{S + T_{GL}} \frac{2W}{T_{BL}} L_1^2 \delta_{BL} \right\} ; \tag{118}$$

Again neglecting terms expressing second order effects, and introducing:

$$x = \frac{T_{GL}}{S} ; \tag{119a}$$

$$y = \frac{T_{BL}}{2W} ; \tag{119b}$$

gives, from eq. (110), (118), and (119a and b):

$$\frac{\Delta P_R}{P_{d,mp}} \approx x + y - \frac{1}{3} \frac{j_{mp}}{V_{d,mp}} \left\{ R_{sh,FL} \left(\frac{S}{2}\right)^2 \delta_{FL} + R_{sh,GL} \frac{1}{x} W^2 \delta_{GL} + R_{sh,BL} \frac{1}{y} L_1^2 \delta_{BL} \right\} ; \tag{120}$$

Differentiating eq. (120) with respect to x and setting equal to zero to find the extrema, yields:

$$\frac{d \frac{\Delta P_R}{P_{d,mp}}}{dx} = 0 = 1 + \frac{1}{x^2} \frac{1}{3} \frac{j_{mp}}{V_{d,mp}} R_{sh,GL} W^2 \delta_{GL} ; \tag{121}$$

or:

$$\frac{T_{GL}}{S} = W \left(\frac{1}{3} \frac{|j_{mp}|}{V_{d,mp}} R_{sh,GL} \delta_{GL} \right)^{\frac{1}{2}} ; \tag{122}$$

Carrying the derivation out from the full relationships yields practically the same result as given in eq. (122) since the second order terms cancel each other in the process, so that only the higher order terms would enter the final relationship.

Taking the derivative of eq. (120) with respect to y yields the corresponding relationship:

$$\frac{T_{BL}}{2W} = L_1 \left(\frac{1}{3} \; \frac{|j_{mp}|}{V_{d,mp}} \; R_{sh,BL} \; \delta_{BL} \right)^{1/2} ; \qquad (123)$$

Equations (122) and (123) give the optimum grid line width and bus line width, but expressed relative to the spacing S between adjacent grid lines and 2W between adjacent bus lines, respectively. These expressions are valid when the grid and bus lines are metal layers of given sheet resistances $R_{sh,GL}$ and $R_{sh,BL}$, respectively.

It is important to note that eq. (122) and (123) represent only an expression of the optimum design compromise between shading and voltage drop for the grid lines alone and the bus lines alone, respectively, as eq. (120) and (121) indicate. The optimum design is still dependent on the grid line spacing, which determines the voltage drop from current flow within the semiconducting front layer, as described by the first term in the brackets of eq. (120). Clearly, the total voltage drop and shading are minimized for S=0, with the grid line shading T_{GL}/S held constant according to eq. (122). Similarly, the grid line voltage drop (second term in brackets in eq. (120) is minimized

when the bus line spacing 2W approaches zero, again holding the bus line shading $T_{BL}/2W$ constant. In reality, there is no need to go this far in reducing the spacings, as other losses, such as the shadings and the bus line voltage drops, remain constant. Thus, it is adequate to reduce S and W to the level at which the losses controlled by these two quantities become insignificant relative to the constant losses.

For the grid lines, this approach may still result in a grid line width T_{GL}, which is difficult to produce. Then, in practice, the metallization designer will select the smallest grid line width $T_{GL,pract}$ which can be cost-effectively produced, considering process costs and yields as well as differences in solar cell value consequent to the efficiency differences, which result from the metallization design variations.

When such a lower limit is set on the grid line width, the determination of an optimum shading ratio according to eq. (122) is no longer appropriate. By using a grid line shading ratio larger than the optimal value obtained from eq. (122), the relative front layer sheet voltage drop can be considerably reduced, since it is proportional to S^2. In fact, when the grid line width is held constant, eq. (120) can be optimized with respect to the grid line spacing S. Setting the derivative of eq. (122) with respect to S equal to zero, yields:

$$S^3 + 2 \frac{R_{sh,GL}}{R_{sh,FL}} \frac{W^2}{T_{GL,pract}} S^2 - \frac{6 V_{d,mp}}{|j_{mp}|} \frac{T_{GL,pract}}{R_{sh,FL}} = 0; \quad (124)$$

The solution of a cubic equation is generally cumbersome. However, if:

$$\frac{R_{shGL}^3}{R_{sh,FL}^2} << \frac{|j_{mp}|}{V_{d,mp}} \frac{T_{GL,pract}^4}{3^4 (2W)^6}; \quad (125)$$

the following approximate solution is valid:

$$S_{opt} = \left(\frac{6 V_{d,mp}}{|j_{mp}|} \frac{T_{GL,pract}}{R_{sh,FL}}\right)^{1/3} - \frac{2^{4/3}}{3} \frac{R_{sh,GL}}{R_{sh,FL}} \frac{W^2}{T_{GL,pract}}; \quad (126)$$

In many cases, the second term of eq. (126) is small compared to the first.

It may also be noted that the application of bus lines is only indicated when their sheet resistance is significantly lower than that of the grid lines. When the sheet resistances of the two types of lines are equal ($R_{sh,Lines}$), assuming the shape factor δ to be unity, then, with use of the optimum shading ratios T_{GL}/S and $T_{BL}/2W$ according to eq. (122) and (123), respectively, eq. (120) becomes:

$$\frac{\Delta P_{R,mp}}{P_{d,mp}} = \left(\frac{|j_{mp}|}{3 V_{d,mp}} R_{sh,Lines}\right)^{1/2} 2 (L_1 + W) + \frac{|j_{mp}|}{3 V_{d,mp} R_{sh,FL}} \left(\frac{S}{2}\right)^2; \quad (127)$$

It is readily shown that, for a structure containing only grid lines, this time of length L_1, the same relationship as in eq. (127) is obtained, except that W does not appear. Thus, the addition of bus lines is, in this case, detrimental.

This can be demonstrated by the following examples:

For a 10 cm x 10 cm cell with $|j_{mp}| = 0.03$ mA cm^{-2} and $V_{d,mp} = 0.5V$, and a grid line sheet resistance $R_{sh,GL} = 1.7 \cdot 10^{-3}\ \Omega$, corresponding to 10 μm thick lines of copper with bulk resistivity, and without bus lines, the optimum shading ratio T_{GL}/S is 5.83%. At a grid line spacing of 2 mm, and a line width of 117 μm according to the shading ratio, the total series-resistance-connected losses of the front structure amount then to 12.4% of the ideal solar cell output. In this number are contained, outside of the shading, relative voltage drops of 5.83% in the grid lines and 0.7% in the front layer itself. Reducing the grid line width and spacing further, while keeping the shading ratio at its optimum value, would not yield a significant improvement, since the total losses could at most be reduced by 0.7 percentage points, or 5.6% of the total losses.

For a system with bus lines of the same sheet resistance as the grid lines, and all data equal to those of the preceding example, eq. (123) yields a bus line shading ratio of 5.83%. With this, the relative bus line voltage drop according to the fifth term on the right hand side of eq. (120) also becomes 5.83%. Choosing a bus line spacing 2W = 1 cm, the

optimum bus line width is thus 583 μm. With this bus line spacing, the optimum grid line shading would then be, according to eq. (122), 0.29%. With the minimum practical line width taken, for this example, as 20 μm, the grid line spacing S_{opt} would be 6.86 mm. The relative grid line voltage drop, according to the fourth term of eq. (120), is then also 0.29%, and the relative front layer sheet voltage drop, according to the third term of that equation, 8.2%. Thus, the total series-resistance-connected front structure losses are 20.4% of the ideal power output, compared to 12.4% for the grid-line-only structure.

This design, while giving the lowest possible bus line and grid line losses, does not provide the lowest total loss, since a lower practical limit was set for the grid line width. It is readily seen that increasing the shading ratio by a factor of four, that is to 1.17%, which means reducing S to 1.72 mm, decreases the relative front layer sheet voltage drop by a factor of 16, so that the sum of all losses becomes 13.4%, still more than in the grid-line-only case. It may be noted that eq. (126) gives 1.738 mm for the optimum value of S with the chosen value of $T_{GL,pract}$.

As it has been found that the application of bus lines of the same sheet resistance as the grid lines is of no use, and as the front structure losses, even with the lowest practically achievable sheet resistance in deposited metal layers, are near 12% in 10 cm x 10 cm solar cells, the attention will necessarily shift to thicker bus lines, which can yield at

least an order of magnitude lower sheet resistance. This means an overlay of a bulk conductor, such as a copper wire. In this case, T_{BL} becomes equal to the wire diameter, and the "effective sheet resistance" is then:

$$R_{sh,BL} = \rho_{BL} \frac{4}{\pi\, T_{BL}} ; \tag{128}$$

where ρ_{BL} is the resistivity of the bus line (wire) material. Introducing eq. (128) into the fifth term of the right hand side of eq. (120) yields:

$$\frac{\Delta P_{R,mp}}{P_{d,mp}} = \frac{T_{GL}}{S} + \frac{T_{BL}}{2W} + \frac{|j_{mp}|}{3\, V_{d,mp}} \Bigg\{ R_{sh,FL} \left(\frac{S}{2}\right)^2 \delta_{FL} + R_{sh,GL} \frac{S}{T_{GL}} W^2 \delta_{GL} + \frac{4}{\pi} \rho_{BL} \frac{2W}{T_{BL}^{\;2}} L_1^{\;2} \delta_{BL} \Bigg\} ; \tag{129}$$

It may be noted that the use of a wire with constant diameter along its length leads to $\delta_{BL} = 1$, just as a parallel grid line system entails $\delta_{FL} = 1$.

Equation (127) can, in contrast to eq. (120), be optimized for T_{BL} alone, rather than the shading ratio $\frac{T_{BL}}{2W}$, since the bus line sheet resistance is now also a function of T_{BL}. Thus:

$$\frac{d\left(\frac{\Delta P_{R,mp}}{P_{d,mp}}\right)}{d\, T_{BL}} = 0 = \frac{1}{2W} - \frac{|j_{mp}|}{3\, V_{d,mp}} \frac{16}{\pi} \rho_{BL} \frac{W L_1^{\;2}}{T_{BL}^{\;3}} ; \tag{130}$$

which resolves to:

$$T_{BL} = \left(\frac{32}{3\pi} \frac{|j_{mp}|\, \rho_{BL}}{V_{d,mp}} W^2 L_1^{\;2} \right)^{1/3} ; \tag{131}$$

ORIGINAL PAGE IS
OF POOR QUALITY

TABLE IV

DESIGN		OPTIMUM	NEAR OPTIMUM	THIN Cu	Ni	PLATED BUS LINES	NEAR OPTIMUM	SCREEN PRINTED Ag
NO. OF BUS LINES (SPACING)	- (cm)	7 (1.428)	→	→	→	→	3 (3.333)	→
BUS LINE WIDTH (DIAMETER)	mm	0.255 DIA	→	→	→	0.75	0.361 DIA	→
BUS LINE THICKNESS (GAUGE)	μm (B&S)	(30 GA.)	→	→	→	10 (Cu)	(27 GA.)	→
NO. OF GRID LINES (SPACING)	- (mm)	65 (1.53)	→	→	→	→	40 (2.50)	→
GRID LINE WIDTH	μm	12.5	25	→	→	→	→	127
GRID LINE THICKNESS	μm	5	10	2	10	→	→	10 (FIRED)
GRID MATERIAL	-	Cu	→	→	Ni	Cu	→	SINTERED Ag
BUS SHADING	%	1.79	1.79	1.79		5.25	1.08	1.08
BUS LOSS	%	0.96	0.94	0.94		4.46	1.12	1.03
GRID SHADING	%	0.82	1.63	1.63		1.55	1.00	5.08
GRID LOSS	%	0.42	0.10	0.51		0.09	0.94	0.49
FRONT LAYER LOSS	%	0.41	0.41	0.41		0.39	1.11	0.98
BASE LOSS (200 μm 1Ωcm; 10 μm Cu)	%	0.46	0.46	0.48	1.82	0.44	0.49	0.47
TOTAL POWER LOSS	%	4.9	5.3	5.8	7.1	12.2	5.7	9.1
CELL EFFICIENCY	%	16.36	16.29	16.20	15.98	15.10	16.22	15.63
MODULE EFFICIENCY	%	15.34	15.27	15.19	14.98	14.16	15.21	14.65
CELL VALUE	$/m²	86.31	85.46	84.49	81.93	71.94	84.73	77.91
	¢/W(PK)	56.3	56.0	55.6	54.7	50.8	55.7	53.2
DIFFERENCE IN VALUE	$/m²	REFERENCE	-0.85	-	-	-	-1.58	-
			REF.	-0.97	-3.53	-13.52	REFERENCE	-6.82

ORIGINAL PAGE IS
OF POOR QUALITY

Inserting the optimum grid line shading ratio from eq. (122) and the optimum bus line width T_{BL} from eq. (131) into eq. (129) permits determination of the actual relative power loss experienced in the front structure:

$$\frac{\Delta P_{R,mp}}{P_{d,mp}} = \frac{|j_{mp}|}{3\, V_{d,mp}} R_{sh,FL} \left(\frac{S}{2}\right)^2 + 2W \left(\frac{|j_{mp}|}{3\, V_{d,mp}} R_{sh,GL}\, \delta_{GL}\right)^{1/2}$$

$$+ \left(\frac{9\,|j_{mp}|\, \rho_{BL}}{2\pi\, V_{d,mp}} L_1^{\,2}\right)^{1/3} \cdot \frac{1}{W^{1/3}} ; \qquad (132)$$

The first term on the right hand side of eq. (132) describes the relative voltage drop in the front layer sheet, the second term the sum of the equal shading and voltage drop losses from the grid lines, and the third term the shading and voltage drop losses from the bus lines. Equation (132) is a function of the bus line spacing W, which exhibits a definite minimum in the sum of the grid line and bus line losses for the appropriate value of W. This optimum bus line spacing, for the use of round wires for the bus lines, is given by:

$$2W = \left(\frac{3}{\pi^2} \frac{\rho_{BL}^{\,2}\; V_{d,mp}}{R_{sh,GL}^{\,3}\; \delta_{GL}^{\,3}\; |j_{mp}|}\right)^{1/8} L_1^{\,1/2} ; \qquad (133)$$

With such use of round wires as bus line overlay, the losses connected with the front structure in 10 cm x 10 cm solar cells can be reduced to under 5%, from about 12% with grid lines only, or with grid lines plus plated bus lines.

The sensitivity of the performance of large area solar cells to the grid and bus line design is illustrated in Table IV.

In the computations for this table, it was assumed that deposited metal layers can be produced only with a 2.5:1 aspect ratio, that is, that the width of the line has to be at least 2.5 times its thickness. The first column shows the data for the optimum design, based on deposited grid lines of 5 μm thickness and bulk conductivity of copper. The bus lines are copper wires of circular crossection. The semiconducting base region and the metal base contact, assumed to cover the entire back surface with 10 μm thick copper of bulk conductivity, contribute together a loss due to voltage drop of 0.46%. All contact resistances have been assumed to be zero. Including this loss from the base, the total shading and voltage drop loss is 4.9% of the ideal power output.

In the second column, a grid line width of 25 μm has been used instead of the 12.5 μm width in the optimum design. Simultaneously, the grid line thickness has been increased to 10 μm. The consequence is, that this "near optimum design" has 0.4 percentage points higher loss than the optimum design, for a total loss of 5.3%.

The third column is split, showing equal sheet resistances by use of either a 2 μm thick copper deposit or 10 μm of nickel for the grid lines. In the latter case, the base contact was also assumed to be of 10 μm thick nickel. While the former case has only a small influence, the latter results in total losses of 7.1%.

The fourth column displays data on a case with plated bus

lines, similar to some discussed above.

While the bus structure in these first four columns contained seven bus lines with 1.43 cm spacing, column 5 shows another "near optimum design" with three bus lines of somewhat heavier gauge wire, and a reduced number of grid lines, namely forty. This design shows a total power loss of 5.7%.

Column 6 uses the same design as column 5, but applies printed thick film silver at the projected minimum line width of 127 μm for the grid lines. The line thickness is 10 μm after sintering, about the maximum achievable with a single printing. The conductivity is approximately one third that of bulk silver, as generally experienced with sintered thick film silver layers. The disadvantage of the use of the thick film silver lies primarily in the large shading resulting from the increased line width, which leads to a total relative power loss of 9.1%.

The line marked "cell efficiency" in Table IV shows the efficiency which would be obtained by use of the various metallization designs on an otherwise identical cell. The following line below, labelled "module efficiency", is obtained from the cell efficiency by multiplying with 0.96 and 0.975 to account for packing factor and assembly losses. Using an area related BOS price of $\$60/m^2$ as an example, and a module materials and assembly price of $\$28/m^2$, an economical "cell value" can be established for which the complete system can deliver power at an equal price. This cell value is a function of the efficiency. These cell values, expressed both in $\$/m^2$

and in \$/W(peak), are given in the two lines below the module efficiency. The last two lines, finally, show the differences in the economic value resulting from the efficiency differences due to the design variations in the various columns. The second to last line uses the cell value of the "optimum design" of column 1 as the reference, and lists the value differences of the two "near optimum designs" of column 2 and 5. In the last line, the values of the cells with "near optimum design" have been taken as reference, and the value differences of the cells with design variations from these given. It is seen that the differences in cell value form a substantial part of the entire metallization process cost and are therefore very worthwhile investigating. It has, however, also to be observed that these cell values are based on the $\$60/m^2$ area related BOS price assumption, and that the differences will be larger or smaller for higher or lower BOS prices, respectively.

The use of "high" bus lines, such as round wires, while extremely beneficial from the efficiency viewpoint, can cause problems. The first is that of thermal expansion, which leads to the need for longitudinally periodic, rather than continuous attachment of the bus wire to the solar cell, with provision for stress relief between the attachement points. Next, the high bus lines will require changes in module assembly procedure, requiring either preformed cover glass to avoid too thick a gap to be filled with potting material, or a conformal coating.

VIII. Design Rules for Front Metallization for Large Area Solar Cells

From the preceding analysis, a definitive set of design rules for the front metallization of large area solar cells has been derived (Table V). Their observation should help cell designers to avoid many of the previously experienced pitfalls and to utilize the most cost-effective contact design and metallization system.

It should be noted that these design rules are not concerned with the problem of contact resistance which still seems to be in need of adequate explanation and reduction to engineering design principles.

C-2

TABLE V

DESIGN RULES
for Front Metallization for Large Area Solar Cells

1. Observe: Careless metallization design is costly.

2. Select conductor metal of the highest practical conductivity.

3. Select deposition processes which approach bulk conductivity as closely as practical.

4. Each higher level in the hierarchy of conductors needs a much lower sheet resistance than the preceding level. This leads to the "sky scraper rule" for the bus lines: Build high rather than wide.

5. If the bus lines cannot have a sheet resistance small compared to the grid lines, omit the bus lines. Proceed directly to 10.

6. Select the bus line spacing, for bus lines of round wire, according to:

$$2W = \left(\frac{3}{\pi^2} \frac{\rho_{BL}^{2}}{R_{sh,GL}^{3} \delta_{GL}^{3}} \frac{V_{mp}}{|j_{mp}|} \right)^{1/8} L_1^{1/2}$$

7. Select bus line wire diameter according to:

$$T_{BL} = \left(\frac{32}{3\pi} \frac{|j_{mp}| \rho_{BL}}{V_{mp}} L_1^{2} W^2 \right)^{1/3}$$

8. For rectangular bus wires of height-to-width ratio k, replace each π by 4k.

9. For bus lines of constant sheet resistance $R_{sh,BL}$, rather than thickness directly proportional to width, as in round or rectangular wires, the relationship:

$$\frac{T_{BL}}{2W} = L_1 \left(\frac{|j_{mp}|}{3 V_{mp}} R_{sh,BL} \delta_{BL} \right)^{1/2}$$

applies, instead of 6.) and 7.). Choose W then as small as practical, considering 13.) and 14.).

10. Arrange grid lines normal to bus lines, and parallel to each other.

11. Select grid line width T_{GL} as small as practical, commensurate with acceptable production costs and yields, considering the differences in solar cell economic value which are a consequence of the efficiency variations resulting from the grid line width design.

12. Select the grid line spacing S according to:

$$S = \left(\frac{6\,V_{mp}}{|j_{mp}|}\frac{T_{GL}}{R_{sh,FL}}\right)^{1/3} - \left(\frac{2}{3}\right)^{4/3}\frac{R_{sh,GL}\,\delta_{GL}}{R_{sh,FL}}\frac{W^2}{T_{GL}}$$

13. The "shape factor" δ varies from 0.75 for fully tapered grid lines to unity for uniform width lines of equal shading.

14. Determine the total relative, series resistance connected losses, and check the design by inserting the obtained values into:

$$\frac{\Delta P_R}{P_{d,mp}} = \frac{T_{GL}}{S} + \frac{T_{BL}}{W} - \frac{1}{3}\frac{j_{mp}}{V_{d,mp}}\left\{R_{sh,FL}\left(\frac{S}{2}\right)^2\delta_{FL} + R_{sh,GL}\frac{S}{T_{GL}}W^2\,\delta_{GL} + R_{sh,BL}\frac{2W}{T_{BL}}L_1^2\,\delta_{BL}\right\};$$

where $R_{sh,BL}$ may be replaced by $\rho_{BL}/(\frac{\pi}{4}\,T_{BL})$ for round wire or $\rho_{BL}/(k\,T_{BL})$ for rectangular crossections. The first 2 terms represent the shading losses, those within the bracket the series resistance losses. In a good design, the shading losses and the series resistance losses associated with the same component (GL or BL) are of approximately equal magnitude. Also, the grid line and the bus line losses will be of comparable magnitude. The front layer loss (1st term in brackets) should be small compared to the grid line and bus line losses, but there is no reason to reduce S beyond the point at which the front layer loss becomes insignificant. If the grid line shading loss $\frac{T_{GL}}{S}$ is too large, try to iterate according to point 11. If the grid line thickness-to-width ratio is limiting, reduce the thickness (increase $R_{sh,GL}$), to find T_{GL} and $R_{sh,GL}$ values for least power loss.

IX. BRIEF DESCRIPTION OF THE METALLIZATION OPTIONS

A. General

Metal can be deposited in selected areas either by chemical or by physical processes. The chemical processes are usually called "plating". They are all so-called "wet" processes which means that deposition occurs from a solution. In the physical processes, metal is transferred in physically finely divided form, either as neutral or charged atoms or molecules, or as a powder, and re-constituted on the substrate as a contiguous metal layer.

B. Chemical Deposition Processes

The three major processes by which plating can occur from solution are immersion, electroless, and electrolytic plating. In immersion and electroless plating, all areas of the silicon wafer, which are not to be covered by metal, must be masked, that is covered by an adequately thick dielectric layer.

1. Immersion Plating

Immersion plating, which is normally used to plate "strike" layers of noble metals, such as Pd or Au, on bare silicon, is mainly due to a simple displacement reaction at the substrate surface.[2] This reaction between the silicon atoms and metal cations results in an oxidation of the substrate and a reduction of the plating material. Probably the initial contribution of electrons to the metal cations

PRECEDING PAGE BLANK NOT FILMED

comes from the accessible dangling silicon bonds, followed by the breaking of silicon-silicon bonds which then leads to the formation of free silicon cations. The silicon ions then move into the bulk of the solution, and their charge is compensated for by the ambient anions. Because the plating cations entering the surface boundary region are reduced, which means converted to neutral atoms by the substrate, maintenance of charge neutrality at the substrate surface requires that equivalent substrate ions enter the solution. The chemistry of immersion plating can be elucidated by examining a Pd-plating solution whose constituents are approximately 1 wt% NH_4F, 1 wt% $HC\ell$, 0.0025 wt% $PdC\ell_2$, and 98 wt% H_2O. The $HC\ell$ increases the solubility of the $PdC\ell_2$ via the formation of weak complexes, while the NH_4F probably helps in keeping the oxidized substrate ions in solution. One possible displacement or immersion reaction at the substrate surface is:

$$2Pd^{+2} + Si^{o} = Si^{+4} + 2Pd^{o}\downarrow \quad (134)$$

or the reduction/oxidation might occur in stages, as in,

$$2Pd^{+2} + Si^{o} = Si^{+2} + 2Pd^{+} \quad (135)$$

$$2Pd^{+} + Si^{+2} \rightarrow Si^{+4} + Pd^{o}\downarrow . \quad (136)$$

In any case, the final products are the plated palladium metal and the Si^{+4} ion. After the silicon cation leaves the surface boundary regime, its positive charge attracts choride and fluoride ions, which by formation of complexes,

help to keep the silicon cation in solution. One possible complex formation is

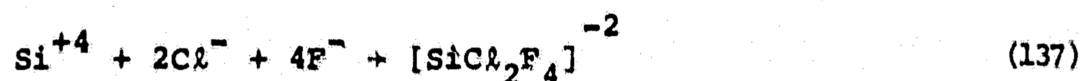

$$Si^{+4} + 2C\ell^{-} + 4F^{-} \rightarrow [SiC\ell_2F_4]^{-2} \qquad (137)$$

There is only a small possibility for the formation of gaseous $SiC\ell_4$ since the silicon cation will hydrolysize (react with water) before it can form covalent bonds with a choride anion.

For the immersion reaction to proceed, the material to be plated, or substrate, has to be more reactive than the plating metal. Too great a reactivity difference between the substrate and the plating cations in the solution would lead to a plating rate too high for the formation of dense and coherent deposits. The relative reactivity of the substrate and the plating cation can be adjusted by the addition of complexing agents such as a cyanide, ethylenedinitrolotetraacetic acid, (EDTA), or disodium salt. The complexing agent can, by binding with the oxidized substrate, drive the immersion reaction forward (reac (134) to the right) by effectively decreasing the concentration of those ions. Similarly, the driving force of the immersion reaction can be decreased by lowering the effective plating cation concentration by complexing.

One would anticipate that the immersion layer thickness would be limited to about 10 Å, as the displacement reaction should cease, once the substrate is covered with a few atomic layers of plated metal. However, inhomogeneities or holes

in the thin plating layer permit the continuation of the displacement reaction. The holes result in local galvanic currents that keep driving the immersion reaction forward until the layer thickness is approximately 50-100 Å.

A disadvantage of the immersion plating solution is its limited capacity. The depletion of the metal cations, contamination from the plating surface, and side reactions contribute to the short life of immersion solutions.

2. Electroless Plating

In order to build up a thicker layer than can be achieved by immersion plating, electroless plating is often used. The material most commonly plated on solar cells using this technique is nickel.[3)] Also palladium, chromium, and copper can be plated electrolessly on silicon. In electroless plating, an oxidation-reduction reaction occurs catalytically at the substrate surface where the plating solution selectively reduces the plating cation. For example, in the nickel plating solution, the oxidation of phosphorus in a hypophosphite anion to an orthophosphite anion produces hydrogen atoms which are adsorbed on the substrate. It is the adsorbed hydrogen atoms (shown as H(ad) in reac (138) that reduce the nickel cations to metallic nickel. The reaction mechanism in a basic, usually ammonium hydroxide, solution is thus:

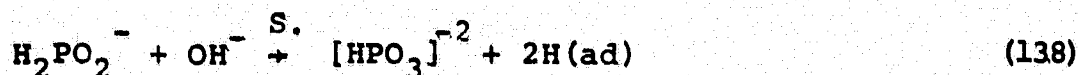

$$H_2PO_2^- + OH^- \xrightarrow{S.} [HPO_3]^{-2} + 2H(ad) \qquad (138)$$

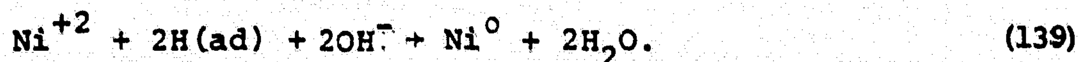

$$Ni^{+2} + 2H(ad) + 2OH^- \rightarrow Ni^0 + 2H_2O. \qquad (139)$$

For simplicity, the NH_4^+ and Na^+ cations, and the Cl^- anions are not shown in the above reactions. The notation S. indicates that the reaction only occurs at the substrate surface.
Since hydrogen is readily adsorbed on a palladium surface, a palladium layer is sometimes applied prior to the electroless nickel plating. Also, nickel can be plated directly on silicon, since there are hydrogen adsorption sites on silicon and silica. The density of potential adsorption sites on silicon, and consequently perhaps the coherence of the nickel film on this surface, is lower than on a Pd-surface. Another problem with plating nickel directly on silicon is that the thickness of the silica layer, which is always present on bare silicon, is thought to be a major factor in determining the adherence of the nickel. Also, too thick a native silica layer (> 50 Å) should result in excessive contact resistance and simultaneously poor adherence of the nickel. At the other extreme, a silica layer only a few atomic layers thick should permit a displacement reaction between the silicon and the nickel chloride to occur (immersion plating), so that the plating layer should not be expected to deposit smoothly.

The plating efficiency of the electroless nickel plating solution is lowered by several competing reactions that consume the hypophosphite anion without the production of adsorbed hydrogen. Two of these reactions are:

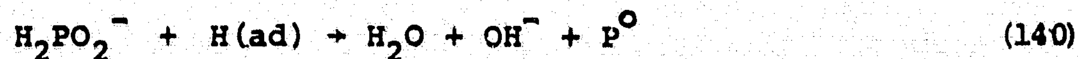

$$H_2PO_2^- + H(ad) \rightarrow H_2O + OH^- + P^o \qquad (140)$$

and

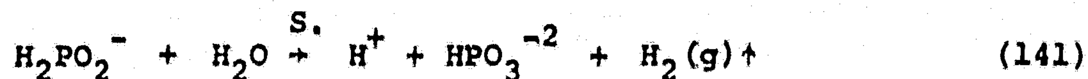

$$H_2PO_2^- + H_2O \overset{S.}{\rightarrow} H^+ + HPO_3^{-2} + H_2(g)\uparrow \qquad (141)$$

Because of the common ion effect, reaction (140) will occur to a greater extent in an acidic solution while reaction (141) will be more favored in a basic solution. To keep the electroless solution effective, precipitation must be minimized. Otherwise, the solution could plate out on itself, or on the container walls, starting with precipitated particles. In the nickel and chromium electroless plating solutions, sodium citrate, a chelating agent, is therefore used to keep the metal cations in solution. Another major constituent of the electroless plating solution is a buffer (weak acid or base and the salt of that acid or base). The buffer is used to maintain the pH of the solution in face of the hydronium ion consumption or production by the plating reactions.

3. Electrolytic Plating

Electrolytic plating, or electrolysis, is a very common commercial process, used either to deposit conducting, protective, or decorative surface layers, or to purify metals. Its first commercial application occured over a century ago in the fabrication of silverware by silver plating. Electroplating can be used to deposit layers of substantial thickness and bulk metal properties, including conductivity. It differs from the two previously mentioned plating procedures in that energy for the plating is provided from an external

voltage source instead of a chemical reaction. The plating apparatus consists of an anode (the metal that is to be plated) and a cathode (substrate to be plated), both submerged in an electrolytic solution, usually parallel to one another and about 15 to 30 cm apart. Electrical connections have to be made to each workpiece (substrate), as well as the anode, from a dc power source capable of supplying the required current at a voltage between 4 and 9 volts (DC). Oxidation of the metal takes place at the anode, producing metal cations which are then transported, both under the influences of the applied potential gradient and of convection currents, to the cathode where the ions are reduced and thus plate out. In this process, the principal work of the external voltage is the movement of electrons from the anode to the cathode.

Since plating is a steady state situation (i.e., the number of electrons in the solution does not change in time), the mass of oxidized metal is equal to the mass of plated metal. The deposition rate can be derived from the current flow, using Faraday's Law which states that 96,500 coulombs will deposit one chemical equivalent. As one mole of electrons has a charge of 96,500 coulombs, a "chemical equivalent" has one mole of electronic charge.[4)] Thus, one chemical equivalent represents one mole deposition of singly charged cations, but only half a mole of doubly charged cations. Therefore, a current density of 1 mA/cm^2 would give a deposition rate of about 1×10^{-8} equivalents/sec-cm^2. This holds only if

the cathode and anode efficiencies are 100%. The electrode efficiency is defined as the actual mass deposited divided by the amount calculated by Faraday's Law.

In copper plating, the electrolytic solution consists chiefly of sulfuric acid and copper sulfate. The sulfuric acid is present in order to lower the resistivity of the plating solution, to prevent the precipitation of copper salts, and to increase the reactivity of the anode surface, while the copper sulfate is needed to charge-balance the oxidized copper in solution. Small quantities of molasses or other organics are sometimes added to the H_2SO_4-$CuSO_4$ solution to obtain finer grain deposits. The applied voltage for copper plating is 6 - 12 volts (DC), and the current density of the cathode is 40 - 60 mA/cm^2. A higher voltage cannot be used to increase the current density, or the plating rate, since the reaction rate is limited by the diffusion of cations through the boundary layer (the Helmholtz double layer) from the bulk to the substrate surface. For electroplating copper directly onto an electroless deposited layer, or strike surface, of nickel, a H_2SO_4-$CuSO_4$ solution may not be suitable because of the possibility of an immersion reaction between the $CuSO_4$ and Ni. Immersion deposited copper is undesirable because it is not very adherent. Therefore, the nickel has to be initially coated with copper using an electroless solution, or with an electrolytic solution containing a copper complexing agent. The complexing agent effectively decreases the concentration

of copper in the solution, and hence, the driving force for a displacement reaction.

C. Physical Deposition Processes

The physical deposition processes are best separated into those transporting material divided into particles of molecular size, and those using much larger powder particles. The latter group is usually connected with the name "printing" processes, of which a substantial variety exists, but only one has gained significant application for metal layer formation in the electronic industry: screen printing. The first category includes those processes where the material is "vaporized" by heat, including that generated by an electron beam ("vacuum evaporation") or ion bombardment (sputtering), and then transferred as neutral particles by free flight through a gap narrow compared to a mean free path, to the substrate on which they are to be deposited. The other group in this category includes those processes where the particles are ionized and then accelerated by an electric field for their transfer to the substrate. These processes include plasma deposition and ion plating, a low-voltage variant of ion implantation.

1. Vacuum Deposition, including sputtering.

In vacuum deposition, the source (metal to be deposited) and the substrate (for instance silicon wafers covered with suitable masks) are both located in a vacuum chamber, where

the metal is evaporated and physically tranferred onto the wafer. There are several methods for supplying sufficient thermal energy to vaporize the metal. A common laboratory method is to place chunks of wire pieces of the metal directly on a coiled filament, which is then heated by passing an electric current through it. This technique works well when the metal and filament wet each other, so that the filament will support the molten metal, when the vapor pressure of the metal is several orders of magnitude greater than that of the filament, and when there is no alloying between the metal and filament. The batch nature of this method and the small amount of metal that can be contained by the filament limit its practicality for large scale cell processing. In production processes, larger amounts of the metal to be deposited are contained in a crucible of graphite, refractory metal such as tungsten, or ceramic. The crucible is heated either by passing current through the crucible, or by a resistance furnace external to the crucible. A cap with a small orifice is usually placed on the crucible to avoid splattering and to gain directionality of the emitted metal vapor.

The coating thickness (t) obtained from a point vapor source of unrestricted opening angle to a planar surface follows Knudsen's cosine law,[5] or:

$$t = \frac{m' \cos\Theta}{4\pi r^2 \rho} , \qquad (142)$$

where m' is the mass of metal evaporated and ρ its density, Θ is the incidence angle, and r is the distance between the source and the deposition area. In terms of the vertical (h) and horizontal (δ) distances between the source and the target,

$$t = \frac{m'h}{4\pi\rho(h^2 + \delta^2)^{3/2}}, \tag{143}$$

or

$$t = \left[(1 + (\delta/h)^2\right]^{-3/2} t_o , \tag{144}$$

where t_o is the plating thickness obtained directly above the source at distance h ($\delta = \theta = 0$). In order to obtain uniform deposition from a point source, the target should lie on the surface of a sphere. The thickness is then equal to $m/4\pi\rho R^2$, where R is the radius of the sphere. In depositing from a capped crucible, the locus of the uniform deposition surface can be ovalized because of the directionality, or beaming, imposed by the crucible orifice.

To reduce crucible temperature and thus crucible-metal interaction, the metal can be heated directly by bombarding it with an electron beam, rather than indirectly by heating the crucible. A hot cathode, such as a tungsten filament, provides the electrons, and a magnetic field is used to direct the electron beam to the vapor-emitting surface. The highest temperature region is thus shifted from the crucible to the metal. In fact, the crucible can be cooled, or omitted completely by heating of a puddle in a block of the metal to be

evaporated, thus eliminating potential contamination from the crucible altogether.

To maximize the adhesion of the vaporized metal to the substrate, its surface should be free of oxides, grease, adsorbed water, or other contaminants. Heating the substrate usually enhances bonding, but very high substrate temperatures reduce the deposition rate by re-evaporation of some of the plated metal.(6) Ionization of the vaporized metal often helps surface adhesion. Ionization can be accomplished in an rf field or a plasma, usually a discharge in noble gases. In the plasma, only about 3% of the metal atoms are ionized, but the Argon ion bombardment of the substrate which results from the plasma which is formed by a discharge in Argon, increases metal adhesion by "hammering-in" the metal atoms. Unfortunately, entrapment of Argon in the metallized layer reduces its conductivity. Because an electric field is applied to the substrate when the vaporized atoms are ionized, the deposition thickness does not follow Knudsen's cosine law.

Another way to vaporize the source metal is to sputter it, which means bombard it with ions. The ions, usually produced in a glow discharge in Argon, are accelerated towards the metal, or target, with a voltage of about 500 volts. Sputtering of the metal occurs because of the transfer of momentum from the discharge gas. A threshold voltage (around 300-400 volts) is required to overcome the work function of the metal, before sputtering can set in. Above the threshold

voltage, the sputtering rate (Q) is directly proportional to the applied voltage (V) and inversely proprotional to the pressure of the discharge gas (p) and the distance between the cathode and the target (d), or

$$Q = \frac{kV}{pd} \quad (145)$$

To maintain a constant sputtering rate, the gas flow rate must be adjusted to maintain a constant voltage and current density. In addition, the cathode temperature must be kept constant, since the current density increases with cathode temperature. The sputtering rate increases with the atomic weight of the discharge gas and decreases with the latent heat of evaporation of the target.

The sputtering efficiency, or the ratio of the latent heat of evaporation of the target to the impinging ion energy needed to vaporize one atom, is usually only 1%. Most of the excess energy is contained in the vaporized atoms which have about two orders of magnitude greater energy than thermally vaporized atoms. The greater energy of the sputtered atoms facilitates crystal formation of the deposited layers, within the practical limits imposed by re-evaporation. Since the sputtered atoms follow the cosine law, slightly modified by the collisions of the discharge gas and sputtered atoms, the target and substrate are usually arranged as planar surfaces parallel to each other, at a distance of approximately 5 cm, to achieve uniform deposition. As the center of the target is somewhat shaded

from the plasma by the substrate, the target is usually chosen about 50% larger than the substrate to attain sufficient sputtering.

2. Thick Film Screen Printing

Screen printing has been used for hundreds of years in printing fabric patterns and metal designs on china. It is a fairly simple process requiring only: (1) a screen to define the printed pattern; (2) a squeegee to transfer the "ink" from the top of the screen to the substrate; and (3) a fixture to hold the screen and substrate in their proper relative positions, while allowing movement of the squeegee. Downward pressure on the squeegee pushes the screen against the substrate and forces ink through the "open" parts of the pattern of the screen. The amount of ink that sticks to the substrate is a function of the screen's filament diameter and spacing, the emulsion thickness, the width of the line to be printed, the initial distance between the screen and substrate (snap-off distance), the viscosity and rheology of the ink, and the adherance of the ink to the substrate. If the ink cannot wet the substrate, then printing will be negligible. The ink used in screen printing of solar cells generally consists of: a metal powder (silver) with 5-10 μm diameter grain size; an organic vehicle composed of a solvent, such as butyl carbitol, and a binder (ethyl cellulose); and a frit, which could be a glass such as lead borosilicate. Recently, experiments have been performed replacing the frit by a flux, such as $AgPO_3$.

The screen may be either a mesh of wire or nylon fibers, with the grid line pattern defined by use of an emulsion which closes the pores in the mesh in desirable areas, to prevent ink flow there, or an etched metal screen. The greater flexibility of the nylon screen is a disadvantage to resolution, because of its larger snap-off distance. The etched metal screen has very good resolution and a small snap-off distance, but is more expensive. Similar results can often be obtained with a cheaper, fine wire mesh screen. A 325 wire mesh can yield lines as narrow as 125 μm, although 175-200 μm line width is more commonly considered as the practical limit of the present technology for a reliable process with acceptable yield. It is expected that this limit can be pushed to 125 μm in the future. The thickness for the printed lines is limited to about 25 μm before firing. The limit arises from adherence of the ink to the sides of the emulsion on the mesh.

After application of the ink, the printed parts are dried and then sintered, both in the air. The drying and sintering shrinks the ink volume by 20 to 50%. When sintered, the silver inks have an open matrix structure with a solid fill factor between 50 and 60%. The conductivity of the printed and sintered silver lines is at most 60% of the bulk conductivity for equal metal mass in the line, due to the limited area contacts between the silver grains.

A screen will last for about 10,000 cycles, a squeegee for a tenth of that. The squeegees need to be hard enough to

retain a sharp edge, yet soft enough not to unduly wear out the screen. The repetitive application of simple operations in screen printing lends this process readily to automation.

X. Comparative Evaluation of the Metal Deposition Options

A. General

In this section, the attributes of the various applicable metal deposition options will be compared against each other. Such a comparison of the deposition options alone is only a first step in a comparative evaluation of the metallization process options, since the complete metallization process consists of a sequence of several steps - such as surface preparation, masking, pattern definition, conduction layer build-up, removal of mask, sintering, etc. The options for the complete metallization process thus form a submatrix to the matrix of the solar cell process options. In this submatrix, the number of process steps varies between options, as well as the interfaces to the main process matrix.

As an example, the various plating processes require the additional steps of masking, further conduction layer build-up, and mask removal, which are all not needed in thick film printing of silver. This process, however, requires a relatively high temperature sintering step to reduce contact and conductor resistance to acceptable values, which is usually not needed for plating. Also, some processes require some additional operations. For instance, in vacuum evaporation, the commonly used contact mask gets covered with deposition metal and must be periodically removed for cleaning. In the interface area, the suitability of some processes depends on preceding processes or the cell structure chosen. As an example, it does not seem advisable to screen

print on texture etched cells due to potential damage to the peaks from the pressure of the squeegee. Even worse, some of the process steps in the metallization submatrix may be combined with process steps in the main matrix, such as AR-coating. For wet chemical plating options, for instance, a dielectric mask is required to define the metal pattern. But, since there is no metal deposit on the mask itself, the mask does not have to be removed if it can serve as, or complement, the AR-coating.

The various metallization options also result in differing conductor attributes, such as conductivity and minimum line width. These attributes determine not only the design of the solar cell, but also its ultimate performance. On large area cells, to achieve high performance, the front metal pattern should have a grid line width of 25 μm or less. This is well beyond the projected capabilities of some processes (e.g. thick film screen printing), and depends on the mask attributes for others (wet chemical plating and vacuum evaporation). The thickness of the metal layer also has a practical upper limit, which has, in generality, been taken as 10 μm for the lines of 25 μm or greater width, and as 40% of the line width for narrower lines.

Postponing these complications to a later point in the evaluations, the following discussion will, as a first step, examine the metal deposition only.

Some of the metal deposition options represent, by themselves, a variety of sub-matrices. For instance, for the electroless Ni plating process, several variations of surface preparation have been explored with conflicting results. They include nickel deposition on: bare, HF-dipped wafers; a Pd-layer applied by immersion plating; a Pd-layer applied by immersion plating, and built up electrolessly; a thin (50-100 Å) gold layer. The type of strike surface used determines the sintering conditions to be applied to the Ni layer. A few general requirements have emerged from the theoretical study of the influence of metallization design on solar cell performance. Foremost among these is that, to simultaneously minimize the losses from series resistance and from surface area coverage which causes current loss from shadowing, the sheet resistance of the grid line needs to be as low as possible. This requires high metal conductivity and large thickness. The use of copper with its high conductivity, second only to silver, is therefore indicated. It is further imperative that the deposition process yields a layer of bulk conductivity, and not only about one third of it, as the powder deposition and sintering processes do.

According to their general nature, outlined in the preceding section, the discussion of the metallization options will deal with them as four major groups: the wet chemical plating, which includes immersion, electroless, and electrolytic plating; vacuum deposition, including

Table VIA

Metallization Process Options

Process	Applicable Metals	Coating Thickness (um)	Purpose of Coating	Typical Sintering Requirements	Major Steps	Remarks
Electro less Plating	Ni on Si	0.5	Pattern for chief Cond. or barrier	300°C; 30 min	HF dip, plate, rinse and dry, sinter.	Adherence to Si and contact resistance is variable
	"	5	Chief cond.	Optional	Plate, rinse and dry.	–
	Ni on Pd	0.5	Pattern for chief cond. & or barrier	None	Plate, rinse and dry.	–
	"	5	Chief Cond.			
	Ni on Au	0.5	Pattern for chief cond.	None	Plate, rinse & dry.	Shouldn't be exposed to high temperatures (>300°C)
	Pd on Si or on Pd_2Si	0.01	Ohmic contact and barrier against Ni	300°C; 15 min in N_2	HF dip, plate, rinse and dry, sinter,	Forms Pd_2Si when sintered
Immersion Plating	Ae on Ni	5	Chief cond.	None	Plate, rinse, and dry.	Only recently has solution stability been acceptable.
	Pd on Si	0.01	Ohmic contact and barrier against Ni	300°C; 30 min in N_2	HF dip, plate, rinse & dry, sinter, hi-pressure scrub, HF dip, plate.	Forms Pd_2Si when sintered

TABLE VIA (Continued)

Metallization Process Options

Process	Applicable Metals	Coating Thickness (um)	Purpose of Coating	Typical Sintering Requirements	Major Steps	Remarks
Electroless Immersion Plating	Au on Si	0.002	Strike layer	None	HF dip, plate	Shouldn't be exposed to high temperature (>300°C)
Electrolytic Plating	Cu on Ni	8-10	Chief Cond. layer	None	Plate, rinse & dry.	Must avoid direct Cu-Si contact.
"	Ni on Si_2	8-10	Chief Cond.	300°C; 30 min in N_2	HF dip, plate, rinse & dry, sinter	Need organics in plating solution.
"	Ag on Ni	5	Chief Cond.	None	Plate, rinse and dry.	Current density between 10-20 mA/cm^2

resistance and electron beam heating as well as sputtering and ion plating; thick film screen printing; and deposition from the melt, such as solder dipping, which is at times used for conduction layer build-up. The processing parameters for each metal deposition option are considerably affected by the type of metal applied. An extreme case in this respect is the thick film process, where it has been found practically necessary to work with noble metals (e.g. silver) to avoid oxidation of the metal powder in the binder burn-off step. However, the high cost of the noble metals, including gold, silver, and palladium, will severely limit their use in the manufacture of solar cells and modules for large scale terrestrial application. As a consequence, grid patterns of base metals are preferred, but their successful application by thick film methods requires further development. The wet chemical plating options appear not to be the most appropriate for applying base metal grids; the operating conditions lead to a reduction of the grid metal. Even though oxidation of the substrate or silicon surface might seem to be a problem in wet chemical plating, the thickness of the silica layer covering the silicon may be reduced when exposed to the plating solution, at least in electroless nickel plating, as recent studies have shown[7].

A summary of the metal deposition process options, used or being considered for low-cost silicon solar cells, is contained in Tables VIA-C. In these tables, the normally applied

metal thickness (which determines the function of the metal layer), the metals, to which the process is normally applied, and the major processing steps are listed. The Midfilm process has been listed separately in these tables, as it represents a cross between a photolithographic and a thick film process.

B. Chemical Deposition Processes.

1. Electroless Plating.

The first set of options listed in Table VIA refers to electroless plating which is now mostly used to apply only a thin layer (up to ∿ 5000 Å) as a pattern for further conductor build-up. Electrolytic plating, just as the older method of solder dipping, is primarily used for additional conductor build-up. If copper is applied as the main conductor, then a "barrier layer" is needed to prevent copper penetration into the silicon wafer. Nickel has been found to provide an effective barrier against copper diffusion, and it is convenient that it can be applied by electroless plating.

In electroless nickel plating, the nickel is deposited by the chemical reactions described by reac (138) and (139) in the preceding section. Approximately three moles of hypophosphite anions are consumed for each mole of plated nickel due to two side reactions. One is the break-up of the hypophosphite anion into H_2O, OH^-, and phosphorus caused by reaction with the adsorbed hydrogen atoms, such as:

$$H_2PO_2^- + H(ad) \rightarrow H_2O + OH^- + P^O. \qquad (146)$$

The other side reaction is the evolution of gaseous hydrogen, instead of adsorbed hydrogen, from the reactants in reac (138). This reaction is:

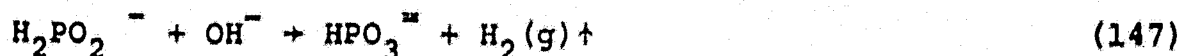

$$H_2PO_2^- + OH^- \rightarrow HPO_3^= + H_2(g)\uparrow \qquad (147)$$

There is still some debate over the type of surface which nickel can be most advantageously applied on. The three organizations which examined electroless nickel plating under the JPL/LSA project, applied three different procedures for surface preparation. Before applying the nickel layer, Motorola covers the grid pattern with a Pd-layer, applied by immersion plating and in some cases built up further with electroless plating. Photowatt applies the nickel layer over a thin gold layer which is formed by immersion plating, while Solarex deposits the nickel directly on the silicon surface by electroless plating. It is to be noted, that the surface preparation prior to the metal deposition process has a major influence on the sucess of the plating process. First, the electrical conductivity of the semiconductor plays a role, with the more heavily doped materials being easier to plate. Second, the mechanical surface structure has a significant influence, with the coarser surfaces (sandblasted, coarsely lapped) resulting in better adhesion. And finally, the chemical cleaning processes used immediately prior to plating, including an HF dip with or without subsequent short rinse, are recognized as important steps in a successful plating process.

The electroless nickel plating options are listed in Table VIA. Even though the electroless application of a bulk nickel conductor is shown in Table VIA, it is now more commonly proposed that the nickel be used only as a thin layer, as the brittleness of the electrolessly plated layer (due to the presence of phophorus in the Ni deposit) causes thicker layers to peel relatively easily from the silicon during temperature cycling.

With proper care of the electroless nickel plating solution, by cleaning the wafers of particulates possibly carried into the bath and by filtering out precipitates to avoid having the solution plate out on itself, and by adding a replenisher solution which contains NH_4OH to maintain the proper pH, and $NiCl_2$ to replace the plated-out nickel, the solution lifetime can be quite extensive. In current cost studies for electroless plating of nickel, it is assumed that one liter of solution could effectively plate, without re-plenishment, 34 m^2 of polished cells with 5% front area coverage to a layer thickness of 5,000 Å. It may be noted, that the high mobility of nickel cations in the solution allows the indiscriminate plating of textured surfaces, which, because of the greater surface area of the texture etched cells, decreases the capacity of the plating solution. The nickel plating solution consists of 2.5 wt% $NiCl_2 \cdot 6H_2O$, 5 wt% NH_4OH, 1 wt% $NaH_2PO_2 \cdot H_2O$, 4 wt% NH_4Cl, 7 wt% $Na_2C_6H_5O_7 \cdot 2H_2O$ and 80 wt% H_2O. The $NiCl_2 \cdot 6H_2O$ is the

metal source, the ammonium hydroxide and the ammonium chloride maintain the pH of the solution, the sodium citrate is a chelating agent, and the sodium hypophosphite is the reducing agent for the nickel. Increasing the pH might increase the rate of production of adsorbed hydrogen atoms and plated nickel (reac (138) and (139), but it also increases the rate of a conflicting reaction (reac (147). Raising the temperature of the plating solution increases the plating rate, but the stability of the plating solution decreases. A solution temperature of 90°-95° C gives acceptable plating rates and solution stability. It would first be expected that the plating rate could be increased by using more sodium hypophosphite than listed above. However, too much sodium hypophosphite decreases the stability of the solution, so that it could plate anywhere, not just on the silicon or cleaned metal surface. The ammonium chloride acts as a buffer and aids in maintaining the solution pH since it is a salt of the weak base NH_4OH. The complexing agent sodium citrate helps to keep solution particles and metal ions in solution. Solid particles not only cause a rough deposition, but can also act as catalytic nuclei that lead to solution decomposition. The electroless plated nickel layer generally shows good uniformity, with few pores and a fine crystalline structure. Part of this is due to the presence of between 3 and 15 wt% phosphorus in the nickel layer due to reac (135). The phosphorus gives the nickel layer a high corrosion resistance,

but also brittleness compared to a pure nickel layer. The resistivity of the Ni-P layer is about an order of magnitude higher than that for pure nickel - 60 μΩ cm compared to 6.35 μΩ cm. As the electroless plated nickel layer normally serves a sensitizing function, its high resistivity does not form a handicap. However, the diffusion of phosphorus from the nickel layer into the wafer can electrically influence an underlying p or p^+ layer. Also, care must be exercised in heating the electroless nickel layer, since the compound Ni_3P is formed at about 400° C. The nickel phosphide affects the hardness of the metal layer due to crystallite growth.

Both the adherance of the electroless nickel layer and the unit area contact resistance (desired to be $\leq 10^{-4}$ ohm·cm^2) are dependent on the nature of the substrate and on sintering temperature and time. Although nickel can be (and has been in production quantities) successfully plated electrolessly directly on silicon, and even without sintering, its adherance and contact resistance have been found to be difficult to control. The former could be due to variations of the nickel layer thickness. The brittleness and thermal expansion coefficient mismatch between the nickel and silicon become more apparent, as the thickness of the layer increases. In one series of experiments(8) it was found that 5000 Å thick layers adhered well to silicon, while 10,000 Å layers separated easily. The silica layer thickness also affects adherance and contact resistance. If the silica layer is

too thick (> 50 Å) to readily permit tunneling, then it will act as a dielectric layer, and electroless plating will not occur. If there is no silica present on the silicon surface, then a displacement reaction will occur with the plating solution between the nickel and silicon, due to the high reactivity of silicon. This is thought to create a porous interface layer between the silicon and the nickel, and thus to decrease the adherence of the deposits.

It has been shown recently[7] that the silica layer thickness decreases in the electroless nickel bath, and that the plating does not actually commence until the silica layer thickness has been adequately reduced, i.e. to near 50 Å to allow a sufficient amount of electron tunneling. This decrease of the silica layer thickness could result from a reduction of the silica by the ammonium hydroxide, and its dissolution by complexing with the sodium citrate in the solution. Since different silica thicknesses thus would require diffferent processing times, it would be desirable to maintain a standardized silica layer thickness in a production line situation. This might be accomplished with a dilute HF dip immediately prior to the electroless plate. Processing times and temperatures for depositing 5000 Å of Ni on "bare" silicon are 5 to 6 min at 80 to 90° C.

To form an ohmic contact on non-degenerate silicon, i.e. not heavily doped and/or sandblasted silicon, the nickel layer has to be sintered after plating, which is thought to

result in the formation of Ni_2Si. The sintering temperature has to be kept low, to minimize the formation of Ni_3P in the metal layer and the diffusion of nickel into the silicon wafer. Nickel atoms in the depletion region can lower the cell efficiency through the formation of recombination centers, while nickel aggregates can even short out the junction. The sintering conditions for electroless deposited nickel are therefore usually 300° C for 30 min in an inert atmosphere. On cells which are solder dipped, a separate sintering step is usually not performed. It is possible that the short heat cycle connected with the solder dipping operation is adequate for the Ni_2Si formation.

To shield the wafer against nickel penetration, and to ensure contact adherence as well as coherence, a palladium layer is sometimes electrolessly deposited prior to the nickel plating, in a "sensitizing bath". The palladium forms a barrier against nickel penetration, and it presents a very active surface for the adsorption of hydrogen atoms. The palladium layer is usually sintered for 30 min at 300° in a nitrogen atmosphere to establish an ohmic contact by the formation of palladium silicide. No additional sintering is then needed after deposition of the nickel layer. A gold strike layer, approximately 20 Å thick, can be deposited in lieu of the Pd layer prior to the nickel plating. The role of this gold layer is not well understood. It probably does not act as a barrier to nickel penetration, and gold itself

penetrates readily into silicon and forms recombination centers there. However, the presence of a gold layer aids in providing an adherent and ohmic nickel layer without the need for sintering. The absence of a sintering step in the Au-Ni layer minimizes the metal penetration problem during the solar cell fabrication process. In one reported sequence, the gold layer is plated by immersion of the wafers for 30 seconds into a basic electroless solution which contains 0.2 wt% potassium cyanaurate as the gold source, 6.6 wt% ammonium chloride, 4.4 wt% sodium citrate, and 1 wt% sodium hypophosphite. These chemical constituents serve the same purposes as they do in the electroless Ni plating solution. The solution is maintained at a pH between 7 and 7.5 by addition of ammonium hydroxide. It has been found that the addition of 1 wt% HF to the electroless gold solution reduces its best operating temperature from the 90°-95° C range to room temperature. Whether the HF increases reactivity of the solution or of the surface, is not known. It could also be that it is simpler to precisely control the thickness of the thin gold layer by keeping the gold solution at room temperature where its reactivity is lower. Just prior to exposure to the gold plating solution, the wafers are dipped in concentrated HF (48 wt%) for 30 seconds. After the gold layer is applied, the wafers are rinsed thoroughly with DI H_2O for 5 minutes before being electrolessly nickel plated.

In another process sequence, palladium is applied via

immersion plating and then built up with electroless plating prior to the electroless nickel plate. The immersion Pd-layer is about 50 Å thick, while the electroless layer is 1000 Å thick. The palladium immersion solution contains $PdCl_2$ as the Pd-source, $HC\ell$ to help dissolve the $PdC\ell_2$, and NH_4F to complex with the silicon cations by formation of fluorides. Control of the immersion reaction rate is important; too rapid a rate leads to non-adherent or spongy deposits. The silica layer thickness is minimized by dipping the wafers in a 1 wt% HF solution just prior to plating.

In the Motorola process sequence, the immersion plating, which takes 5 min, is done twice, with DI H_2O rinses, a short aqua regia dip (5 sec), and a 20 sec 1 wt% HF dip between the immersion plating steps. After the second plating operation, the cells are rinsed with DI H_2O, dried, and sintered for 15 min at 300° C in a nitrogen atmosphere. The palladium layer is then built up by electroless Pd plating. The composition of the electroless Pd-solution is very similar to that for the nickel solution, save that $PdC\ell_2$ is the metal source. The cells are placed for 45 sec in the electroless Pd-solution which is kept at 50° C and a pH of 9.7. The cells are then rinsed with DI H_2O, dried, and sintered at 300° C for 30 min in a N_2 atmosphere. It might not be necessary to have such a thick Pd-layer prior to the nickel plating. More recently, Motorola has been able to fabricate good cells by electroless plating of nickel over an immersion Pd-layer. Sintering is then done only after the nickel is plated.

2. Electrolytic Plating.

Electrolytic plating is considered in solar cell fabrication primarily for the deposition of copper for the purpose of conduction layer build-up. The most common solution used for plating copper is an acid which consists of approximately 150 to 200g of copper sulfate ($CuSO_4 \cdot 6H_2O$) and 30g of concentrated sulfuric acid in a liter of water.[4] The copper sulfate transports the copper from the anode to the cathode. But because only about 25% of the $CuSO_4$ is ionized in an aqueous solution, the conductivity of a $CuSO_4$ solution is low. Therefore, one of the chief purposes of the sulfuric acid is to increase the conductivity of the electrolytic solution. The conductivity of a 1 n H_2SO_4 is about 6 times larger than that of an equivalent $CuSO_4$ solution - 0.200 mho cm^{-1} compared to 0.035 mho cm^{-1}. In addition, the sulfuric acid promotes anode reduction by reacting with it, and further, by attacking copper aggregates, the sulfuric acid fosters a smooth deposition. Colloidal particles, such as starches, in the electroltic solution also promote smooth deposition by accumulating at the high points of the wafer. Since the high points of the substrate are closer to the anode, heavier deposition is normally experienced there. However, an excessive deposition on high points is reduced by the presence of colloids. Also required for smooth deposits is good wetting of the substrate or cathode surface, since beading of the electrolyte would concentrate deposition into selected areas.

During the electroplating, the solution is kept at a moderately high temperature ($\sim 50^{0}$ C) since the conductivity of the solution increases with temperature. However, the stability of the electrolytic solution sets an upper limit to its operating temperature. Also, the solution has to be agitated during plating, to redistribute the ions and prevent charge accumulation at the electrodes. Further, the electrolytic solution should be constantly filtered through diatomaceous earth to rid it from particulates. The filtering rate should be fast enough to turn over the electrolytic solution once an hour. The accumulation of precipitates, or solid particles, would affect the coherence of the deposition. Since the grid lines are only 5-10 μm thick and 40-120 μm wide, the inclusion of particulates in the grid pattern could be detrimental to the grid line integrity. Another technique, besides filtering, to minimize deposition of solid particles, is to place bags around the electrodes. One suggestion [9] is to use a 10-12 oz. cotton flannel inner bag with a napped polypropylene outer bag.

Unlike electroless and immersion plating, which could be done in a simple flow tank with a recirculating system, electrolytic plating requires fairly large plating tanks. These tanks have to be electrically insulated towards the solution and are therefore normally made of steel with a rubber lining, such as Koroseal from Goodyear. Before a new tank can be used for plating, the tank has to be leached with a

weak alkali solution to remove any loose organics. In order to plate 2400 solar cells of 10 cm x 10 cm size per hour, assuming a cycle time of 5 minutes for the plating operation, two tanks would be required, each of approximately 185 cm x 215 cm surface area and of adequate depth to accommodate one cell placed vertically. In this setup, the tank would contain six anodes parallel to each other along the long side of the tank, placed 30 cm apart. Equidistant from the anodes and the tank walls are five cathode racks, each rack containing 20 wafers, being plated on both sides simultaneously. A plating current density of 60 mA/cm^2 will give a coating thickness of about 6 μm in 5 min using the acid plating solution.[10] In this scheme, it is assumed that an electrical connection can be made to each of the 100 wafers that are in a tank simultaneously. This would require loading and unloading 10 racks with 20 wafers each every 5 minutes, probably by automatic means. It may be noted that the plating current amounts to 6 A per solar cell, or 600 A per tank. It is also to be observed that the tank can be made deeper, and thus accommodate a multiple of the 100 cells per load discussed. This can be used to eliminate the second tank and/or increase plating time or throughput.

For plating copper directly on a nickel grid pattern, the acid bath solution may not be desirable because of the possible displacement reaction between copper ions and nickel metal. The displacement reaction, which occurs because

nickel is more reactive than copper, would result in incoherent deposits. To avoid this reaction, wafers with an electroless nickel coating, could, prior to copper plating, be dipped in an alkaline "coppering" solution. This solution both cleans the surface and deposits, by immersion plating, a thin layer of copper on the nickel surface. The coppering solution is composed of: 50 g of NaOH, to emulsify oil; 50 g NaCN, for complexing metal ions; 50 g of Na_2CO_3, to give the proper pH; and 25 g of CuCN, as the source of copper; and one liter of water.[11] The cyanide complexes with the copper cation, effectively decreasing the copper activity.

Another common electrolytic plating method, which does not require a preceding "coppering" bath, utilizes a copper cyanide plating solution.[4] This solution contains Rochelle Salt ($NaKC_6H_4O_6 \cdot 4H_2O$) which is also a complexing agent, copper cyanide, sodium cyanide, sodium carbonate, and sodium hydroxide. Sodium cyanide complexes with copper as follows:

$$CuCN + 2\ NaCN = Na_2Cu(CN)_3. \qquad (148)$$

The desired operating pH of the Rochelle salt solution is 12.6, which is adjusted by the addition of NaOH or H_2SO_4, depending whether it is desired to raise or lower the pH. The operating temperature of this solution is between 50° and 90° C, and current densities used are between 20 mA/cm^2

and 50 mA/cm^2. Besides being able to plate active metals without a displacement reaction, electrolytic solutions containing cyanide have good throwing power, or the ability to produce even deposits on irregular surfaces. The throwing power of the cyanide containing solution is about five times larger than that of the $CuSO_4$ - H_2SO_4 solution.

It has also been proposed to electroplate nickel grid patterns directly on the silicon wafers. It is undesirable to plate copper directly on silicon because of the detrimental results on cell performance of copper penetration into the junction. The lower conductivity of nickel would require that its plating thickness be about four times larger than that for copper, which, however, may not be practical. The equipment and procedures for nickel plating are similar to that for copper plating, except, of course, for the difference in electrolytic solution and the anode material. To prevent rough deposits, the nickel anodes should be double bagged. One liter of nickel electrolytic solution consists commonly of 327 g of nickel sulfamate ($Ni(SO_3NH_2)_2$), as the nickel carrier, and 30 g of boric acid which acts as a buffer. There are also traces of chemicals added to increase the anode reactivity and the deposition smoothness. Since pure nickel is a fairly inactive anode, a sulfur depolarized nickel anode is used. The optimum operating conditions for the nickel sulfamate solution are a temperature of 49° C,

a pH of 4.0, a current density of 60 mA/m^2, and a voltage between 4 and 8 volts (DC). Approximately 1 mℓ of nickel replenisher solution should be added for every ampere-hour of charge passed through the tank.

C. Thick Film Screen Printing

Screen printing appears to be a very simple process for applying the bulk conducting layer on a solar cell. The application of the conductor in the desired pattern is essentially a one-step operation using a screen printer, requiring neither prior pattern definition nor further conduction layer build-up. The pattern is defined by a wire mesh or metal screen which can be re-used about 10,000 times. However, the currently available thick film procedures are incompatible with the requirements of a low-cost solar cell production line. For one, the only metal that can be practically used for applying contacts to silicon solar cells by screen printing is silver, primarily because of the need for burning off the binder in the ink before sintering the layer. This burning-off of the organic material requires oxygen, which, at the same time, would cause oxidation of the metal particles in the ink, were they of non-noble metals. In the quantities required, silver is too expensive to permit meeting the price goals for the modules. Secondly, the conductance of a layer of screen printed and sintered silver, containing an equal mass of metal as a bulk layer of the same metal,

Table VIB

Metallization Process Options

Process	Applicable Metals	Coating Thickness (um)	Purpose of Coating	Typical Sintering Requirements	Major Steps	Remarks
Thick Film Screen Printing	Ag on Si	12	Chief Cond.	125°C; 15 min for drying followed by 675°-700°C; 90-120 sec.	Screening, sintering	Gridline density is 50-60% of bulk; line width 250 um; Polished surfaces preferred.
"	Sn:MoO3 (75:25). on Si	15	Pattern for chief cond. (solder)	400°C; 5 min to burn out C, followed by 700 °C for 30 min in N_2 and H_2 mixture	Screening, sintering	Small quantities of Ti (20 ppm) decreases contact resistance. Polished surfaces preferred
"	Cu on Si	10-15	back contact only	550°C, 5 min in N_2 for adherence followed by 550° C for 8 min in N_2	Screening, sintering	Cu paste contains AgF_2 to act as a flux and Al-Si eutectic to promote ohmic contact
"	Al on Si	15	back surface field	850°C, 20 sec	Screening, sintering, removal of acess Al	Al-Si eutectic formed during sintering which results in a high conc. of Al in the Si.

is only about half that of the bulk silver layer, due to the limited contact area between adjacent grains in the sintered layer. Therefore, twice as much metal has to be placed on the wafer in a screen printed layer than in a wet chemical or vacuum deposition process. In addition, as the screen printed and sintered lines contain a lot of voids, with a density factor between 40% and 60% of bulk density (see Table VIB), about four times the volume of a bulk metal line is needed for equal conductance. However, the thickness of a screen printed and sintered layer is limited to approximately 20 μm for a single screen printing. A second layer could be applied after sintering the first layer, but this would involve pattern registration and would appear to be even more uneconomical. Thus, a single screen printed layer is equivalent in performance to a 5 μm thick plated layer. Thirdly, the line width in screen printing is, today, still practically limited to 175 to 250 μm minimum, with about 125 μm projected for the future. This limitation causes more shadowing of the cells than experienced by other deposition processes which are capable of smaller line width.

The composition of the screen printing ink usually includes the following: metal particles with a mean diameter of approximately 5 μm; a glass frit to foster metal flow and adherence during sintering (a common type is the Drakenfeld frit which is a lead borosilicate glass $PbO:B_2O_3:SiO_2$ in the mixture 80:10:10 (wt%)); a binder, such as triethyl cellulose,

to hold the ink together; and a solvent, such as trichlor-ethylene or butyl carbitol, to give the ink the correct viscosity. After the ink is applied with a screen printer, it is dried at approximately 125°C for 5-15 min to evaporate the solvent, and then sintered at approximately 700°C for a minute or two, to coalesce the metal particles to each other and to the surface of the wafer. An automatic screen printing machine is projected to print up to 2400 10 cm x 10 cm wafers an hour with a line resolution of 125 μm, using 325 mesh wire screen. A metal screen could print lines with about 50% higher precision than a wire screen, but is considerably more expensive. The function of the screen printing machine is to firmly hold the silicon wafer and screen in fixed position relative to each other, with a close and uniform spacing between them, apply a fixed amount of ink, and to move the squeegee over the screen in order to push the ink through the screen onto the wafer's surface. During the printing or "striking" step, the screen is pushed into contact with the wafer by the squeegee. After the squeegee has passed, the screen "snaps-off" from the wafer, imparting a large sheer force to the ink, and thus hardening it so it can retain its shape. As mentioned earlier, the grid pattern's uniformity and quality is affected by the speed, pressure, and attack angle of the squeegee (angle that the squeegee makes with the screen), and the snap-off (substrate-to-screen) distance. Typical conditions are a squeegee speed of 8.4 cm/sec with

an attack angle of 45°, and a snap-off distance of 0.064 cm[12]. Since the snap-off distance should be constant over the wafer's surface, and because the squeegee excerts a significant downward force on the wafer, it might be difficult to print warped wafers with acceptable yield. The squeegee speed affects the flow properties of the ink. Normally, silver screen printed inks are thixotropic, i.e. they exhibit a hysteresis, which means a finite recovery period after snap-off. A thixotropic ink, as opposed to a pseudoplastic one, will retain its low viscosity for a short time after snap-off.

The ratio of the printed ink's line thickness to width decreases with increasing line width, since relatively more ink sticks to the screen for thinner lines. For 125 μm wide lines, the largest wet ink thickness may be about 20 μm, which results in 10 to 16 μm thickness of the sintered line. This, coupled with the relatively low conductance of the screen-printed lines means, that larger series resistance connected losses will have to be accepted, if screen-printed lines are selected over some other metallization process options.

The current cost of screen-printing silver is dominated by the cost of the silver ink, which in turn is determined by the silver price. A silver price of \$0.40/g (∿ \$12.50/troy oz) has been assumed for these calculations. With a price of \$0.30/g for the glass frit, binders, solvents, and formulation, the total ink price will be \$0.70/g. The process details included in Table I were obtained from "Format A"

information supplied by the respective organizations. In some cases, the process data given were not complete, e.g. screen and squeegee costs were left out.

In order to fit thick film screen printing into the LSA framework, the screening of base metals is being explored. The two principal examples of this effort are the screen printing of an ink based on a mixture of Sn and MoO_3 powder, and one of copper using a AgF flux. (Table VIB). The last process has been used primarily for the formation of the back contact. The thick film application of aluminum to the back surface will not be discussed in this context, since it is applied primarily to form a heavily doped p^+ layer and a high-low junction by the alloy-regrowth process, and usually requires further conduction layer build-up.

The tin:molybdenum oxide screening is a primary step to define the grid for conduction layer build-up by solder dipping.[E3] The ink solids consist of a 3:1 wt ratio of Sn to MoO_3, with one part in 50,000 of $TiSi_2$ added. The titanium silicide is supposed to lower the contact resistance. The ink solids are used in a vehicle which is composed of 75 wt% solvent, e.g. trichlorethylene, and 25 wt% binder, e.g. ethyl cellulose. Two parts of powder are used with one part liquid. After the $Sn:MoO_3$ ink is applied to the wafer by screen printing, the wafer is air dried, heated to 400°C in air to burn-out the carbon, and then sintered at 700°C for half-an-hour in a reducing atmosphere consisting of

hydrogen (40%) and nitrogen (60%). After cool-down, the wafers can be solder dipped.

The application of copper ink using a AgF flux is still in the experimental stage.[14] The AgF which composes about 2 wt% of the ink, melts at 435°C and dissociates at 460°C, with the nascent fluorine reacting with the silicon dioxide and reducing the silica layer thickness. After the Cu:AgF ink is applied by screen printing, it is activated by firing for 5 min at 500°C in nitrogen atmosphere, and then sintered for 8 min in a hydrogen atmosphere at 550°C. The first firing establishes the adherence of the metal to the silicon, the second the bonding of the copper particles to each other. The process does not involve any organic binder which would need to be burnt off, nor any oxide containing flux. Thus, the process can be carried out in an oxygen-free environment and therefore be applied to base metals such as copper. It is still subject to the other limitations of the thick film processes, and it involves handling of the quite costly AgF in a completely dry atmosphere, since it decomposes with very small amounts of moisture.

Currently, adherent and coherent copper contacts have been made to silicon with apparently little cell degradation from copper contamination. Using copper inks, doped with aluminum germanium or aluminum silicon eutectics, to form the back contacts, bare cells with efficiencies of 9.4% have been produced.[15]

Table VIC

Metallization Process Options

Process	Applicable Metals	Coating Thickness	Purpose of Coating	Typical Sintering Requirements	Major Steps	Remarks
Midfilm	Ag on Si	8.5	Chief Cond.	650°C, 60-100 sec; 700°C, 30-70 sec in air	Applying Midfilm, exposure, applying metal, sintering	Works best with spherical particles resolution about 50 um
"	Cu:Sn	Not available	-	700°C for 5 mm in N_2	Same as above	Sucessfully fired on Si wafers only
Vaccuum deposition	Ti:Pd:Ag on Si	0.01:0.01:5	Bonding:barrier Chief cond.	None	Load, evaporation unload	Used for space cells
	Ni:Cu on Ng	0.5:10	Barrier: chief cond.	None	Load, evaporation, unload	Modification of above procedure
Solder dipping	Sn:Pb (60:40) on Ni	>55	Chief cond.	None	Flux dip, solder dip, clean, rinse and dry	Must have metal pattern. Thicker on bus bars.

D. Physical Vapor Deposition.

Physical vapor deposition, particularly in the form of vacuum evaporation, has also been used in large scale manufacturing of various products. Although it often is reputed to be a high-cost process, it has been applied, for instance, for the mass production of metallized plastic parts for low-priced merchandise, such as toy cars. The process is also capable of automation, as the successful operation of several fully automated vacuum process lines for the low-cost deposition of precision four-layer optical interference coatings at OCLI (Santa Rosa, CA) shows.

Physical vapor deposition (PVD), or vacuum evaporation, has been employed for years in the fabrication of space solar cells, as well as in much of integrated circuit manufacture. The generally used metal layer combination for space cells includes an about 100 Å thick titanium layer directly on the silicon to ascertain an ohmic contact as well as the adherance of subsequent layers. The Ti layer is followed by a 100 Å thick Pd-layer which protects the titanium layer from oxidation and hydrolization. The last layer is about 5 μm of silver to serve as the bulk conductor.

One of the attributes of the physical vapor deposition process is that it has to be carried out in a controlled environment, namely in a high vacuum in the case of vacuum evaporation or ion plating, or a low pressure gas such as argon in the case of sputtering. This causes some complica-

tion for the loading and unloading of the work in process. In laboratory type and small production equipment, the chamber is opened to the atmosphere for unloading and loading. Subsequently, the chamber is closed and pumped down to the required vacuum level. This pump-down requires some time, often 15 to 30 minutes, during which the relatively capital intensive equipment, and often also its operator, are not productive. Installation of larger capacity pumps - an additional capital investment - can reduce this pump-down time to approximately 5 to 10 minutes. For mass production purposes, continuously operating conveyerized systems have been investigated about ten years ago. These systems are always open at the loading and unloading sides, although the openings are restricted as far as possible. Thus, in front and behind the actual process chamber in which a high vacuum is continuously maintained, a sequence of pumps has been installed to achieve a suitable pressure gradient between the outside environment and the pressure in the process chamber. This approach requires large equipment and considerable energy consumption for the continuous maintenance of the pressure gradient. This equipment is therefore not considered economical, and is no longer produced. The alternative for mass production is a quasi-batch operation with airlock chambers for the loading and unloading of the work in process. These airlocks are located between the ambient and the process chamber which, in this approach, is also

continuously maintained at the high operating vacuum. For entry or exit of work in process, the airlock is opened to the ambient, while closed to the process chamber. The gate to the ambient is then closed vacuum tight, and the airlock pumped down to the pressure of the process chamber. Subsequently, the gate to the process chamber is opened to permit passage of the work in process between the airlock and the process chamber. After closing this gate again, the pressure in the airlock is raised to the ambient pressure, usually simply by admitting outside air. For large production systems, two airlock chambers are usually provided, to permit separate entry and exit means for the work in process, and to permit a smoother material flow.

Energy is continuously consumed in vacuum deposition systems for the pumping to maintain the required pressure in the process chamber, and somewhat more intermittently for the pump-down in the airlock chambers. In addition, the substrates are sometimes electrically heated to an elevated temperature during the deposition process. Finally, energy is needed for heating and evaporating the material to be deposited. This heating is now frequently done by an electron beam.

The vacuum deposition process is a highly controllable process, both with respect to the quality of the deposited materials and to the layer thickness, as well as their uniformity. However, even in a high vacuum process (about 10^{-6} Torr) there are some residual gases in the process

chamber, some originating from backstreaming of oil from the vacuum pumps. These gases can interact with the material to be deposited or enter into the deposited layer, somewhat modifying its properties. Through proper vacuum chamber construction and maintenance, however, this contamination problem can be adequately controlled. In the systems which are equipped with airlocks, and where the process chamber is continuously maintained at the operating vacuum level, the possibilities for contamination are greatly reduced in comparison to those systems which are periodically opened to the atmosphere.

Since there is no significant chemical reaction at the wafer surface during physical vapor deposition, adherence to the substrate depends mostly on van der Waals forces. Therefore, coating adherence depends strongly on surface condition. The presence of water vapor, adsorbed gases, carbon layers or grease on the wafer's surface, can greatly reduce adherence. The wafer, therefore, has to be thoroughly washed, degreased, (possibly by vapor degreasing with appropriate solvents), rinsed, and dried before placement in the vacuum chamber. Additional cleaning can be done in the vacuum chamber after pump-down. One method employs a low energy glow discharge, which provides ions which can knock loose contaminants from the surface. Baking out of the water at up to 300°C is another method. It will remove water vapor and other adsorbed gases. However, a carbonaceous layer may form from the cracking of residual hydrocarbons.

One of the major problems with vacuum deposition is that the material evaporated from the source does not deposit only on the desired areas. The evaporated material leaves the "source" on straight line trajectories and deposits on all surfaces in its path. While simple laboratory type sources deposit material into a hemisphere around the source, more sophisticated sources, or "boats", incorporate baffles and "chimneys" to restrict the exit angle and deposit material predominately in a cone which does not have to be significantly larger than that containing the work in process. Nevertheless, there is always some overspray, as well as material transport to gaps between individual pieces of the work in process, which results in a deposition of material on parts of the equipment. Thus, the equipment has to be opened periodically and partially torn down to permit removal of this unwanted deposit. It is noteworthy that about 75% of this spuriously deposited material can be reclaimed.

Patterns in the deposit can be readily defined by repeatably usable "shadow masks" which are positioned close to the work in process in the path of the evaporated material. An alternative is the application to the work in process of a temporary mask, a "resist", such as a photoresist. Where mechanical shadow masking is used, evaporated material will gradually build up on the mask, and will restrict its pattern openings. Thus, after a certain period of time, the mask has to be removed and cleaned, requiring

the expenditure of labor and chemicals. Again, about 50% of the material deposited on the mask can be reclaimed. As a result of these handling and cleaning operations, however, the mask life becomes limited.

In many applications, the source boats have to be brought periodically to rather elevated temperatures and cooled down again, which reduces their useful life. A further life limitation of the source boat is, at times, caused by interaction between the boat material and the material to be evaporated. Nevertheless, 1000 lbs of copper have been evaporated from one graphite source boat in a large production system.[16]

Vacuum evaporation has the following attributes which are beneficial for large scale solar cell production: a well controllable, automatic process, capable of yielding very fine line (< 10 μm) patterns, and of providing layers of bulk material properties, and capable of pattern generation with reusable masks. It has, however, also a number of undesirable attributes which include impracticality of simultaneous deposition on both sides of the wafer, thus essentially doubling the capital costs[16], material loss through overspray and deposition on the masks, which result in the need for cleaning masks and chamber, need for periodic replacement of masks, source boats, and pump oil, and considerable, though tolerable, energy consumption. These attributes tend to make the process more costly than some

of the wet chemical options.

These problems tend to make the process unsuitable for the deposition of thick, fine line patterns. When a pattern of 10 μm thick conductors of 25 μm line width, as found desirable in the pattern optimization studies, is to be produced, then the 10 μm deposit would tend to reduce the width of the openings in the mask so much as to require cleaning after only a few depositions. This would drive the costs up intolerably. The alternative would be to use a disposable mask, a resist, on the wafer. With the required small line width, the resist application may require photolithography, a process of higher, but probably tolerable costs. However, a 10 μm thick film has a significant lateral strength. This thickness may not be adequately reduced at the steps between masked and unmasked areas to permit separation of the deposited film there without significant weakening or even destruction of the bond between metal and semiconductor in the unmasked areas. Such separation is usually no problem on thin films, with perhaps up to a micrometer thickness. These problems would not occur in depositions on the back of the wafers without masking.

Table VII

Principal Metallization Process Options

I. Contact Masking

A. Standard positive or negative photoresist procedures (Kodak, Shipley, etc.)

B. Midfilm process (developmental) (Spectrolab)

C. Printing of resist (offset, screen, etc.)

D. Spraying of resist

E. Plasma etching (shadow mask) of AR coating (Motorola)

II. Plating

A. Pd (immersion + electroless)/Ni(electroless)/solder (dip) (Motorola)

B. Pd (immersion + electroless)/Ni(electroless)/Cu (electrolytic) (Motorola)

C. Pd (immersion)/Ni(electroless)/Cu(electrolytic) (Motorola)

D. Ni (electroless)/Cu(electrolytic) (ASEC)

E. Au (electroless)/Ni(electroless)/solder (dip) (Photowatt, Solar Power, Solar Systems)

F. Ni(electroless)/solder (dip) (Solarex)

III. Thick-film screen printing

A. Ag ink with glass frit (ARCO Solar)

B. MoO_3:Sn ink (developmental) (SOL/LOS)

C. Fritless Ag or Cu ink using AgF and germanium or silicon alloys as fluxes (developmental) (Bernd Ross Assoc.)

IV. Vacuum deposition

A. Ti-Pd-Ag evaporation (Spectrolab, ASEC)

B. Ti-Pd evaporation followed by electroplating of Ag (Spectrolab, ASEC)

C. Ti-Pd evaporation followed by electroplating of Cu (Westinghouse)

XI. The Principal Metallization Process Options

From the large matrix of potentially useful metallization process options, the more important processes are listed in Table VII. In regular manufacture of solar cells, so far only the plating processes E and F have been applied, as well as the thick film printing process III A, and the vacuum deposition process IV A. The latter, as a system of proven high reliability on high performance solar cells, has been applied primarily in the fabrication of cells for application on spacecraft. The remaining processes are either developmental or have been used in pilot line fabrication of solar cells. However, a few of these processes, such as II D or IV C, may become production processes in the near future.

Not mentioned in Table VII have been sintering steps, which are used with all thick film processes, and have also been applied after most immersion or electroless plating steps, as well as after the vacuum deposition of silver. The metallization processes which include a solder dip, have generally been carried out without a separate sintering step. The brief heating cycle connected with the solder dip, however, may have a similar effect as a sintering step.

Through the years, it has been found again and again, that electroless plated layers without a subsequent sintering step tend to show occasional incidences of weak contact adhesion. Experience has also shown that the electroless plating of nickel on silicon is a process which is difficult

Table VIII

A. Plating

1) Pd-Ni-solder (Motorola)

a) Immersion Pd Coat and Sinter

1. Dip for 10 sec in a 10:1 H_2O:HF solution, followed by a DIH_2O rinse (30 sec in a 50:1 H_2O:HF solution, no DIH_2O rinse).

2. Immersion Pd for 2 min, followed by DIH_2O rinse (immersion Pd for 3 min, followed by a 5 min DIH_2O rinse.)

Option A.

(3) Aqua regia dip for 5 sec, followed by a 15 min DIH_2O rinse.

(4) Dip for 20 sec in a 50:1 H_2O:HF Solution

(5) Immersion Pd for 5 min, followed by a 5 min DIH_2O rinse.

(6) Spin dry and inspection.

(7) Sinter for 15 min @ 300°C with N_2 purge.

(8) Dip for 20 sec in a 50:1 H_2O:HF solution.

(9) Immersion Pd coat for 2 min, followed by a 2 min DIH_2O rinse.

Option B.

3. Spin-dry and inspection.

4. Sinter for 30 min @ 300°C with N_2 purge.

5. High pressure scrub (both sides).

6. Dip for 5 sec in 10:1 H_2O:HF solution, followed by DIH_2O rinse.

7. Immersion Pd coat for 15 sec, followed by a DIH_2O dip.

b) Electroless Pd Coat and Sinter

1. Electroless Pd coat for 95 sec, followed by DIH_2O rinse. (electroless Pd coat for 45 sec, followed by a 10 min DIH_2O rinse).
2. Spin-dry and inspection.
3. Sinter for 30 min at 600°C with N_2 purge (300°C for 15 min with N_2 purge).

c) Electroless Ni plating

1. Electroless Ni plate for 5 min at 80°C, followed by 10 min DIH_2O rinse.
2. Spin-dry and inspection.

---

d) Solder

1. Immerse cell in solder flux (type RA, Kester 1544), and allow excess to drain.
2. Immersion in solder (Kester 60:40 Sn:Pb) at 240°C for 1 sec.
3. Remove excess flux by agitating in TCE.
4. Second dip in TCE.
5. let stand in acetone for 5 min.
6. Rinse in DIH_2O and spin-dry.

Note: The process details listed as Option A as well as those shown in parenthesis at other steps were obtained from the LSA Process Specification Format supplied by Motorola.

The remaining details were obtained from Motorola Quarterly and Final Reports, as well as by private communication of H. Goldman with Motorola personnel.

2) <u>Au-Ni Plating (Sensor Technology)</u>

1. Dip for 30 sec in concentrated 48% HF.

2. Electroless gold coating dip for 30 sec, followed by a DIH_2O rinse for 4 min (Small quantities of HF have been added to the gold solution for the reaction to proceed at RT).

3. Electroless Ni plating at 83°C for 4 min, followed by two deionized water rinses of 4 min each.

4. Spin-dry and inspection.

Note: Solar Power Corp. and Solar Systems, Inc. also do electroless Ni plating, apparently with preceding electroless gold plating, but their detailed procedures are not available.

B. Thick Film Processes (Screen-Printing)

1) Thick Film Screen Printing (RCA)

1. Mixing of metal powder (90 wt% Ag) and frit (10 wt% lead borosilicate) with organic vehicle (6 wt% ethyl cellulose (N-300) and 94 wt% Carbitol).

2. Screen printing of metal pattern on wafer (includes preparation, mounting, and cleaning of screen).

3. Heat treatment of wafer for drying and removing volatiles: 15 minutes at 125°C; followed by a 90-120 sec sinter at 675-700°C.

2) Thick Film Screen Printing of MoO_3:Sn (SOL/LOS)

1. A 4:1 wt mixture of Sn:MoO_3 is blended in a 2:1 wt ratio with an organic vehicle which consists of 25 wt% ethyl cellulose and 75 wt% trichloroethylene. Traces of titanium resins are added to the ink (to ensure an ohmic contact?).

2. Screen printing of wafers.

3. The wafers are air dried to remove volatiles, baked at 400°C to burn out carbon, and heated at 700°C for 0.5h in a nitrogen and hydrogen atmosphere to reduce the MoO_3 and sinter the metal contact.

3) Thick Film Screen Printing of an Al BSF and Contact (Spectrolab)

1. Etch back-surface with HF for 15-60 sec, DIH_2O rinse and dry.

2. Screen print Al ink using a 200 mesh screen. The ink consists of 70% Al, 28% terpineol, and 2% ethyl cellulose. Size of Al particles is 6-8 μm.

3. Air dry at 250°C for 10-15 min.

4. Melt in air at 900°C for 30 sec.

5. Removal of oxidized Al by dipping in 1% NaOH solution, followed by ultrasonic cleaning.

C. Photoresist Type Processes

1) Typical Photoresist Process (Kodak)

1. Application of Koday Micro Positive Resist 809 photoresist to wafer with spinning at 5200 rpm for 30 sec.
2. Pre-baking of wafer for 30 min at 90°C.
3. Exposure through a mask with a 200 Watt high pressure Hg lamp for 8-10 sec (energy flux $\geq$ 170 mW/cm^2).
4. Development with agitated Micro Positive Resist Developer diluted 1:1 with H_2O, followed by a deionized water rinse for 30 sec.
5. Air dry with jet of nitrogen.
6. Post-bake at 90°C for 30 min.
7. Mild HF etch.
8. Application of metal (i.e. by vapor deposition, dipping, plating, etc.).
9. Washing away of undeveloped resist with isopropyl alcohol for 30 sec, followed by a 5 sec deionized water rinse.

2) MIDFILM Process (Sepctrolab)

1. Application of MIDFILM photoresist resin either by spin-on or spray-on. Wafers are first rinsed with trichloroethane.
2. Exposure of coated wafer with a mercury lamp through a mask (28 mW/cm^2 for 3 sec).
3. Application of metal powder and removal of excess powder.
4. Sintering of wafer at 600°-800°C for 40-60 sec.

D. Vacuum Metal Deposition and Plating

1) Ti-Pd-Aℓ-Ni deposition followed by Ag plating (Westinghouse).

1. Wafers are loaded into the entrance airlock portion of the vacuum deposition system which is pumped down for 15 minutes. The wafers are then transported into the deposition chamber. The metal fluxes are: 0.09 g/m^2 for Ti, 0.242 g/m^2 for Pd, 8 g/m^2 for Aℓ, and 0.054 g/m^2 for Ni. After this, the wafers are transported into the exit airlock portion of the system where they are brought up to atmospheric pressure.

2. Dip in a buffer solution for 15 min.

3. Stripping of photoresist with overlying metal in acetone for 20 min.

4. Sintering for 20 min at 400°C in N_2 atm.

5. Electroplating of silver for 5 min.

6. DIH_2O rinse and dry.

to control. To improve process control, a number of organizations prefer to precede the electroless nickel plating by one or more electroless plating steps depositing gold or palladium layers. At times, however, these processes have exhibited their own control problems, which led to a lively debate of their real merits. Since statistics on the process control problem or the associated cell yields are not available, this variable between the different process options could not be entered into the economic analysis.

Details of the process sequences, as they were given in various progress reports by contractors of the LSA program, are summarized in Table VIII. Such detailed process descriptions can form the starting point for an economic analysis.

In the thick film (screen printing) processes, the printing inks are found to be the major cost item. The formulation of these inks has become the basis of an industry of apparently prosperous small companies, except that one of the major suppliers is E.I. DuPont de Nemours and Company. The industry jealously guards its "trade secrets" in the largely empirically evolved formulation of these inks, although they seem to be quite well known within the industry. Under the LSA program, two companies have given details on the formulation of these inks. This information is summarized in Table IX. It is noteworthy that these inks generally have a relatively low metal content. Consequently, upon drying and sintering, the volume of the ink shrinks to approximately 50% of that

PRECEDING PAGE BLANK NOT FILMED

Table IX

Comparison of the Compositions of the Inks Used by RCA and Lockheed

A) RCA Ink: (80 wt% solid, 72 wt% Ag)

Source: RCA Process Specification for Thick Film Screen Printed Metallization

The ink constituents are:

	Wt%	ρ (g/cm^3)	Vol %
		Solids	
Ag	90.3	10.49	85.0
glass frit	9.7	6.376	15.0
		Vehicle	
butyl carbitol	94	0.99	94.3
ethyl cellulose	6	1.13	5.7
		Ink	
Solids	80	9.872	28.8
Vehicle	20	0.997	71.2

The density of the solids is equal to:

$$\rho_{solid} = (0.903/10.49 + 0.097/6.376)^{-1}$$
$$= 9.872 \text{ g/cm}^3,$$

while the vehicle density is:

$$\rho_{veh} = (0.94/0.99 + 0.06/1.13)^{-1}$$
$$= 0.997 \text{ g/ml}.$$

The ink density is then:

$$\rho_{ink} = (0.20/0.997 + 0.80/9.872)^{-1}$$
$$= 3.552 \text{ g/cm}^3.$$

It can be readily shown that the volume fraction of the solids in the wet ink is given by:

$$V_{solid} = \frac{\rho_{ink} - \rho_{veh}}{\rho_{solids} - \rho_{veh}} = 0.288$$

During drying and firing, the ink has been reported to shrink to about half its volume. Therefore the solid volume fraction in the sintered ink should be 57.6%.

B) Lockheed (65 wt% Ag, Dupont 7095 ink)

Source: Lockheed, Final Report DoE/JPL 954898-78/4, p. A-29 (10/78).
W. Robson, Dupont, private communication (9/79).

The ink constituents are:

	Wt%	ρ (g/cm³)	Vol %
		Solids	
Ag	93 †	10.49	81.6
Glass Frit	7 †	3.5	18.4
		Vehicle	
Dupont 8250	95 *	0.94	95.8
ethyl cellulose	5 *	1.13	4.2
		Ink	
Solids	69.9 †	9.203	19.3
Vehicle	30.1 †	0.9480	80.7

Using the procedures as shown in the first part of this Table, the following values are obtained:

$$\rho_{solid} = 9.203,$$

$$\rho_{veh} = 0.948,$$

$$\rho_{ink} = 2.541,$$

and

$$V_{solids} = 19.3\% .$$

Lockheed reports a volume shrinkage of 50% in drying, which would lead to solids volume of 38.6% in the dried ink. There may be additional shrinkage upon sintering.

* estimated
† given by DuPont.

of the wet ink, as applied. Also, because of ink viscosity and screen geometry, the maximum application thickness of the wet ink is usually considered to be 20 to 25 μm, resulting in a line thickness near 10 to 12.5 μm after sintering. RCA, however, has been able to formulate an ink which can repeatably be applied in 25 μm thickness (wet), and which shrinks only to about 80% of its original volume upon sintering, that is, to a line thickness of about 20 μm.

Six generic metallization processes have been selected for a more detailed comparative analysis. The available information on these processes has been tabulated on UPPC formats which are contained in Appendix I. These six processes are: thick film screen printing as a process which requires neither masking nor a strike or barrier layer; electroless nickel plating for the formation of a strike or barrier layer; vacuum evaporation for consecutive deposition of a nickel barrier layer and a copper conduction layer; sputtering of a copper conduction layer; electrolytic plating of a copper conduction layer; and, finally, solder dipping for build-up of a conduction layer over a metal strike layer which, for this case, usually is nickel.

The thick film screen printing process is essentially a state-of-the-art process, using automatic cassette unloaders and loaders, automated single wafer handling including a collator between the screen printer output and the belt furnace (or furnaces) used for drying and sintering.

The electroless plating process described here is a conceptual scale-up of the current, essentially beaker-type plating operations, projected to use automatic wafer handling into and out of the baths, as well as automatic liquid recirculation and replenishment of the plating and rinsing baths. The vacuum evaporation process is based on a large scale, fully automated deposition system with continuous evaporation. Similar systems have been built and operated successfully, although not in the semiconductor or solar cell industries. The wafers would move past the evaporation boats on their wafer/mask holders on a one meter wide track, that is about nine 10 cm x 10 cm cells abreast, and the source material would be evaporated from approximately one meter long graphite boats which are heated by electron beams. The wafer/mask holders would enter the system in batches through an airlock and be disassembled from the batches into a continuous flow within the deposition chamber. After complete metal deposition on one side, the wafer/mask holders are turned over for deposition on the second side, as all evaporation takes place upward from the source boats. After completion of the deposition on the second side, the wafer/mask holders are reassembled into batches for exit from the system through a second airlock.

The sputter deposition would proceed in a way similar to that projected for the vacuum deposition. Here, the deposition of only one metal has been considered. Also,

the system studied here has a lower capacity than that investigated for vacuum deposition. While the sputter deposition system does not need the electron beam guns and their power supplies, which the vacuum deposition system incorporates, it needs rf power supplies to maintain the glow discharge for sputtering. Also, the sputter targets need to be replaced periodically, while the source metal can be supplied continuously for vacuum deposition. Further, the sputter system needs gas pressure and flow control. Beyond this, the systems should be quite similar.

For the electrolytic deposition of copper over a pre-existing strike layer, two different types of automated plating systems have been proposed by two different fabricators of such systems. The one is an inline tank system, called a finger plating system, where each individual cell would, after unloading from a cassette, be automatically attached to a holder ("finger") which also makes the electrical cathode contacts.[17] These fingers are attached to a belt or chain. They immerse the cells sequentially and for the appropriate times into the various plating and rinse tanks. The required immersion times and the belt speed determine the physical lengths of the tanks, which turns out to be of the order of 60 feet for the throughput rates required here. The wafers are assumed here to be plated on both sides simultaneously. The second plating system is a "carousel" machine where holders, with groups of cells attached, are immersed in a tank for a

given time period, then removed and transported to the next tank in a circular movement, and immersed there.[18] While the finger plating machine is based on continuous, linear movement, the carousel machine works with periodic movement. Here, the tanks have only to be large enough to hold the required number of holders in essentially stationary fashion. Both machines function equally automated, and their prices, for the same throughput rate, are comparable, that is approximately a quarter million dollars. Exact prices will be available only after such a machine has been fully specified and pre-designed.

XII. Selection of Metals for the Conduction Layer

The question of a process sequence, or several sequences ultimately to be selected for the low cost fabrication of high performance solar cells, is closely connected with the selection of the metal to be used for the conduction layer of the solar cell. Since this layer constitutes a significant amount of metal on the cell, the cost of the raw metal alone can make a major process cost contribution. In addition, a given process usually is not capable of depositing any selected metal. Thus, the selection of the metal will, to a degree, determine the ultimate process selection. This may be illuminated by the example of the thick film processes. The conventional thick film processes are principally of very low cost in their execution. They use relatively inexpensive equipment of high throughput rates, with little labor required for the operation. However, in the conventional form of these thick film processes, reasonably good conductance in the metal layers can be achieved only by the use of silver which is a rather expensive metal. Of the two developmental processes in thick film deposition, the molybdenumtrioxide/tin process uses tin for the conduction layer which also is rather expensive in the thicknesses needed to achieve adequately low sheet resistance, while the fritless process which is still in relatively early development, could apply the inexpensive copper.

PRECEDING PAGE BLANK NOT FILMED

TABLE X

Physical and Cost Data of Various Metals of Interest for Solar Cell Metallization

1	2	3	4	5	6	7	8
Metal	Resistivity μΩcm	Density g/cm^2	1975 Price ¢/g	Thickness needed for 1.67 mΩ sheet resistance μm	Mass needed to cover 1m^2 at this thickness g/m^2	Cost of metal for this layer ¢/m^2	Cost of metal for a 100 Å thick layer ¢/m^2
Aluminum (Al)	2.655	2.7	0.05 [1]	15.9	42.9	3.86	0.002
Copper (Cu)	1.67	9.0	0.14 [1]	10.0	90.0	12.6	-
Molybdenum (Mo)	5.2	10.2	7.0 [3]	31.1	317	2220	0.71
Nickel (Ni)	6.85	8.9	0.485 [1]	41.0	365	177	0.04
Gold (Au)	2.35	19.3	450 [1]	14.1	272	122,460	86.9
Palladium (Pd)	10.8	11.4	177 [3]	64.7	738	130,550	20.2
Platinum (Pt)	10.5	21.45	514 [1]	62.9	1349	693,490	110
Silver (Ag)	1.6	10.5	16.14 [1]	9.6	100.8	1627	1.7
Solder (50:50 Sn:Pb)	15	8.9	0.7 [3]	89.8	799	559	-
Tin (Sn)	11	7.3	0.67 [1]	65.9	481	332	0.05
Titanium (Ti)	43	4.5	7.0 [2]	257.5	1159	8110	0.32
Tungsten (W)	5.65	19.3	7.0 [3]	33.8	652	4570	1.35
Zirconium (Zr)	41	6.5	48 [3]	245.5	1596	7660	3.12

1. Electronic News, 20 (1060) (12/75).
2. SAMICS Cost Account Catalog, ERDA/JPL-954800-77/21 (9/77).
3. MC/B Chemical Reference Manual (6/73).

These metal cost considerations are illustrated in Table X which lists the more likely metals to be used in the metallization process, the thickness of a layer needed to achieve the same sheet resistance as a 10 μm thick layer of copper, and the costs of a square meter of such a layer. It is seen that this metal cost alone of such a layer covers five orders of magnitude, and that for only two candidate metals, aluminum and copper, the cost is in a range where it does not make a major contribution to the total cost of metallization. Even tin, whose price per unit mass does not differ greatly from that of aluminum or copper, has to be used in such a thick layer that the metal cost for a layer of comparable conduction is two orders of magnitude above that of the other two metals. This large required thickness is the consequence of tin's relatively high resistivity.

In contrast to the requirements of the conduction layer, a number of metals are applicable for use in strike or barrier layers. In this application, the metals may be used in layer thicknesses in the order of twenty to a few hundred Angstroms. To permit an evaluation of the metal cost for use in such strike or barrier layers, the cost of a one-hundred Angstrom thick layer of metal has also been listed in Table X.

It may be noted that outside of the resistivity, the density of the metal plays a significant role towards its ultimate cost. An example of this is a comparison between aluminum and copper. As the resistivity of aluminum is

proximately 50% higher than that of copper, the layer thickness needed for equal sheet resistance is also approximately 50% higher. However, the density of aluminum is less than 1/3 of that of copper, so that the total mass of aluminum needed on a square meter is less than half of that of copper. Since the metal prices are always based on unit mass, and the aluminum price is approximately 2/3 of that of copper for equal mass, the final cost of the conduction layer for aluminum ends up being less than 1/3 of that of copper.

It may be noted that this discussion has not provided the complete picture for the cost of metal used in a particular process. As was discussed in section X of this report, not every type of process results in bulk conductivity of the deposited metal layer. Thus, a larger amount of metal may actually be needed to achieve the same sheet resistance as a layer of bulk conductivity. In addition, different deposition processes utilize the metal at differing efficiencies. This means that frequently, only a fraction of the metal used is actually deposited on the desired areas of the cell. This leads to significant variations in the cost of the metal actually used in the different processes.

XIII. Metal Utilization in the Various Deposition Process

The electroless and electrolytic plating systems, as well as the solder dipping of partially metallized semiconductors, generally deposit material only on the areas to be plated, either because they are already covered by a strike layer or because the not-to-be-plated areas are covered with a contact mask (resist). Also, the metal contained in the plating baths can be utilized very effectively, particularly through the praxis of "replenishing". Consequently, these processes have a high "plating efficiency", which refers to the source metal utilization.

In contrast, the vacuum deposition methods "spray" the deposition material in a cone from the source, and deposit it both on the to-be-plated and the not-to-be-plated areas. This causes large differences in the so-called plating efficiency. A significant fraction of the spuriously deposited material can, however, be recycled, that is repurified and formed into the shape required for the source material of the deposition process. For copper deposition, the primary requirement is adequate purity of the metal, and freedom from oxygen. For vacuum deposition, the copper is fed in wire or rod form to the source boats, while in sputter deposition, the material has to be brought into the shape of the targets, which usually are flat plates. Also, the sputter targets cannot be fully utilized, so that a part of the target material has to be recycled. Consequently, in the following analysis,

the material usage is divided into that of virgin material and that of recycled material.

Of the total material evaporated from the source, only a fraction ends up on the desired areas of the substrate. Other fractions of the material are deposited on the walls and other interior parts of the vacuum evaporation chamber, on the mechanical device which holds the substrates and masks in their relative positions, (usually called the substrate holder), and on the masks themselves. A part of this spuriously deposited material can be reclaimed. Consequently, two prices for the source material will be applicable. One will be the price of the "virgin" material, which is composed of the commercial raw material price plus the price of further processing to the desired purity level and the physical shapes required. These may be rods or pellets for vacuum evaporation, or flat plates for the targets of sputter systems. The other is the price of the recycled material which may contain the price of further purification costs, depending on the condition and purity of the reclaimed material, and of physical shaping.

Four different quantities relative to the amount of source material used are of interest. The first one is the gross amount of material used which is the amount of material evaporated or sputtered from the source. This quantity is of importance for determining the life of the source boat or of the sputter target, and for determining the rate at which the source material has to be supplied. A second quantity

is the amount of material which actually ends up on the substrate. This is the real "direct material". The third quantity is the net amount of source material used, which is the material deposited on the substrate plus the amount of material lost in one cycle of the process. This is the amount of source material to be bought at the price of the virgin material. The fourth quantity finally is the amount of material reclaimed, which can be replaced at the recycling price.

The "gross deposition area" is determined by the holder. This area is composed of the projected area of the holder itself, excluding any open areas, and the area of the masks, including their openings, A_{mask}. This gross deposition area shall be designated as the "holder area" A_{hold}. Only a fraction of the material which leaves the source boat is actually deposited on this holder area. This fraction is commonly called the deposition efficiency η_{dep}.

Deposition will generally be carried out until a certain thickness d of the deposited layer has been reached. Since, in the case of solar cells, metal has to be deposited both on the front and the rear surfaces of the substrate, two different thicknesses d_F and d_R for the front and rear deposited layers, respectively, may be involved. The mass M_{evap} of the gross amount of source material used is then determined by:

$$M_{evap} = \frac{A_{hold}}{\eta_{dep}} (d_F + d_R) \; \rho_{Met} \; ; \tag{149}$$

where ρ_{Met} is the density of the source material. The deposition efficiency is an empirical quantity which depends on the set-up of the given deposition apparatus. It will normally be determined experimentally from the holder area and the gross amount of material evaporated, in inverse application of eq. (149). A number of 70% has been quoted for the deposition efficiency as representative of experience data in large area depositions, as discussed here.

The mass M_{subs} of the material deposited on the desired areas of the substrate is given by:

$$M_{subs} = (A_{subs,F} d_F + A_{subs,R} d_R) \; \rho_{Met} \; ; \tag{150}$$

This quantity is part of the net amount of metal used, whose mass M_{net} is expressed by:

$$\begin{aligned} M_{net} = A_{hold} \rho_{Met} \Bigg\{ & \frac{1-\eta_{dep}}{\eta_{dep}} (d_F + d_R)(1-r_{wall}) \\ & + (1-f_{hold})(d_F + d_R)(1-r_{hold}) + f_{hold} \\ & \cdot \Big[(1-f_{mask,F}) \; d_F + (1-f_{mask,R}) \; d_R \Big] \; (1-r_{mask}) \Bigg\} \\ & + M_{subs} \; ; \end{aligned} \tag{151}$$

In this equation, the first term in the large brackets represents that amount of material which is deposited on the walls and other parts of the vacuum system, and which is not

recycled. It is expressed as the gross amount of material evaporated minus the material deposited on the holder area, multiplied by $(1-r_{wall})$ where r_{wall} is the fraction of this material whicl is recycled. The second term in the large brackets of eq. (151) gives the fraction of the material deposited on A_{hold}, but excluding the material deposited on the mask area A_{mask}, expressed by the factor $(1-f_{hold})$. Again, the fraction $(1-r_{hold})$ of this material is not recycled.

Finally, the last term in the large brackets describes the material which is deposited on the masks, but excluding that deposited on the substrate areas which are represented by the openings in the mask. Again, the fraction $(1-r_{mask})$ is not recycled and enters here. The last term outside of the brackets finally is the material deposited on the desired areas of the substrate (M_{subs}), as given by eq. (150).

The mass of the material that is recycled, finally is given by:

$$M_{recl} = A_{hold}\rho_{Met} \left\{ \frac{1-\eta_{dep}}{\eta_{dep}} (d_F + d_R)\, r_{wall} + (1-f_{hold})(d_F + d_R)\, r_{hold} + f_{hold} \left[(1-f_{mask,F})\, d_F + (1-f_{mask,R})\, d_R \right] r_{mask} \right\} \tag{152}$$

This relationship essentially contains the three terms in the large bracket of eq. (151), except that the fractions recycled, r, appears rather than $(1-r)$.

XIV. Comparative Economic Evaluation

So far, only the metal deposition processes by themselves have been evaluated, that is excluding any masking or mask removal steps, where these are separate from the metallization process itself. In these evaluation activities, it has been found more difficult to attain adequate process data for a meaningful evaluation than it has been with the processes analyzed previously. Part of this difficulty is probably attributable to the larger variety of processes used in this area. Beyond this, however, it was found more difficult even to attain a consistent set of data on an existing process with a good experience base. Such an economical data set of a well-understood process has been used as the basis for extrapolation to the future large-scale processes in the other process areas. In addition, it appears that the jump in process technology from the processes currently used for solar cell metallization, to those to be applied in the future is, at least in the automation part, larger in this process area than in those analyzed previously. This is best illustrated by the fact that a significant part of current metallization is based on a vacuum deposition process which, although called automated, does not differ significantly from those used with laboratory type evaporation systems. Much of the alternate metallization used on current production lines is based on the electroless nickel plating process, which is carried out in a manner very close to a

beaker type of operation, that is on a near laboratory scale. The only process used to some extent in current solar cell production which is close to an automated large scale process, is the thick film process. This process, however, will be less attractive for the future because of the high metal cost and the limit on achievable line width.

To achieve a comparison basis for the principal process options, projections have been made to the performance of these processes at comparable production rates, and with equipment of comparable levels of automation. For this comparison purpose, the six generic processes listed in section II of this report have been selected and subjected to these extrapolations. One of these processes includes the pattern definition as such: the thick film deposition process. The other processes require masking of one type or another for the pattern definition, and their costs have not been included in the present analysis. In some cases, the AR-coating serves as the mask, and thus does not contribute additional costs.

In physical vapor deposition, the masks can be of either of two types. They can be contact or temporary masks (resist), or they can be shadow masks which can be reused many times. A third possibility exists which involves the deposition of metal over the whole substrate area, application of a resist over the areas on which deposition is desired, and subsequent removal of the material (etching) from

the areas on which deposition was not desired, followed finally by removal of the resist from the remaining deposited material. Particularly where the area of desired deposition is relatively small, as on the front areas of the solar cells, this process is relatively cumbersome and expensive. In addition, it seems that the deposited and resist materials can never be completely removed, so that the surfaces would remain in a somewhat altered state after application of this procedure. Consequently, this approach will not be discussed further.

The method most commonly used in physical vapor deposition employs the shadow mask. It is very practical where only thin films are deposited, perhaps up to a few thousand Angstroms in thickness, or where the open area in the mask is very large and the opening dimensions are not critical. These conditions are not fulfilled for the front area of the solar cell, where the desired mask open area is only about 3.4% of the total area, and the line width may be near 25 µm. With a deposit of 10 µm thickness, the openings in the mask would be substantially reduced during the course of a single deposition. Thus, the mask would have to be removed from the holder after only a few depositions, and the deposited material cleaned off. This consumes not only labor and chemicals (with subsequent disposal and reclaiming problems) but it also significantly shortens the life of the mask.

The second alternative consists in the application of a temporary mask, usually in the form of a photoresist.

At the edge of the resist to the open areas, a step in height occurs. In the deposition, the thickness of the deposited layer is generally reduced at this step. In the subsequent removal of the resist, the deposited layer usually separates at this step, so that the part of the layer which was deposited over the resist, can be readily removed with the latter. At a 10 μm thick deposition, however, as considered here for deposition of the conduction layer, the material deposited over the step will still be of sufficient thickness and consequently mechanical strength, that removal of the deposit over the mask without damage to the deposited layer in the open areas cannot be expected.

Although the vacuum deposition (or sputter deposition) of 10 μm thick copper layers is basically one of the economically feasible processes, the problems encountered with the masking for fine line pattern generation make it unfeasible for the deposition of the conduction layer on the front of large area solar cells. The process can, however, be economical and practical for the deposition of thin strike or barrier layers in preparation for the deposition of the conduction layer by other processes, such as electrolytic plating. In this case, the direct material component of the costs may be reduced to near negligible levels, except when palladium should be used, and the cost of the vacuum system may be cut in half because of the greatly reduced deposition time. Thus, the total process may, for

PRECEDING PAGE BLANK NOT FILMED

Table XI

Comparative Tabulation of Direct Material Consumption and Cost for the Principal Metallization Options

Option		Metal	Thickness	Metal Mass on Cell (a)	Plating Effic'y.	Recycl. Rate	Net Metal eff.	Gross Metal Required	Approximate Cost of Metal	
			μm	g/m^2	%	%	g/m^2	g/m^2	¢/g	$\$/m^2$
3.5.01-01	T.F. Screen Printing	Ag w/frit	20[b]	6.5 front (c)	90	50	94.7	12[i]	70[i]	8.40
3.6.03-03	Vacuum Evaporation	Ni/Cu	0.1 Ni, 10 Cu	3.1 front 90 back	1.7 front 50 back (d)	75,50 (e)	51(v) 25.7 overall	181.5(v) 178.5(r)	0.3(v)(f) 0.13(r)	0.78 Cu + 0.02 Ni
3.6.03-02	Sputtering	Cu	10	dto.	dto.	75,50 (h)	7.23	188(v) 263(r) (j)	0.33(v) 0.15(r)	1.015
3.6.04-02	Electroless Plating (g)	Ni	0.5	4.6	90	-	90	5.1 18(h)	6.50(h)	0.289
3.6.04-01	Electrolytic Plating	Cu	10	92.4	95	-	95	97.3	0.200	0.195
3.6.04.03	Solder Dip	60:40 Sn:Pb	55	520[c]	95	-	94.7	547.4	1	5.474

a. Metals assumed to cover 3.4% of front area (25 μm line width), 100% of back, unless noted otherwise.
b. For layer after sintering, contains 50% by volume Ag.
c. Grid line/bus coverage taken as 6.2% commensurate with minimum line width of 125 μm.
d. Refers to metal on grid line.
e. Numbers refer to recycling efficiency of metal on machine's interior and holder, and that on mask, respectively.
f. Price of copper.
g. Used as a "strike" or "barrier" layer prior to electrolytic deposition, vacuum evaporation, or sputtering of other metals, or to solder dipping.
h. In the form of $NiCl_2 \cdot 6H_2O$.
i. Refers to complete ink including frit, binder, formulating, etc.
j. Includes recycled target material.
(v) Applies to the virgin material used.
(r) Applies to the additional recycled material used

thin layer deposition, be only 1/3 to 1/2 of that found for conduction layer deposition, and may become competitive with the wet chemical processes.

As has been done previously, the UPPC forms have been used as a combination guide and checklist for the accumulation of detailed process information. For the six generic processes discussed, the filled-in forms are included as Appendix I. To facilitate the comparison of the important attributes of these processes, the relevant data have been compiled in Tables XI through XV.

Table XI contains a comparative tabulation of the direct material consumption and its costs. It is evident that the screen printing process and the solder dipping process incur direct material costs, which are as much as a factor of 40 above those of the lowest cost process. Clearly, costs of \$5 and \$8 per square meter of cells for the direct materials alone place these processes out of competition for a low cost, large scale production line. This conclusion is amplified by the fact that both of these processes cannot generate very narrow line widths, and thus result in cells of inherently lower than optimum efficiency. Such a reduced efficiency constitutes another economic penalty.

It may also be noted that the data given in Tables XI to XV for the thick film screen printing process apply only to the metallization on the front surface of the cells, in contrast to those for the remaining processes which apply to

Table XII

Comparison of Indirect Material Consumption For The Principal Metallization Options

Option		Consumable	Cost of Consumables $/m^2$	Description of Supplies (Unit Cost)	Cost of Supplies $/m^2$	Electricity Name-plate Rating (and duty cycle) and Consumption	Electricity Cost $/m^2$ (a)	Total Indirect Mat. Cost $/m^2$
3.5.01-01	T.F. Screen Printing of Ag	Xylene Solvent ($0.52/lb)	0.030	Print Screens ($25 ea.) Squeegees ($0.40 ea.) Thermocouples and misc.	0.275 0.035 0.10 0.410	35 kW(50%) 1.5kWh/m^2	0.075	0.515
3.6.03-03	Vacuum Evaporation of Ni/Cu	Pump oil ($30/qt, 4 qt/wk) Graphite crucible ($1000 ea.)	0.017 0.800 0.817		–	80 kW(30%) 200 kW(45%) 2.4 kWh/m^2	0.12	0.937
3.6.03-02	Sputter Deposition of Copper (10 μm)	Argon ($100/332$ft^3$) Pump oil (as under 3.6.03-03)	0.049 0.017 0.066	–	–	20 kW(75%) 45 kW(30%) 1.06 kWh/m^2	0.053	0.119
3.6.04-02	Electro-less Plating of Ni (0.5 μm)	Plating solution	0.494	–	–	20 kW(75%) 0.5 kWh/m^2	0.025	0.519
3.6.04-01	Electrolytic Plating of Cu (10 μm)	Replenishing solution ($13/gallon)	0.282	–	–	5 kWh/m^2	0.250	0.532
3.6.04-03	Solder Dipping (55 μm)	Flux ($6.75/gal) DI$H_2O$ ($6.60/$m^3$)	0.363 0.053 0.416	–	–	15 kW(95%) 0.27 kWh/m^2	0.013	0.429

a. Unit cost is $0.05/kWh

front and back metallization. If metallization would also be applied to the back surface by screen printing to a thickness adequate for a low sheet resistance, the metal costs (silver) for this back surface layer would be completely prohibitive. However, Dr. D'Aiello of RCA Laboratories has shown that an adequately low effective sheet resistance can be obtained when the back surface is covered with only 0.4 μm of silver, but overlaid with several bus lines over the whole length of the cell. The bus lines may be of bulk metal ribbon or wire. For a layer of this thickness, the total costs of a screen printed back layer would equal those of the thick film front layer shown as option number 3.5.01-01.

Table XII summarizes the indirect material costs for the six generic processes. Interestingly, the total indirect material costs all fall within one order of magnitude. In vacuum evaporation, the cost of the graphite crucibles accounts for most of the indirect material costs. Since the sputter system does not use crucibles, but obtains the source material from the sputter targets, the corresponding costs are shifted from the indirect materials category to the direct materials category, as the fabrication of the target plates is more costly than that of rod or wire for the evaporation source material. In the thick film process, the replacement costs for the print screens and the squeegees account for the major part of the indirect material cost, while in the wet chemical plating processes, the cost of the chemicals for the plating

Table XIII

Comparison of Labor Requirements For The Principal Metallization Options

	Option	Gross output (m^2/h)	Uptime	Net Output (m^2/g)	Labor Type	Hourly Rate $/h	Effort per Station %	Direct Labor Cost (a) $\$/m^2$	Indirect Labor Cost (b) $\$/m^2$	Total Labor Cost $\$/m^2$
3.5.01-01	T.F. Screen Printing of Ag	12	95	11.4	Assembler Maint. Mech.	5.65 7.40	25 20	0.264 0.277 0.541	0.135	0.676
3.6.03-03	Vacuum Dep. of Ni/Cu (10 μm)	48	85	41	Assembler Maint. Mech.	5.65 7.40	50 20	0.147 0.077 0.224	0.056	0.280
3.6.03-02	Sputter Dep. of Cu (10 μm)	30	90	27	Assembler Maint. Mech. Elec. Tech.	5.65 7.95 7.40	100 10 10	0.446 0.063 0.058 0.567	0.142	0.709
3.6.04-02	Electroless plating of Ni (0.5 μm)	30	88	26.4	Assembler	5.65	100	0.456	0.114	0.570
3.6.04-03	Electrolytic plating of Cu (10 μm)	30	95	28.5	Assembler	5.65	100	0.422	0.106	0.528
3.6.04-03	Solder dipping (55 μm)	30	88	26.4	Assembler	5.65	100	0.456	0.114	0.570

a. Includes a load factor of 113% for benefits and 8280 h/year staffing
b. Taken as 25% of direct labor cost

solutions makes the predominant contribution. It is interesting to note that the electricity consumption appears considerably greater in the electrolytic plating process than in the vacuum evaporation or sputter deposition processes, although the latter require the pumping power besides the power needed for the vaporization of the source material.

In the six projected generic processes, the total labor costs fall into a rather narrow range (Table XIII). The only observation to be made is that the largest throughput system shows the lowest labor costs per unit area of cells metallized, while the lowest throughput system , the thin film screen printing process, is near the peak of the labor costs. The relatively high labor content of the sputter deposition system is probably more due to the estimation of the individual making the projection than to actual experience data.

In the capital equipment area, summarized in Table XIV, the prices of the automated screen printing machine and the furnaces are probably the most reliable ones, as they represent the current state of the art. The prices for the vacuum deposition, sputtering and electrolytic plating systems are estimates given by the manufacturers of such equipment. The plating equipment costs shown include an allocation of about one third of the total for the relatively high installation and chemical waste treatment system costs. The vacuum evaporator and the sputter system costs apply to fully automated systems. Since double-sided deposition

Table XIV

Comparison of Capital Requirements For The Principal Metallization Options

Option		Annual Output 10^5 m^2/y	Cycle Time Min	Equipment Needed (Unit Cost)	Equip Cost (a) $\$/m^2$	Facility Area m^2	Facility Cost (b) $\$/m^2$	Total Capital Cost $\$/m^2$
3.5.01-01	T.F. Screen Printing of Ag	0.94	0.05	Screen Printer (50k) Dryer (20k) Furnace (35k)	0.113 0.045 0.070 0.237	40	0.076	0.313
3.6.03-03	Vacuum Dep'n. of Ni/Cu (10 μm)	3.38	55	Evaporator ($ ~ 2 Mill)	1.264	97.5	0.052	1.316
3.6.03-02	Sputtering of Cu (10 μm)	2.23		Sputterer (~ 3 Mill)	2.865	60	0.048	2.913
3.6.04-02	Electroless Plating of Ni (0.5 μm)	2.18	20	Compl. System ($44k)	0.053	8.4	0.007	0.060
3.6.04-03	Electrolytic Plating of Cu (10 μm)	2.36	15	Autom. Plating Machine ($60k)	0.543	90	0.068	0.611
3.6.04-03	Solder Dipping (55 μm)	2.18	1	Soldering System ($50k)	0.049	9.3	0.022	0.071

a. Using an annual charge rate of 21.35%
B. Using an annual charge rate of 179.13$/m^2

is needed, the turn-over of the cell and mask holder in the deposition chamber and a second set of source material boats, including all their controls, are required. Consequently, the manufacturer has given the system cost as twice that of a system for single-sided deposition, which is more common. The capital equipment costs for the electroless nickel plating and solder dipping equipment represent relatively unsophisticated projections from the current operation which is essentially manual, and may thus be viewed as the least reliable estimates, probably being on the low side.

Table XV provides the summary of the cost comparisons contained in Tables XI through XIV. In addition, it gives the add-on price for the individual processes, computed according to the SAMICS-IPEG methodology. The first two lines of Table XV describe two processes which provide the total metallization, including the barrier layer below the copper layer in the case of vacuum deposition. But, as discussed before, vacuum evaporation is really not suited for full conduction layer deposition on the front surface because of the masking problem for fine line deposition of thick layers. It can therefore be readily applied only to the rear surface metallization or the deposition of a barrier or strike layer. In the latter case, the price may be in the range of one third to one half of that shown in the last two columns. It may also be reiterated that the thick film silver process applies only to the front layer metallization,

Table XV

Cost Summary For The 6 Principal Metallization Options

Process Option		Remarks	COSTS Metal $/m^2$	Indirect Mat'ls. $/m^2$	Tooling etc. $/m^2$	Elect. Power $/m^2$	Labor $/m^2$	Capital Equip't $/m^2$	Facility $/m^2$	Price $/m^2$	Price ¢/W(pk)
3..5.01-01	Thick Film Ag	Front only Rear at 0.4 μm thickness gives equal cost	8.40 [1]	0.030	0.410	0.075	0.676	0.237	0.076	13.150	8.77
3.6.03-03	Vacuum Deposition of Nickel Barrier and Copper Conduction Layers	Both sides Cu ∿ 10 μm thick	0.797	0.817	–	0.12	0.28	1.264	0.052	5.772	3.85
3.6.03-02	Electroless Ni Strike or Barrier Layer	Both sides. Requires contact mask. ∿ 0.5 μm thick	0.289 [2]	0.494	–	0.025	0.06	0.053	0.007	1.908	1.3
3.6.-04-07	Solder Dipping	Both sides. Requires ∿ 0.5 μm thick Ni or other solderable metal.	5.668	0.416	–	0.013	0.569	0.49	0.022	8.997	6.0
3.6.04-01	Electrolytic Plating of Copper Conduction Layer	Both sides. ∿ 10 μm thick. Requires Ni strike layer.	0.195	0.282	–	0.250	0.556	0.543	0.068	3.216	2.14
3.6.04-03	Sputter Deposition of Copper Conduction Layer	Both sides. ∿ 10 μm thick. Requires barrier layer, registration.	1.015	0.066	–	0.053	0.708	2.865	0.048	9.221	6.15

1. Cost of ink
2. Cost of $NiCl_2 \cdot 6H_2O$ crystals

and that its price would have to be doubled if rear surface metallization is to be included.

The third line in Table XV gives the cost summary for a nickel strike or barrier layer, deposited by electroless plating. Its price is approximately 1.9 $\$/m^2$, or 1.3¢/W(peak). It is thus seen that the price of vacuum deposition of such a barrier or strike layer may be competitive with that of an electroless plated layer, particularly in consideration of the fact that the former does not require separate masking/ demasking steps. The last three lines of Table XV all contain conduction layer metallization processes. It is seen that the electrolytic plating of copper is clearly the conduction layer deposition process of lowest cost. The thick film silver deposition process and the solder dipping are clearly out of range because of the high metal costs. The sputter deposition of a conduction layer on the front surface suffers under the same masking problem as the vacuum evaporation process. In addition, the major price difference between sputter deposition and vacuum deposition seems to lie in the capital equipment costs. This difference is based on the equipment manufacturers estimates, and may disappear once a proper price determination for this type of equipment has been carried out.

The conclusion to be drawn from this economic analysis, as evident from Table XV, is that the electroless deposition of a strike or barrier layer, and the plating of a copper conduction

layer seem to be the lowest cost processes among the available options. In addition, these two processes are capable of the best line resolution and therefore of producing the highest efficiency solar cells. The vacuum deposition of a strike or barrier layer, using fully automated, high-throughput equipment, can possibly be competitive with the electroless plating approach.

XV. Preparation of SAMIC Format A Input Information from the UPPC Forms

The Format A has been developed to present the important cost data of any solar cell manufacturing process in a standardized form, and thus facilitate the entry of such data into the SAMIC computer program. Consequently, the information to be entered on Format A represents a summary of the results of an elaborate information collection and pre-processing effort. The UPPC forms have been developed specifically for the purpose of facilitating this information collection and pre-processing effort, and of documenting all the detail information which is needed for the proper evaluation of a process. They have also been intended to form a guide and a check list for the information collection, with space provided for the work-up and explanation of the data entered or arrived at by calculation. In a secondary application, the forms can be used for a manual evaluation of the costs and prices of the process being studied. This evaluation normally follows the SAMIC-IPEG methodology.

The UPPC system is composed of 16 individual forms (Appendix III), each dedicated to the collection of specific types of information. Each form may be used as many times as space is needed to document the available information, or may not be used at all. Therefore, Form 1 is used in essence as a Table of Contents, to document the complete set of forms used for the description of a particular process. Form 2 contains the general description of the individual process and the specifications

for the input work-in-process. Form 3 contains a listing of the direct materials used, including their specifications, the quanities required, and the unit cost. The similar Form 4 is devoted to the information collection for the indirect materials used. In Form 5, the expendable tooling needed for the execution of the process and the energy consumption in the process are listed. This form also contains a summation of the direct and indirect material costs and the costs of expendable tooling and energy. Form 6 accumulates information about the direct labor needed for the execution of the process, separated by labor categories and job activities. Entries are made for the amount of labor required at the process station, the labor rate, and the loading. The latter, according to the SAMIC-IPEG system, includes the employee benefits and the cost of replacement personnel to achieve staffing for 8280 hours per year. In addition, the form contains provisions for similar listing of the indirect labor. Form 7 is dedicated to the collection of information on the capital equipment needs, including installation costs, throughput rates and availability, as well as provision for servicing costs, which may include labor as well as parts or outside service. In addition, the useful life and the capital charge rate are to be entered. Form 8 is concerned with the facility needs of the individual process, including the floor area and the charge rate. There is additional provision for determination of the energy used in the facility

for heating, air-conditioning and lighting, as well as the cost of maintenance of the facility broken down into labor, supplies, and outside services. Forms 9-1, 9-2 and 9-3 are devoted to the determination of the amounts of salvaged work-in-process, direct, and indirect materials, respectively, as well as to the determination of their salvage credits with or without incurring reprossing costs. Forms 10 and 11 are dedicated to the accumulation of data relating to the solid, liquid or gaseous wastes or by-products possibly generated in carrying out the individual process, including specification of the types of wastes, their toxicity, biodegradability, and other characteristics of interest with respect to disposal, as well as their energy content, the amount generated, and the costs of waste treatment and disposal, or credits achievable by salvage. In the LSA program, data of this type have not yet become available, but as the processes are proceeding towards the pilot line stage, the accumulation of such data will become more urgent. Forms 12, 13-1 and 13-2 facilitate the summation of the cost data accumulated in the preceding forms and a manual price calculation according to the SAMIC-IPEG methodology. Forms 14 and 15 are devoted to a process performance evaluation and the specification of attributes of the output work-in-process, respectively, but have usually not been used. Form 16, finally, is a generalized work sheet to be used for the documentation of additional data or of calculations carried out in preparing

entries for any of the preceding forms.

The transformation of the information accumulated on the UPPC forms to that required for entry into the SAMIC Format A has been found to be best carried out in the following way:

a. UPPC Form 2 contains the process description to be summarized on line A-2 of Format A. It also contains the input work-in-process description needed for item A25 in Part 6 of Format A.

b. The process description on UPPC Form 2 usually includes the throughput rate of the process. Otherwise, the throughput rate will be found on Forms 7 and 8. Multiplying this throughput rate with the yield contained in item 7.42 or 7.44 of UPPC Form 12, provides the output rate for item A6 of Part 2 of Format A. (The throughput rate on the UPPC forms may be expressed as an hourly or a yearly rate, and has to be converted to a rate per minute for entry into Format A.)

c. The process description of UPPC Form 2 frequently includes the time of the product at the individual station, to be entered in item A7 of Format A.

d. UPPC Forms 3, 4, and 5 contain the data for direct and indirect materials, as well as expendable tooling and energy consumption, for direct transfer to items A20 through A23 in Part 5 of Format A. The UPPC forms contain the consumption rates in any practical units, such as grams

per square meter of solar cell area. These numbers have to be converted to consumption per minute for entry into Format A by use of the throughput rate discussed under point b. above. As far as the materials of the proper specifications can be found in the Cost Account Catalog, the catalog number and price from this Cost Account Catalog will normally have been entered in the UPPC forms.

e. The direct labor costs of UPPC Form 6 can be directly transferred to items A16 through 19 of Part 4 of Format A. Again, the Cost Account Catalog data will have been used in filling out the UPPC forms. (Indirect labor data, if they should have been entered on the UPPC forms, will not be transferred to Format A.)

f. The equipment data of UPPC Form 7 will be directly transferred to items A9 through 14 in Part 3 of Format A. (The current version of the UPPC Form 7 does not provide for entry of a base year for the equipment price or for the salvage value. The latter has usually not been available, and therefore been assumed as zero.)

g. Form 7 also contains the machine availability, or up-time fraction to be entered into item 8A of Part 2 of Format A.

h. The facilities data from UPPC Form 8 are directly transferable to items A16 through 19 of Part 5 of Format A.

i. Salvage credits or costs of waste or by-product processing or disposal, eventually to be contained in UPPC

Forms 9 through 11, will normally be entered into items A20 through 23 in Part 5 of Format A.

j. Form 12, in items 7.41 through 7.44, contains the data for conversion rate and yield to be entered into items A26 and A27 of Part 6 of Format A.

Making the transfers and conversions discussed in these points a. through j., Format A's were readily filled out for the six generic processes discussed in sections XI to XIV of this report. These Formats A are included in Appendix II of this report.

PRECEDING PAGE BLANK NOT FILMED

Table XVI

No.	Potential Process Sequence (Add-on prices in $/m^2$)				Total Price
1.	Apply Mask ~3.-(E)	Electroless Metal Ni-Sinter-Ni ~4.- (UP) Au-Ni 6.24 (PhotoW.) Pd-Sinter-Pd-Ni 4.14(Mot.)	Remove Mask ~1.-(E)	Solder Dip ~1.30+5.70 Metal	15.- to 18.-
2.	Apply Mask ~3.-(E)	Electroless Metal Pd-Sinter-Pd-Ni 4.14(Mot.)	Electrolytic Metal Cu 3.22(UP)	(Remove Mask) ~1.-(E)	~11.40
3.	Vac. Deposit Metal Ti-Pd-(Ni) 2.84(West.)(UP)	Sinter 0.10(Mot)	Electrolytic Metal Cu 3.22(UP)	-	~6.16
4.	Screen Print Silver 7.30+14.30 Ag(Lockh) to 10.30+9.30 Ag(RCA)	Dry/Sinter	-	-	~20.- to 22.-
5.	Apply "Midfilm" 2.77+2.09 Ag(Front Only)	Powder Metal Ag	Sinter	Conductor Layer Build-up (Electrolytic Cu) 3.22	8.08

(E) = estimated

XVI. Potential Metallization Process Sequences

Applying the data from Table XV as well as data from the LSA contractors contained in numerous progress reports, potential process sequences can be constructed and evaluated. A small sample of such potential process sequences is shown in Table XVI. These sequences contain all the associated process steps required for complete metallization, particularly masking where required.

Table XVI leads to several observations. The first is, that the data from the various sources have become quite consistent. The second is that process sequences can produce complete metallization in the \$6.- to 12.-/m^2 (4 to 8¢/W(peak)) range, and that the processes including thick film silver or solder dipping fall significantly above this range. It is also seen that the vacuum deposition of a strike/barrier layer (sequence 3) may be competitive with the electroless plating process (sequence 2). In the latter, significant costs are incurred in contact masking and mask removal. However, it is not clear that the sequence 3 will result in high efficiency and long life solar cells, without use of a contact mask. The vacuum deposition through a shadow mask can result in "underspray" with consequently reduced light transmission. Further, the electrolytic plating over the strike layer may bring copper in contact with the silicon at the edges of the strike layer, and result in degradation of performance in time. Clearly, the approach of using the

AR coating as a permanent plating mask is appealing since it can eliminate this latter problem. It would, however, likely eliminate the vacuum deposition process for the strike/ barrier layer, since it would require the additional process step of registration of the shadow mask to the contact mask (AR-coating), and involve the difficulty of maintaining this precise registration throughout all subsequent handling until the strike layer deposition is complete.

It has also to be determined whether electrolytic plating-up of a sintered silver layer resulting from the Midfilm process is possible. On small area cells, such build-up may not be necessary, as the sheet resistance may be adequately low for grid lines of small length. The other alternative, for large area cells, would be to design a metallization pattern with a larger number of bus lines.

The SOL/LOS Mo/Sn process has not been considered further, since it relies on tin as the main conductor and therefore will not be cost effective, at least as intended to be applied now. The fritless copper thick film process has basic merit, but requires a lot more development until it can be considered competitive with the more established processes.

It has thus been seen that a few basic process options exist for the low-cost metallization of large area, high performance solar cells. But it has also been seen that potential pitfalls exist with at least some of these options,

and that some pilot line experience with careful attention to ultimate process cost, controllability and yield, and potential initial or long term solar cell performance degradation is needed, possibly with subsequent further development work.

XVII. Conclusions

The analysis of the metallization pattern design for the front surface has provided considerable insight into the requirements to be fulfilled in a low-loss design for large area solar cells. These requirements have been compiled into a set of Design Rules, contained in Table V. It has been shown that the total shading and voltage drop losses can be held to about 5% in 10 cm x 10 cm solar cells, but that not every metallization process is capable of meeting the requirements of the low-loss design. Without close observation of the design rules, the combined series resistance related losses can easily increase to 10 and even 20% of the ideal power output. It has also been shown that these low losses can be achieved only by use of several bus lines containing a bulk conductor, such as a wire of circular or rectangular crossection. Without bus lines, and with a sheet resistance of $1.7 \cdot 10^{-3}$ Ω (10 μm thick Cu of bulk resistivity) of the deposited metal for the grid lines, the total losses of the front structure (semiconductor front layer of 35 Ω sheet resistance and metallization) cannot be reduced below 11.7% of the ideal power output in 10 cm x 10 cm cells. Applying bus lines that are not of significantly lower sheet resistance than the grid lines does not improve this situation.

Several process sequences have been identified which should be capable of producing the required metallization

PRECEDING PAGE BLANK NOT FILMED

for large area, high performance solar cells in the $6.- to 12.-/$m^2$, or 4 to 8¢/W(peak) price range. Any process relying on the use of a conduction layer of tin, or lead-tin alloy, or of thick film silver, falls above this price range. Electroless plating processes for strike or barrier layer formation, and electrolytic plating of the conduction layer, primarily considering copper, appear as the more cost-effective processes. Vacuum deposition of the strike or barrier layer, based on use of a variety of metals, may be competitive with the electroless plating processes. The use of the AR coating as a plating mask is very attractive, but not compatible with the vacuum deposition of strike or barrier layers. Vacuum or sputter deposition of the conduction layer for the front of solar cells appears impractical because of masking problems. Some of the other process sequences also may contain hidden problems of potentially significant consequences. Thus, a careful evaluation of the pilot line operation of the most hopeful process sequences will be needed to reveal such potential problems which may effect process controllability and yield or cause an initial or a gradual degradation of solar cell performance. Once such problems are recognized, additional development work may be needed.

Aluminum could be an alternative to copper as the conduction layer metal. The impracticality of depositing it by wet chemical methods, the problems of masking in vacuum evaporation for the front metallization, and the limitations

in lead bonding to aluminum, however, have lead to its omission from the discussion.

XVIII. References

1. Mardesich, N., Spectrolab, Inc., Quarterly Report No. DOE/JPL-955725-80/1, Appendix I.

2. J.A. Murphy, editor, "Surface Preparation and Finishes for Metals", pp. 226-228; McGraw Hill, New York, N.Y., 1971

   E. Raub and K. Müller, "Fundamentals of Metal Deposition", pp. 72-77; Elsevier, Amsterdam, 1967, (J.K. Dennis and T.E. Such, "Nickel and Chromium Plating", pp. 220-291, Newnes-Butterworth, London, 1972.)

3. J.A. Murphy, editor, "Surface Preparation and Finishes for Metals", pp. 203-226, McGraw Hill, New York, N.Y. 1971. J.K. Dennis and T.E. Such, "Nickel and Chromium Plating", Newnes-Butterworth, London, 1972.

4. E. Raub and K. Müller, "Fundamentals of Metal Deposition", pp. 18-28, Elsevier, Amsterdam, 1967. F.A. Lowenheim, editor, "Modern Electroplating", pp. 3-39, (E.H. Lyons, "Fundamental Principles") pp. 172-191, (W.H. Safranek, "Acid Copper Plating and Electroforming") pp. 154-171, (R.R. Bair and A.K. Graham, "Copper Plating from Cyanide Baths") J. Wiley and Sons, New York, N.Y., 1963. A.K. Graham, "Electroplating Engineering Handbook", Reinhold, New York, N.Y., 1962.

5. L. Holland, "Vacuum Deposition of Thin Films," Chapman and Hall, London, 1963.

6. Ibid., pp. 199-203.

7. R.C. Peterson, Solarex Corp. (Quarterly Report No. DOE/JPL-954854-80/6, pp. 4-8

8. J.R. Anderson, Solarex Corp., private communication

9. Allied Kelite Berkeley Heights, NJ), Technical Data Sheet on the Barrett Sulfamate Nickel Plating Process.

10. S. Field and A. Dubley, "Electro-Plating", 6th edition, Pitman Publ. (NY, NY), p. 232 (1957).

11. A reference to this method could not be recovered.

12. R.V. D'Aiello, RCA-Labs. "Process Specification for Thick-Film Screen Printed Metallization" (12/78). DOE/JPL Contract No. 954868.

PRECEDING PAGE BLANK NOT FILMED

13. M. Macha, SOL/LOS Inc. (Los Angeles, CA), Presented at the 14th PIM for the LSA program at the Jet Propulsion Laboratory, Dec. 1979. (DOE/JPL Contract No. 955318).

14. B. Ross, Bernd Ross Assoc., Quarterly Report No. DOE/JPL-955164-79/4, pp. 71-75 (12/79).

15. B. Ross, Record 14th Photovoltaic Specialists Conf., IEEE Cat. No. 80CH1508-1, p. 787-792, Jan. 1980.

16. J.L. Hughes, Airco Temescal, private communication.

17. F. Coscina, Napco, Inc., Terryville, CO; private communication.

18. C. Nye, Oxy Metal Industries Corp.; private communication.

APPENDIX I

DETAIL DATA FOR 6 GENERIC METALLIZATION PROCESSES

Process No. 3 . 5 . 01 - 01

Form 1

University of Pennsylvania

PROCESS CHARACTERIZATION

(UPPC)

Process: Device Fabrication

Subprocess: Contact Metallization (Front only)

Option: Thick Film Screen Printing of Silver

INDEX

Form	Pages	Rev.	Date	Remarks
1		1	2-81	
2	1 to 2	2	2-81	
3	1 to 1	2	2-81	
4	1 to 1	1	9-79	
5	1 to 1	2	2-81	
6	1 to 1	1	9-79	
7	1 to 1	1	9-79	
8	1 to 1	1	9-79	
9-1	1 to -			
9-2	1 to -			
9-3	1 to -			
10	1 to -			
11	1 to -			
12	1 to 1	1	2-81	
13-1	1 to -			
13-2	1 to 1	1	2-81	
14	1 to -			
15	1 to -			
16	1 to -			

ORIGINAL PAGE IS OF POOR QUALITY

Revision 2 Date 2-81

Process No. 3 . 5 . 0 1 - 0 1

0.1 Value Added: _____ $/ ___

Process Description: The wafers are unloaded from cassettes, inserted in a screen printer, and the ink is applied. Wafers are then collated and dried and sintered in a belt furnace, and re-loaded into cassettes. The metal area coverage on the front surface is assumed to be 6.2% with a line width of 125 µm and thickness (after sintering) of 20 µm, and 3 bus lines. Output rate of screen printer is 1200 wafers/h and utilization rate is 95% for an effective output rate of 1140 wafers/h, or 11.40 m^2/h. This process description covers only front surface metallization.

(Continuation on Form 2, page 2)

1. Input Specification:

Name of Item: Silicon wafers with N^+PP^+ junctions

Dimensions: 10-cm square and about 300 µm thick

Material: _____

Other Specifications: _____

1.1 Quantity Required: _____ / _____ Unit Cost: _____ $/ _____

1.2 Input Value:	_____ $/ _____
1.3 Input Cost:	_____ $/ _____

Note to Item 1.3: Use price, if input produced in own plant.

Revision 2 Date 2-81

Process No. 3 . 5 . 0 1 - 0 1

0.1 Value Added:	$/

Process Description: The process can apply metallization on one side, and requires duplication in equipment and operations for metal application to the rear surface. A 100% rear surface metallization at 0.4 μm thickness after sintering would have approximately the same material consumption as shown here.

1. Input Specification:

Name of Item:

Dimensions:

Material:

Other Specifications:

ORIGINAL PAGE IS OF POOR QUALITY

1.1 Quantity Required: / Unit Cost: $/

1.2 Input Value:	$/
1.3 Input Cost:	$/

Note to Item 1.3: Use price, if input produced in own plant.

Process No. 3 . 5 . 01 - 01

Form 3
Page 1 of 1

2.1 Direct Materials:

Revision 2 Date 2-81

2.11 Type: Silver ink paste, similar to that described by RCA ;

Specification: Wet layer thickness is 25 µm, application eff. 90%, with 50% of waste ink recycled. ;

Quantity Required: ~ 12 g/ m^2; Unit Cost: 0.70 $/ g*; Cost: 8.40 $/ m^2

2.1_ Type: ;

Specification: ;

Quantity Required: /; Unit Cost: $/; Cost: $/

2.1_ Type: ;

Specification: ;

Quantity Required: /; Unit Cost: $/; Cost: $/

ORIGINAL PAGE IS OF POOR QUALITY

*Includes formulation cost of $0.30/g.

2.1 Subtotal Direct Materials:	8.40 $/ m^2

Process No. 3 . 5 . 0 1 - 0 1

Form 4

Page 1 of 1

Revision 1 Date 9-79

2.2 Indirect Materials (incl. supplies and non-energy utilities):

2.2 1 Type: Xylene, ρ = 0.87g/mℓ;

Specification: Used as a solvent for the ink. Usage is about 30 mℓ/m^2 cells.

Cost is $0.52/lb for reagent grade (J.T. Baker, 12/79)

Quantity Required: 26.1 g/m^2; Unit Cost: 1.146 $/kg; Cost: 0.030 $/$m^2$

2.2_ Type:

Specification:

Quantity Required: ___/___; Unit Cost: ___$/___; Cost: ___$/___

2.2_ Type:

Specification:

Quantity Required: ___/___; Unit Cost: ___$/___; Cost: ___$/___

2.2 Subtotal Indirect Materials: 0.030 $/$m^2$

Process No. 3 . 5 . 01 - 01

Form 5

Page 1 of 1

Revision 2 Date 2-81

2.3 Expendable Tooling:

2.3 1 Type: Print screens - replaced every shift. (∿ 9000 cells)

Quantity Required: 0.011 screens/m^2 : Unit Cost: 25 $/scr. Cost: 0.275 $/$m^2$

2.3 2 Type: Squeegees - replaced every hour (∿ 1000 cells)

Quantity Required: 0.088 squeegees/m^2 : Unit Cost: 0.40 $/sqe. Cost: 0.035 $/$m^2$

2.3 3 Type: Thermocouples and misc. replacement parts

general estimate Quantity Required: ____ /____ : Unit Cost: ____ $/____ Cost: 0.10 $/$m^2$

2.3 _ Type: ____

Quantity Required: ____ /____ : Unit Cost: ____ $/____ Cost: ____ $/____

2.3 Subtotal Expendable Tooling: 0.410 $/$m^2$

2.4 Energy

2.4 1 Type: Electricity, name plate rating is 35 kW (mostly belt furnace)

Quantity Required: 1.5 kWh/m^2 : Unit Cost: 0.05 $/kWh Cost: 0.075 $/$m^2$

2.4 _ Type: ____

Quantity Required: ____ : Unit Cost: ____ $/____ Cost: ____ $/____

2.4 Subtotal Energy Costs: 0.075 $/$m^2$

2.5 Subtotal 2.1 to 2.4: 8.915 $/$m^2$

2.6 Handling Charge: 5.26 % of item 2.5 0.469 $/$m^2$

2.7 Subtotal Materials and Supplies: (2.5 + 2.6) 9.384 $/$m^2$

ORIGINAL PAGE IS OF POOR QUALITY

Process No. 3.5.01-01

Form 6
Page 1 of 1
Revision 1 Date 9-79

3.1 Direct Labor:

3.11 Category: Semiconductor Assembler (SAMICS B5464D) Activity: machine monitoring and operation
Amount Required: 0.25 h/ h ; Rate: $ 5.65 /h; Load 113 %*; Cost: 0.264 $/$m^2$

3.12 Category: Maintenance Person (SAMICS B5176D) Activity: Repair and service
Amount Required: 0.2 h/ h ; Rate: $ 7.40 /h; Load 113 %*; Cost: 0.277 $/$m^2$

3.1_ Category: ______ Activity: ______
Amount Required: ______ h/ ______ ; Rate: $ ______ /h; Load ______ %; Cost: ______ $/ ______

3.1 Direct Labor Subtotal: 0.541 $/$m^2$

3.2 Indirect Labor: Taken as 25% of direct labor

3.2_ Category: ______ Activity: ______
Amount Required: ______ h/ ______ ; Rate: $ ______ /h; Load ______ %; Cost: ______ $/ ______

3.2_ Category: ______ Activity: ______
Amount Required: ______ h/ ______ ; Rate: $ ______ /h; Load ______ %; Cost: ______ $/ ______

3.2_ Category: ______ Activity: ______
Amount Required: ______ h/ ______ ; Rate: $ ______ /h; Load ______ %; Cost: ______ $/ ______

3.2 Indirect Labor Subtotal: 0.135 $/$m^2$

3.3 Subtotal 3.1 and 3.2	0.676	$/$m^2$
3.4 Overhead on Labor: 5.26 %	0.035	$/$m^2$
3.5 Subtotal Labor	0.711	$/$m^2$

*Includes 36% benefits and the requirement of 1.57 persons/shift.

Process No. 3 . 5 . 0 1 - 0 1

Form 7
Page 1 of 1
Revision 1 Date 9-79

4.1 Equipment

4.11 Type: Screen Print Apparatus with cassette unloader and collator (Welter Model 44-PS)

Cost: 50,000 \$; Installation Cost: - \$; Throughput: 12 m^2 /h;

Plant Oper'g Time 8280 h/y; Machine Avail'ty: 95 %; Machine Oper'g Time 7866 h/y

Servicing Costs: Labor ___ h/y at ___ \$/h; Parts or Outside Service: ___ \$/y

Useful Life: 7 y; Charge Rate: 21.35 % of Cost/y; Capital Cost: 10,700 \$/y — 0.113 \$/m^2

4.12 Type: Drier - dries ink

Cost: 20,000 \$; Installation Cost: - \$; Throughput: 12 m^2 /h;

Plant Oper'g Time 8280 h/y; Machine Avail'ty: 95 %; Machine Oper'g Time 7866 h/y

Servicing Costs: Labor ___ h/y at ___ \$/h; Parts or Outside Service: ___ \$/y

Useful Life: 7 y; Charge Rate: 21.35 % of Cost/y; Capital Cost: 4,270 \$/y — 0.045 \$/m^2

4.13 Type: Belt driven sintering furnace

Cost: 35,000 \$; Installation Cost: - \$; Throughput: 12 m^2 /h;

Plant Oper'g Time 8280 h/y; Machine Avail'ty: 95 %; Machine Oper'g Time 7866 h/y

Servicing Costs: Labor ___ h/y at ___ \$/h; Parts or Outside Service: ___ \$/y

Useful Life: 7 y; Charge Rate: 21.35 % of Cost/y; Capital Cost: 7,470 \$/y — 0.070 \$/m^2

4.1 Subtotal Equipment Cost:	0.237 \$/m^2

Process No. 3 . 5 . 0 1 - 0 1

Form 8
Page 1 of 1
Revision 1 Date 9-79

4.2 Facilities:

ORIGINAL PAGE IS OF POOR QUALITY

4.2.1 Type: Screen Printer and furnace area Floor Area: 40 m^2; Throughput: 94,400 m^2/y

Charge Rate: 179.13* \$/(m^2·y);

Energy Use:

Heating ____ /y at ____ \$/____

Air Cond'g ____ /y at ____ \$/____

Lighting ____ /y at ____ \$/____

Maintenance Costs:

Labor: ____ h/y at ____ \$/h

Supplies: ____ \$/y

Outside Services: ____ \$/y

Total Cost: 7,164 \$/y — 0.076 \$/m^2

4.2_ Type: ____ Floor Area: ____ m^2; Throughput: ____ /y

Charge Rate: ____ \$/(m^2·y);

Energy Use:

Heating ____ /y at ____ \$/____

Air Cond'g ____ /y at ____ \$/____

Lighting ____ /y at ____ \$/____

Maintenance Costs:

Labor: ____ h/y at ____ \$/h

Supplies: ____ \$/y

Outside Services: ____ \$/y

Total Cost: ____ \$/y — ____ \$/____

4.2_ Type: ____ Floor Area: ____ m^2; Throughput: ____ /y

Charge Rate: ____ \$/(m^2·y);

Energy Use:

Heating ____ /y at ____ \$/____

Air Cond'g ____ /y at ____ \$/____

Lighting ____ /y at ____ \$/____

Maintenance Costs:

Labor: ____ h/y at ____ \$/h

Supplies: ____ \$/y

Outside Services: ____ \$/y

Total Cost: ____ \$/y — ____ \$/____

*Includes energy use

4.2 Subtotal Facilities:	0.076 \$/m^2
4.3 Equipment and Facilities Subtotal :	0.313 \$/m^2

Process No. 3 . 5 . 0 1 — 0 1

Revision 1 Date 2-81

7. Process Cost Computation

Item	Value
7.11 Manufacturing Add-On Costs (sum of 2.7, 3.5, 4.3, 6.)	10.408 $/ m^2
7.22 Other Indirect Costs: (0.059 x 4.1 + ~~0.108 x 4.2~~) % of 7.11	0.022 $/ m^2
7.21 Total Operating Add-on Costs of Process:	10.430 $/ m^2
7.22 G & A ______% of 7.21	- $/
7.31 Total Gross Add-On Cost of Process	10.430 $/ m^2
7.32 ~~Credit for Salvaged Material (5.8)~~	- $/
7.33 Cost of Work-in-Process Lost (5.3)	NA $/
7.34 Specific Add-On Cost of Process (7.31 + 7.33)-(7.32)	10.430 $/ m^2
7.35 Cost of Input Work-in-Process Contained in Good Output Work-in-Process (5.4)	NA $/
7.36 Loading on Item 7.35 at Rate ______ %	NA $/
7.37 Cost of Output Work-in-Process (7.34 + 7.35 + 7.36)	$/

Item	Value
7.41 Theoretical Yield (or Conversion Rate, if output units of work-in-process do not equal input units)	NA /
7.42 Practical Yield	99 %
7.43 Effective Yield (7.41 x 7.42)	99% /
7.44 Number of Units of Good Output Work-in-Process per Computation Unit Used up to 7.35	0.99 m^2 / m^2

Item	Value
7.51 Cost of Unit of Good Output Work-in-Process (7.37 ÷ 7.44)	NA $/
7.52 Specific Add-On Cost per Unit of Good Output Work-in-Process (7.34 ÷ 7.44)	10.536 $/ m^2

Process No. 3.5.01-01

Form 13-2
Page 1 of 1

Revision 1 Date 2-81

8.2 Alternate 2 (SAMICS Methodology):

8.21 Profit Computation:

0.9274* 0.237 $/m^2 from Subtotal 4.1 = 0.220 $/m^2

1.946* 0.076 $/m^2 from Subtotal 4.2 = 0.148 $/m^2

Subtotal = 0.368 $/m^2

8.22 Costs of Amortization of the One-Time Cost:

0.192* 9.384 $/m^2 from Subtotal 2.7 = 1.802 $/m^2

0.192* 0.711 $/m^2 from Subtotal 3.5 = 0.137 $/m^2

0.2958* 0.237 $/m^2 from Subtotal 4.1 = 0.070 $/m^2

2.77* 0.076 $/m^2 from Subtotal 4.2 = 0.211 $/m^2

Subtotal = 2.220 $/m^2

8.23 Total Net Cost of Equity (8.21 + 8.22): 2.588 $/m^2

8.24 Profit and Amortization of Start-up Costs per Unit of Good Output Work-in-Process:
(Divide Subtotal 8.23 by 0.99 m^2 / m^2 from 7.44)

2.614 $/m^2

8.25 Price of Process (7.52 + 8.24) 13.150 $/m^2 or 8.77¢/W(peak)

8.26 Price of Work-in-Process (7.51 + 8.24) $/

Process No. 3 . 6 . 0 3 - 0 2

Form 1

University of Pennsylvania

PROCESS CHARACTERIZATION

(UPPC)

Process: Device Fabrication

Subprocess: Contact Metallization (front and rear)

Option: Electroless Ni Plating of Strike or Barrier Layer

INDEX

Form	Pages	Rev.	Date	Remarks
1		1	2-81	
2	1 to 2	1	2-81	
3	1 to 1	1	2-81	
4	1 to 2	1	2-81	
5	1 to 1		12-79	
6	1 to 1	1	12-79	
7	1 to 1	1	2-81	
8	1 to 1		12-79	
9-1	1 to -			
9-2	1 to -			
9-3	1 to -			
10	1 to -			
11	1 to -			
12	1 to 1	1	2-81	
13-1	1 to -			
13-2	1 to 1	1	2-81	
14	1 to -			
15	1 to -			
16	1 to -			

Form 2

Revision 1 Date 2-81

Process No. 3.6.03-02

0.1 Value Added:	$/

Process Description: Wafers with contact mask are dipped in electroless nickel solution at 80 to 90°C for 5 min, and are then rinsed and dried. Two flow hoods are used for processing. Cycle time is 20 min and Wafers are carried in 50 wafer cassettes, which are moved automatically through the system. The plating tank is large enough to hold 5 cassettes. Plating occurs on both sides simultaneously.

Throughput rate is 3,000 wafers/h and machine utilization is 88%. Surface coverage is 3.4% front, 100% rear. Plating thickness is 0.5 µm Plating effeciency is assumed to be 90%.

(Continued on Form 2, page 2)

1. Input Specification:

Name of Item: N^+PP^+ silicon wafer with contact mask

Dimensions: 10-cm square

Material:

Other Specifications:

1.1 Quantity Required: / Unit Cost: $/

1.2 Input Value:	$/
1.3 Input Cost:	$/

Note to Item 1.3: Use price, if input produced in own plant.

Form 2

Revision 1 Date 2-81

Process No. 3 . 6 . 0 3 — 0 2

0.1 Value Added:	\$/

Process Description: One liter of Ni electroless plating solution consists of: 875 mℓ H_2O; 30 g of $NiCl_2 \cdot 6H_2O$; 50 g of NH_4Cl; 84 g of $Na_3C_6H_5O_7 \cdot 2H_2O$; 10 g of $NaH_2PO_2 \cdot H_2O$ and 125 mℓ of NH_4OH (58%).

1. Input Specification:

Name of Item:

Dimensions:

Material:

Other Specifications:

1.1 Quantity Required: / Unit Cost: \$/

1.2 Input Value:	\$/
1.3 Input Cost:	\$/

Note to Item 1.3: Use price, if input produced in own plant.

Process No. 3 . 6 . 0 3 - 0 2

Form 3

2.1 Direct Materials:

Revision 1 Date 2-81

2.1_ Type: $NiCl_2 \cdot 6H_2O$, reagent grade crystals, $\rho = 7.77\ g/cm^3$;

Specification: Coating thickness is 0.5 µm.

$NiCl_2 = (0.05) \cdot (0.5) \cdot (7.77) \cdot (237.71/58.71) \cdot (1/0.9) = 0.87\ g/m^2$. One liter of solution will plate 1.7 m^2 of cells. Cost of $NiCl_2 \cdot 6H_2O$ is $7.29/lb (12/79; J.T. Baker);

Quantity Required: 18 g/m^2; Unit Cost: 16.07 $/kg; Cost: 0.289 $/$m^2$

2.1_ Type: ;

Specification: ;

Quantity Required: /; Unit Cost: $/; Cost: $/

2.1_ Type: ;

Specification: ;

Quantity Required: /; Unit Cost: $/; Cost: $/

2.1 Subtotal Direct Materials: 0.289 $/$m^2$

ORIGINAL PAGE IS OF POOR QUALITY

Process No. 3 . 6 . 0 3 – 0 2

Revision 1 Date 2-81

2.2 Indirect Materials (incl. supplies and non-energy utilities):

2.21 Type: Deionized water for plating solution;

Specification: Need 875 ml of DIH_2O per liter of solution. Consumption is 620 mℓ for 1 m^2 of cells. Cost is $660 for 100 m^3 (SAMICS C1128D).

Quantity Required: 620 mℓ/m^2; Unit Cost: 0.0066 $/ℓ; Cost: 0.004 $/$m^2$

2.22 Type: Ammonium Chloride (NH_4Cl), reagent grade, granular

Specification: Need 50 g/ℓ of plating solution. Consumption is 35 g/m^2 of cells. Cost is $1.15/lb (J.T. Baker, 12/79)

Quantity Required: 35 g/m^2; Unit Cost: 2.535 $/kg; Cost: 0.089 $/$m^2$

2.23 Type: Sodium Citrate, reagent grade crystals

Specification: Need 84 g/ℓ of plating solution. Consumption is 62 g/m^2 of cells. Cost is 1.88 $/lb. (J.T. Baker, 12/79)

Quantity Required: 62 g/m^2; Unit Cost: 4.145 $/kg; Cost: 0.257 $/$m^2$

2.2 Subtotal Indirect Materials: ______ $/______

Process No. 3 . 6 . 0 3 – 0 2

Form 4

Page 2 of 2

Revision 1 Date 2-81

2.2 Indirect Materials (incl. supplies and non-energy utilities):

2.2.4 Type: Sodium hypophosphite ($NaH_2PO_2 \cdot 2H_2O$), reagent grade crystals; ;

Specification: Need 10 g/ℓ of plating solution. Consumption is 7.2 g per m^2 of cells. Cost is $4.22/lb (J.T. Baker, 12/79)

Quantity Required: 7.2 g / m^2; Unit Cost: 9.304 $/ kg; Cost: 0.067 $/ m^2

2.2.5 Type: Ammonium hydroxide (NH_4OH), 58% reagent grade

Specification: Need 125 mℓ/ℓ of plating solution. Consumption is 89 mℓ per square m^2 of cells. Density of NH_4OH (58%) is 0.826 g/mℓ. Cost is $0.47/lb. (J.T. Baker, 12/79)

Quantity Required: 89 mℓ / m^2; Unit Cost: 0.861 $/ ℓ; Cost: 0.077 $/ m^2

2.2_ Type:

Specification:

Quantity Required: / ; Unit Cost: $/ ; Cost: $/

2.2 Subtotal Indirect Materials: 0.494 $/ m^2

ORIGINAL PAGE IS OF POOR QUALITY

Process No. 3 . 6 . 0 3 – 0 2

Form 5

Revision ____ Date 12-79

2.3 Expendable Tooling:

2.3_ Type: ______

______ Quantity Required: ______ ____/____: Unit Cost: ____$/____ Cost: ____$/____

2.3_ Type: ______

______ Quantity Required: ______ ____/____: Unit Cost: ____$/____ Cost: ____$/____

2.3_ Type: ______

______ Quantity Required: ______ ____/____: Unit Cost: ____$/____ Cost: ____$/____

2.3_ Type: ______

______ Quantity Required: ______ ____/____: Unit Cost: ____$/____ Cost: ____$/____

2.3 Subtotal Expendable Tooling:	____$/____

2.4 Energy

2.4 1 Type: Electricity for laminar flow hoods with strong exhaust, heater on plating tank, drier, various motors and instruments, name plate rating estimated to be 20 kW with 75% load factor.

______ Quantity Required: 0.5 kWh/m^2 : Unit Cost: 0.05 $/kWh Cost: 0.025 $/ m^2

2.4_ Type: ______

______ Quantity Required: ______ ______: Unit Cost: ____$/____ Cost: ____$/____

2.4 Subtotal Energy Costs:	0.025 $/ m^2
2.5 Subtotal 2.1 to 2.4:	0.808 $/ m^2
2.6 Handling Charge: 5.26 % of item 2.5	0.043 $/ m^2
2.7 Subtotal Materials and Supplies: (2.5 + 2.6)	0.851 $/ m^2

Process No. 3.6.03-02

Form 6
Page 1 of 1
Revision 1 Date 12-79

3.1 Direct Labor:

3.1[1] Category: Semiconductor Assembler (SAMICS B5464D) Activity: Hood operation

Amount Required: 1 h/ h ; Rate: $ 5.65 /h; Load 113 %[*]; Cost: 0.456 $/ m^2

3.1_ Category: ______ Activity: ______

Amount Required: ____ h/ ____ ; Rate: $ ____ /h; Load ____ %; Cost: ____ $/ ____

3.1_ Category: ______ Activity: ______

Amount Required: ____ h/ ____ ; Rate: $ ____ /h; Load ____ %; Cost: ____ $/ ____

3.1 Direct Labor Subtotal: ____ $/ ____

3.2 Indirect Labor: Taken as 25% of direct

3.2_ Category: ______ Activity: ______

Amount Required: ____ h/ ____ ; Rate: $ ____ /h; Load ____ %; Cost: ____ $/ ____

3.2_ Category: ______ Activity: ______

Amount Required: ____ h/ ____ ; Rate: $ ____ /h; Load ____ %; Cost: ____ $/ ____

3.2_ Category: ______ Activity: ______

Amount Required: ____ h/ ____ ; Rate: $ ____ /h; Load ____ %; Cost: ____ $/ ____

3.2 Indirect Labor Subtotal: 0.114 $/ m^2

3.3 Subtotal 3.1 and 3.2	0.570	$/ m^2
3.4 Overhead on Labor: 5.26%	0.030	$/ m^2
3.5 Subtotal Labor	0.600	$/ m^2

*Includes cost of replacement personnel and benefits.

ORIGINAL PAGE IS
OF POOR QUALITY

Process No. 3 . 6 . 0 3 - 0 2

Revision 1 Date 2-81

4.1 Equipment

4.1 1 Type: Two 6-foot laminar flow exhaust hoods (IAS type LU6-30x)

Cost: 9,000 \$; Installation Cost: ______ \$; Throughput: 30 m^2 /h;

Plant Oper'g Time 8280 h/y; Machine Avail'ty: 88 %; Machine Oper'g Time 7286 h/y

Servicing Costs: Labor ______ h/y at ______ \$/h; Parts or Outside Service: ______ \$/y

Useful Life: 7 y; Charge Rate: 21.35 % of Cost/y; Capital Cost: 1920 \$/y — 0.009 \$/m^2

Fluoro...

4.1 2 Type: Two chemical recirculating systems (fluorocarbon No. 5000)

Cost: 15,000 \$; Installation Cost: ______ \$; Throughput: 30 m^2 /h;

Plant Oper'g Time 8200 h/y; Machine Avail'ty: ______ %; Machine Oper'g Time 7286 h/y

Servicing Costs: Labor ______ h/y at ______ \$/h; Parts or Outside Service: ______ \$/y

Useful Life: 7 y; Charge Rate: 21.35 % of Cost/y; Capital Cost: 3200 \$/y — 0.015 \$/m^2

4.1 3 Type: Drying station and cassette transport system

Cost: 20,000 \$; Installation Cost: 10,000 \$; Throughput: 30 m^2 /h;

Plant Oper'g Time ______ h/y; Machine Avail'ty: ______ %; Machine Oper'g Time 7286 h/y

Servicing Costs: Labor ______ h/y at ______ \$/h; Parts or Outside Service: ______ \$/y

Useful Life: 7 y; Charge Rate: 21.35 % of Cost/y; Capital Cost: 6400 \$/y — 0.029 \$/m^2

4.1 Subtotal Equipment Cost:	0.053 \$/m^2

Process No. 3 . 6 . 0 3 - 0 2

Form 8
Page 1 of 1
Revision ____ Date 12-79

4.2 Facilities:

4.21 Type: Hood Area   Floor Area: 8.36 m^2; Throughput: 218,600 m^2/y

Charge Rate: 179.13* $/($m^2$·y);

Energy Use:

Heating ______ ______/y at ______$/______

Air Cond'g ______ ______/y at ______$/______

Lighting ______ ______/y at ______$/______

Maintenance Costs:

Labor: ______ h/y at ______ $/h

Supplies: ______ $/y

Outside Services: ______ $/y

Total Cost: 1500 $/y   0.007 $/$m^2$

4.2_ Type: ______ Floor Area: ______ m^2; Throughput: ______ ______/y

Charge Rate: ______ $/($m^2$·y);

Energy Use:

Heating ______ ______/y at ______$/______

Air Cond'g ______ ______/y at ______$/______

Lighting ______ ______/y at ______$/______

Maintenance Costs:

Labor: ______ h/y at ______ $/h

Supplies: ______ $/y

Outside Services: ______ $/y

Total Cost: ______ $/y   ______$/______

4.2_ Type: ______ Floor Area: ______ m^2; Throughput: ______ ______/y

Charge Rate: ______ $/($m^2$·y);

Energy Use:

Heating ______ ______/y at ______$/______

Air Cond'g ______ ______/y at ______$/______

Lighting ______ ______/y at ______$/______

Maintenance Costs:

Labor: ______ h/y at ______ $/h

Supplies: ______ $/y

Outside Services: ______ $/y

Total Cost: ______ $/y   ______$/______

4.2 Subtotal Facilities:	0.007 $/ m^2
4.3 Equipment and Facilities Subtotal :	0.060 $/ m^2

*Includes energy use

Form 12
Page 1 of 1

Process No. 3 . 6 . 0 3 – 0 2

Revision 1 Date 2-81

7. Process Cost Computation

Item	Description	Value
7.11	Manufacturing Add-On Costs (sum of 2.7, 3.5, 4.3, 6.)	1.511 \$/ m^2
7.22	Other Indirect Costs: (0.059 x 4.1 + ~~0.108 x 4.2~~) % of 7.11	0.004 \$/ m^2
7.21	Total Operating Add-on Costs of Process:	1.515 \$/ m^2
7.22	G & A ______ % of 7.21	– \$/ –
7.31	Total Gross Add-On Cost of Process	1.515 \$/ m^2
7.32	Credit for Salvaged Material (5.8)	NA \$/
7.33	Cost of Work-in-Process Lost (5.3)	NA \$/
7.34	Specific Add-On Cost of Process (7.31 + 7.33)-(7.32)	1.515 \$/ m^2
7.35	Cost of Input Work-in-Process Contained in Good Output Work-in-Process (5.4)	NA \$/
7.36	Loading on Item 7.35 at Rate ______ %	NA \$/
7.37	Cost of Output Work-in-Process (7.34 + 7.35 + 7.36)	NA \$/

Item	Description	Value
7.41	Theoretical Yield (or Conversion Rate, if output units of work-in-process do not equal input units)	1 m^2 / m^2
7.42	Practical Yield	99 %
7.43	Effective Yield (7.41 x 7.42)	0.99% /
7.44	Number of Units of Good Output Work-in-Process per Computation Unit Used up to 7.35	0.99 m^2 / m^2

Item	Description	Value
7.51	Cost of Unit of Good Output Work-in-Process (7.37 ÷ 7.44)	– \$/
7.52	Specific Add-On Cost per Unit of Good Output Work-in-Process (7.34 ÷ 7.44)	1.530 \$/ m^2

Process No. 3.6.03-02

Form 13-2
Page 1 of 1
Revision 1 Date 2-81

8.2 Alternate 2 (SAMICS Methodology):

8.21 Profit Computation:

0.9274* 0.053 $/ m^2 from Subtotal 4.1 = 0.049 $/ m^2

1.946* 0.007 $/ m^2 from Subtotal 4.2 = 0.013 $/ m^2

Subtotal = 0.062 $/ m^2

8.22 Costs of Amortization of the One-Time Cost:

0.192* 0.851 $/ m^2 from Subtotal 2.7 = 0.163 $/ m^2

0.192* 0.600 $/ m^2 from Subtotal 3.5 = 0.115 $/ m^2

0.2958* 0.053 $/ m^2 from Subtotal 4.1 = 0.016 $/ m^2

2.77* 0.007 $/ m^2 from Subtotal 4.2 = 0.019 $/ m^2

Subtotal = 0.313 $/ m^2

8.23 Total Net Cost of Equity (8.21 + 8.22): 0.375 $/ m^2

8.24 Profit and Amortization of Start-up Costs per Unit of Good Output Work-in-Process:
(Divide Subtotal 8.23 by 0.9[illegible] m^2 / m^2 from 7.44)

0.378 $/

8.25 Price of Process (7.52 + 8.24) 1.908 $/ m^2

or 1.3 ¢/W(peak)

8.26 Price of Work-in-Process (7.51 + 8.24) $/

Process No. 3 . 6 . 0 3 – 0 3

Form 1

University of Pennsylvania

PROCESS CHARACTERIZATION

(UPPC)

Process: Device Fabrication

Subprocess: Contact Formation (Front and Rear)

Option: Vacuum deposition of a nickel barrier layer and copper conducting layer

INDEX

Form	Pages	Rev.	Date	Remarks
1		1	2-81	
2	1 to 2	1	2-81	
3	1 to 1	1	2-81	
4	1 to 1	1	2-81	
5	1 to 1	1	2-81	
6	1 to 1	1	2-81	
7	1 to 1	1	2-81	
8	1 to 1	1	2-81	
9-1	1 to -			
9-2	1 to -			
9-3	1 to -			
10	1 to -			
11	1 to -			
12	1 to 1	1	2-81	
13-1	1 to -			
13-2	1 to 1	1	2-81	
14	1 to -			
15	1 to -			
16	1 to 4	-	2-81	

Form 2

Revision 1 Date 2-81

Process No. 3 . 6 . 03 - 03

0.1 Value Added:	$/

Process Description: Wafers are placed and locked into reversible holders which also hold the shadow mask for the contact and grid metallization pattern definition on the front side. The holders are ca. 1 m wide and hold 10 cells across their width. The holders are placed in batches into the air-lock chamber of the system, from where they proceed into the main chamber after pump-down to the main chamber pressure ($\sim 10^{-6}$ Torr). In the main chamber, the holders are sequentially removed from the batch and passed flat in continuous flow over the evaporation boats which are ca. 1 m long and deposit

(Continued on Form 2, page 2)

1. Input Specification:

Name of Item: N^+PP^+ Silicon cell ready for metallization, with freshly removed oxide layer, without mask.

Dimensions: 10-cm square

Material:

Other Specifications:

1.1 Quantity Required: / Unit Cost: $/

1.2 Input Value:	$/
1.3 Input Cost:	$/

Note to Item 1.3: Use price, if input produced in own plant.

Revision 1 Date 2-81

Process No. 3 . 6 . 0 3 - 0 3

0.1 Value Added:	$/

Process Description: metal simultaneously over the whole width of the holder. The boats are continuously recharged with rod of the appropriate metal. They are electron beam heated. The evaporation rate and speed of the holder movement determine the metal thickness. After deposition on one side, the holders are turned over in the machine and passed over another set of boats. After deposition on the second side, the holders are re-assembled into batches and passed out of the machine through a a second air-lock chamber.

1. Input Specification: (See Notes on Form 16, page 1)

Name of Item:

Dimensions:

Material:

Other Specifications:

1.1 Quantity Required: / Unit Cost: $/

1.2 Input Value:	$/
1.3 Input Cost:	$/

Note to Item 1.3: Use price, if input produced in own plant.

Process No. 3 . 6 . 03 - 03

Form 3

Page 1 of 1

2.1 Direct Materials:

Revision 1 Date 2-81

2.11 Type: Copper, rod, 1/8" dia., oxygen free (99.9% Cu), ρ=8.96 g/cm^3

Specification: Surface coverage is 3.4%, front, 100% back. Evaporation efficiency is 70% on mask and holder, 50% on to mask. Metal recovery rate is 75% for wall and holder deposits, 50% for mask deposits. Usage ~ 120t/y

Quantity Required: 181.5 g / m^2; Unit Cost: ~ 3 $/ kg ; Cost: 0.545 $/m^2

2.12 Type: Copper, rod from recycled material.

Specification: 178.5 g/m^2 copper are recycled at an assumed recycling cost of 1.30 $/kg

Quantity Required: 178.5 g / m^2; Unit Cost: 1.30 $/ kg ; Cost: 0.232 $/m^2

2.13 Type: Nickel wire, (99.9%), ρ = 8.91 g/cm^3

Specification: Plating thickness is 0.1 µm, and evaporation and recovery efficiencies are same as copper's

Quantity Required: 1.8 g/ m^2; Unit Cost: ~ 11 $/ kg ; Cost: 0.020 $/ m^2

2.1 Subtotal Direct Materials: 0.797 $/ m^2

ORIGINAL PAGE IS
OF POOR QUALITY

Process No. 3 . 6 . 03 - 03

Form 4

Page 1 of 1

Revision 1 Date 2-81

2.2 Indirect Materials (incl. supplies and non-energy utilities):

2.2.1 Type: Vacuum pump oil Convoil 20;

Specification: Need 4 qt. per week

3 shift/day at 7 day/wk operation at net output of 41 m^2/h

Quantity Required: 5.8×10^{-4} qt/m^2; Unit Cost: 30 \$/qt; Cost: 0.017 \$/m^2

2.2.2 Type: Graphite boats

Specification: Size 8" x 12" x 30", set in water-cooled structure. Two or more crucibles used for copper, two for nickel. Experience has shown that 1000 lbs of copper can be evaporated from one crucible. At 50% deposition efficiency, 360 g/m^2 copper need to be evaporated, 3.6 g/m^2 nickel.

Quantity Required: $8 \cdot 10^{-4}$ cruc/m^2; Unit Cost: 1000 \$/cruc; Cost: 0.800 \$/m^2

2.2_ Type:

Specification:

Quantity Required: /; Unit Cost: \$/; Cost: \$/

2.2 Subtotal Indirect Materials: 0.817 \$/m^2

Process No. 3 . 6 . 0 3 – 0 3

Form 5

Revision 1 Date 2/81

2.3 Expendable Tooling:

2.3 _ Type: (Masks not charged here.)

Quantity Required: ____ /____ : Unit Cost: ____ $/____ Cost: ____ $/____

2.3 _ Type: ____

Quantity Required: ____ /____ : Unit Cost: ____ $/____ Cost: ____ $/____

2.3 _ Type: ____

Quantity Required: ____ /____ : Unit Cost: ____ $/____ Cost: ____ $/____

2.3 _ Type: ____

Quantity Required: ____ /____ : Unit Cost: ____ $/____ Cost: ____ $/____

2.3 Subtotal Expendable Tooling: ____ $/____

2.4 Energy

2.4 1 Type: Electricity, name-plate rating 100 kW for pumps, 200 kW for e-beams. Energy usage 3kWh/lb evaporated.

Quantity Required: 2.4 kWh/m^2 : Unit Cost: 0.05 $/kWh Cost: 0.12 $\$/m^2$

2.4 _ Type: ____

Quantity Required: ____ : Unit Cost: ____ $/____ Cost: ____ $/____

2.4	Subtotal Energy Costs:	0.12 $\$/m^2$
2.5	Subtotal 2.1 to 2.4:	1.734 $\$/m^2$
2.6	Handling Charge: 5.26 % of item 2.5	0.091 $\$/m^2$
2.7	Subtotal Materials and Supplies: (2.5 + 2.6)	1.825 $\$/m^2$

Process No. 3 . 6 . 03 - 03

Form 6
Page 1 of 1
Revision 1 Date 2/81

3.1 Direct Labor:

3.11 Category: Semiconductor Assembler (SAMICS B5464D) Activity: Loading, unloading, & machine monitoring

Amount Required: 0.5 h/ h ; Rate: $ 5.65 /h; Load 113 %; Cost: 0.147 $/$m^2$

3.12 Category: Maintenance Mechanic (SAMICS B5176D) Activity: Machine service and repair

Amount Required: 0.2 h/ h ; Rate: $ 7.40 /h; Load 113 %;* Cost: 0.077 $/$m^2$

3.1_ Category: Activity:

Amount Required: h/ ; Rate: $ /h; Load %; Cost: $/

3.1 Direct Labor Subtotal: 0.224 $/$m^2$

3.2 Indirect Labor: Taken as 25% of direct

3.2_ Category: Activity:

Amount Required: h/ ; Rate: $ /h; Load %; Cost: $/

3.2_ Category: Activity:

Amount Required: h/ ; Rate: $ /h; Load %; Cost: $/

3.2_ Category: Activity:

Amount Required: h/ ; Rate: $ /h; Load %; Cost: $/

3.2 Indirect Labor Subtotal: 0.056 $/$m^2$

3.3 Subtotal 3.1 and 3.2 0.280 $/$m^2$

3.4 Overhead on Labor: 5.26% 0.015 $/$m^2$

3.5 Subtotal Labor 0.295 $/$m^2$

*Includes benefits (36%) and requirement of 1.57 workers/shift.

Form 7
Page 1 of 1
Revision 1 Date 2/81

Process No. 3 . 6 . 0 3 - 0 3

4.1 Equipment

4.11 Type: Airco Temescal evaporator

Cost: ~ 2,000,000 $; Installation Cost: ______ $; Throughput: 48 m^2 /h;

Plant Oper'g Time 8280 h/y; Machine Avail'ty: 85.5%; Machine Oper'g Time 7038 h/y

Servicing Costs: Labor ______ h/y at ______ $/h; Parts or Outside Service: ______ $/y

Useful Life. 7 y; Charge R[illegible] [illegible].35 % of Cost/y; Capital Cost: 34,160 $/y | 1.264 $/$m^2$

4.1_ Type: ______

Cost: ______ $; Installation Cost: ______ $; Throughput: ______ /h;

Plant Oper'g Time ______ h/y; Machine Avail'ty: ______ %; Machine Oper'g Time ______ h/y

Servicing Costs: Labor ______ h/y at ______ $/h; Parts or Outside Service: ______ $/y

Useful Life: ______ y; Charge Rate: ______ % of Cost/y; Capital Cost: ______ $/y | ______ $/______

4.1_ Type: ______

Cost: ______ $; Installation Cost: ______ $; Throughput: ______ /h;

Plant Oper'g Time ______ h/y; Machine Avail'ty: ______ %; Machine Oper'g Time ______ h/y

Servicing Costs: Labor ______ h/y at ______ $/h; Parts or Outside Service: ______ $/y

Useful Life: ______ y; Charge Rate: ______ % of Cost/y; Capital Cost: ______ $/y | ______ $/______

4.1 Subtotal Equipment Cost:	1.264 $/$m^2$

Process No. 3 . 6 . 0 3 - 0 3

Form 8
Page 1 of 1
Revision 1 Date 2/81

4.2 Facilities:

4.21 Type: Equipment space   Floor Area: 97.5 m^2; Throughput: 337,800 /y

Charge Rate: 179.13* $/(m^2·y);

Energy Use:

Heating	/y at	$/	
Air Cond'g	/y at	$/	
Lighting	/y at	$/	

Maintenance Costs:

Labor: h/y at $/h

Supplies: $/y

Outside Services: $/y

Total Cost: 17,465 $/y   0.052 $/$m^2$

4.2_ Type: Floor Area: m^2; Throughput: /y

Charge Rate: $/(m^2·y);

Energy Use:

Heating	/y at	$/	
Air Cond'g	/y at	$/	
Lighting	/y at	$/	

Maintenance Costs:

Labor: h/y at $/h

Supplies: $/y

Outside Services: $/y

Total Cost: $/y $/

4.2_ Type: Floor Area: m^2; Throughput: /y

Charge Rate: $/(m^2·y);

Energy Use:

Heating	/y at	$/	
Air Cond'g	/y at	$/	
Lighting	/y at	$/	

Maintenance Costs:

Labor: h/y at $/h

Supplies: $/y

Outside Services: $/y

Total Cost: $/y $/

4.2 Subtotal Facilities: 0.052 $/$m^2$

4.3 Equipment and Facilities Subtotal : 1.316 $/$m^2$

Form 12
Page 1 of 1

Process No. 3 . 6 . 03 — 03

Revision 1 Date 2/81

7. Process Cost Computation

Item	Description	Value
7.11	Manufacturing Add-On Costs (sum of 2.7, 3.5, 4.3, 6.)	3.436 $/ m^2
7.22	Other Indirect Costs: (0.059* 4.1 + 0.108* 4.2) % of 7.11	0.080 $/ m^2
7.21	Total Operating Add-on Costs of Process:	3.516 $/ m^2
7.22	G & A ____ % of 7.21	- $/ -
7.31	Total Gross Add-On Cost of Process	3.516 $/ m^2
7.32	Credit for Salvaged Material (5.8)	incl'd $/
7.33	Cost of Work-in-Process Lost (5.3)	- $/
7.34	Specific Add-On Cost of Process (7.31 + 7.33)-(7.32)	3.516 $/
7.35	Cost of Input Work-in-Process Contained in Good Output Work-in-Process (5.4)	NA $/
7.36	Loading on Item 7.35 at Rate ____ %	NA $/
7.37	Cost of Output Work-in-Process (7.34 + 7.35 + 7.36)	NA $/

Item	Description	Value
7.41	Theoretical Yield (or Conversion Rate, if output units of work-in-process do not equal input units)	1.0 m^2 / m^2
7.42	Practical Yield	99 %
7.43	Effective Yield (7.41 x 7.42)	0.99 /
7.44	Number of Units of Good Output Work-in-Process per Computation Unit Used up to 7.35	0.99 m^2 / m^2

Item	Description	Value
7.51	Cost of Unit of Good Output Work-in-Process (7.37 ÷ 7.44)	$/
7.52	Specific Add-On Cost per Unit of Good Output Work-in-Process (7.34 ÷ 7.44)	3.552 $/ m^2

ORIGINAL PAGE IS OF POOR QUALITY

Process No. 3.6.03-03

Form 13-2
Page 1 of 1

Revision 1 Date 2/81

8.2 Alternate 2 (SAMICS Methodology):

8.21 Profit Computation:

0.9274* 1.264 $/ m^2 from Subtotal 4.1 = 1.172 $/ m^2

1.946* 0.052 $/ m^2 from Subtotal 4.2 = 0.101 $/ m^2

Subtotal = 1.273 $/ m^2

8.22 Costs of Amortization of the One-Time Cost:

0.192* 1.825 $/ m^2 from Subtotal 2.7 = 0.350 $/ m^2

0.192* 0.295 $/ m^2 from Subtotal 3.5 = 0.057 $/ m^2

0.2958* 1.264 $/ m^2 from Subtotal 4.1 = 0.374 $/ m^2

2.77* 0.052 $/ m^2 from Subtotal 4.2 = 0.144 $/ m^2

Subtotal = 0.925 $/ m^2

8.23 Total Net Cost of Equity (8.21 + 8.22): 2.198 $/ m^2

8.24 Profit and Amortization of Start-up Costs per Unit of Good Output Work-in-Process:
(Divide Subtotal 8.23 by 0.99 m^2 / m^2 from 7.44)

2.220 $/ m^2

8.25 Price of Process (7.52 + 8.24) 5.772 $/ m^2
3.85 ¢/W(peak)

8.26 Price of Work-in-Process (7.51 + 8.24) $/

Process No. 3 . 6 . 03 - 03

WORKSHEET TO ITEM Process Descrip., FORM 2 PAGE 3

Machine throughput is nominally 48 m^2/h. The uptime fraction is 0.85, for an effective throughput rate of 41 m^2/h. Nickel thickness is 0.1 µm and copper layer is 10 µm thick. Approximately 1 h/shift is required for cleaning the vacuum chamber of metal deposits. Vacuum deposition machine is proposed by Airco Temescal, based on similar machines built by them (John L. Hughes)

With use of a common shadow mask for barrier layer and conduction layer deposition, some deposition of scattered copper atoms outside of an adequate barrier layer may not be avoidable. Even without heat treatment subsequent to metallization, this spurious copper deposit may reduce the effective operating life of the cells. This may be an additional reason, besides the impracticality of using shadow masks for thick deposits with fine line patterns, for the selection of competing processes over physical vapor deposition.

Process No. 3 . 6 . 0 3 – 0 3

Form 16
Page 2 of 4

WORKSHEET TO ITEM Process Descript., FORM 2 PAGE ___

Length of machine ∿ 50 ft ≈ 15 m;

Approximate breakdown of lengths:

Airlock in	2 m
batch disassembler	2 m
evaporation station 1	2.5 m
turn-over	2 m
evaporation station 2	2.5 m
batch re-assembler	2 m
airlock out	2 m
total length of machine	15 m

Throughput 48 m^2 = 48 m long x 1 m wide, means 0.8 m/min travel speed.
Boat width ∿ 12" ≈ 30 cm, means exposure ∿ 0.4 m: evaporation speed Cu ∿ 20 μm/min.
Assume airlock cycle time 15 min; batch size 12 m^2.
To calculate time at station:

Assemble batch for machine:	(1/2 batch)	6 m^2
In airlock in (pump-down ∿ 2/3 of airlock cycle)	(2/3 batch)	8 m^2
Dis-assemble batch in machine:	(1/2 batch)	6 m^2
Moving through process (∿ 8 m long)		8 m^2
Re-assemble batch	(1/2 batch)	6 m^2
In airlock out (air admission ∿ 1/3 of airlock cycle)	(1/3 batch)	4 m^2
Dis-assemble batch for further processing	(1/2 batch)	6 m^2
	Total	44 m^2

Result: Time at station: 55 min.

Process No. 3 . 6 . 0 3 - 0 3

WORKSHEET TO ITEM 2.11 & 2.12, FORM 3 & 4 PAGE 1 ea.

Mass evaporated from boat:

$$M_{evap} = \frac{A_{mask}/f_{hold}}{\eta_{dep}} (d_F + d_R)\ \rho_{Met} = \frac{1\cdot 10^4\ cm^2/0.71}{0.7} \cdot 2\cdot 10^{-3}\ cm\cdot 8.96\ g/cm^3 = \underline{\underline{360\ g/m^2}}$$

Mass on cell:

$$M_{subs} = A_{mask}(f_{mask,F}d_F + f_{mask,R}d_R)\ \rho_{Met} = 1\cdot 10^4\ cm\ (0.034 + 1.00) \cdot 1\cdot 10^{-3}\cdot 8.94 = \underline{\underline{92.6\ g/m^2}}$$

Net metal used:

$$M_{net} = \frac{A_{mask}}{f_{hold}} \rho_{Met} \left\{ \left[\frac{1-\eta_{dep}}{\eta_{dep}} (1-r_{wall}) + (1-f_{hold})(1-r_{hold}) \right] (d_F + d_R) + f_{hold} \left[(1-f_{mask,F})\ d_F + (1-f_{mask,R})\ d_R \right] \cdot (1-r_{mask}) \right\} + M_{subs}\ ;$$

Process No. 3 . 6 . 0 3 - 0 3

WORKSHEET TO ITEM 2.11 & 2.12, cont'd FORM ______ PAGE ______

$$M_{net} = \frac{1 \cdot 10^4\ cm^2}{0.71}\ 8.96\ g/cm^3 \left\{ \left[\frac{0.3}{0.7} \cdot 0.25 + 0.29 \cdot 0.25 \right] \cdot 2 \cdot 10^{-3}\ cm + 0.71 \left[(0.966 + 0) \cdot 1 \cdot 10^{-3}\ cm\ 0.5 \right\} + 92.6\ g/m^2 ;$$

$$M_{net} = 181.2\ g/m^2$$

The following quantities were used:

$A_{mask} = 1\ m^2 = 1 \cdot 10^4\ cm^2$; $\rho_{Met} = 8.96\ g/cm^3$; $d_F = d_R = 1 \cdot 10^{-3}\ cm$; $r_{wall} = r_{hold} = 0.75$;

$r_{mask} = 0.5$

$\eta_{dep} = 0.7$; $f_{hold} = 0.71$; $f_{mask,F} = 0.034$; $f_{mask,R} = 1.0$;

Process No. 3 . 6 . 0 4 - 0 1 Form 1

University of Pennsylvania
PROCESS CHARACTERIZATION
(UPPC)

Process: Device Fabrication

Subprocess: Contact Metallization (Front and Rear)

Option: Electrolytic Plating of Copper over a Nickel Strike Layer

INDEX

Form	Pages	Rev.	Date	Remarks
1		1	2-81	
2	1 to 2	1	2-81	
3	1 to 1	1	2-81	
4	1 to 1	1	2-81	
5	1 to 1	1	2-81	
6	1 to 1	1	1-81	
7	1 to 1	1	2-81	
8	1 to 1	1	2-81	
9-1	1 to -			
9-2	1 to -			
9-3	1 to -			
10	1 to -			
11	1 to -			
12	1 to 1	1	2-81	
13-1	1 to -			
13-2	1 to 1	1	2-81	
14	1 to -			
15	1 to -			
16	1 to -			

Form 2

Page 1 of 2

Revision 1 Date 2-81

Process No. 3 . 6 . 0 4 - 0 1

0.1 Value Added:	$/

Process Description: Copper is electrolytically plated sequentially on both sides of the cells in an automatic plating system, including cassette unload and re-load. The equipment should be capable of of a current density of about 60 mA/cm^2 and a voltage between 4 and 8 volts (DC). The system may resemble a finger plating machine (Napco) with individual racking, or a carousel machine (4 cavity) with jig loading (Oxy Metal Industries). Throughput rate is 3,000 wafers/h (30 m^2/h) and availability

(Continuation on Form 2, page 2)

1. Input Specification:

Name of Item: Silicon wafer with N$^+$PP$^+$ junctions and 0.5 μm thick nickel strike layer in desired metallization pattern on front and back surfaces, possibly contact mask.

Dimensions: 10-cm square

Material:

Other Specifications:

ORIGINAL PAGE IS OF POOR QUALITY

1.1 Quantity Required: ______ /______ Unit Cost: ______ $/ ______

1.2 Input Value:	$/
1.3 Input Cost:	$/

Note to Item 1.3: Use price, if input produced in own plant.

Revision 1 Date 2-81

Process No. 3.6.04-01

0.1 Value Added: $/

Process Description: is 95% for an effective output rate of 28.5 m^2/h. Area coverage is 3.4% front, 100% rear, metal thickness is 10 µm. Cycle time is 15 minutes.

1. Input Specification:

Name of Item:

Dimensions:

Material:

Other Specifications:

1.1 Quantity Required: / Unit Cost: $/

1.2 Input Value:	$/
1.3 Input Cost:	$/

Note to Item 1.3: Use price, if input produced in own plant

Process No. 3 . 6 . 0 4 - 0 1

Form 3

Page 1 of 1

2.1 Direct Materials:

Revision 1 Date 2-81

2.11 Type: Copper electrodes (99.9%);

Specification: Electrolytic Cu anodes. At 1.034 m^2/m^2 and 10 μm thickness, 10.34 cm^3/m^2 or 92.44 g/m^2 deposited on solar cells. Coating efficiency of 95% assumed.;

Quantity Required: 97.31 g/m^2; Unit Cost: ∿ 2.00 $/ kg; Cost: 0.195 $/ m^2

2.1_ Type: ;

Specification: ;

Quantity Required: /; Unit Cost: $/; Cost: $/

2.1_ Type: ;

Specification: ;

Quantity Required: /; Unit Cost: $/; Cost: $/

2.1 Subtotal Direct Materials: 0.195 $/ m^2

Process No. 3 . 6 . 04 - 01

Form 4

Page 1 of 1

Revision 1 Date 2-81

2.2 Indirect Materials (incl. supplies and non-energy utilities):

2.21 Type: Electrolytic Copper Replenisher Solution ;

Specification: Need 1 mℓ per amp-h. Volume of solution is 1 mℓ/amp-h x 1 amp-h/3600 coul x 96,500 coul/0.5 mole x 1 mole/63.54g x 97.31g/m^2.

Cost of solution is $13/gallon when bought in 54 gallon drums.

Quantity Required: 82.1 mℓ / m^2; Unit Cost: 3.434 $/ ℓ ; Cost: 0.282 $/ m^2

2.2_ Type:

Specification:

Quantity Required: / ; Unit Cost: $/ ; Cost: $/

2.2_ Type:

Specification:

Quantity Required: / ; Unit Cost: $/ ; Cost: $/

2.2 Subtotal Indirect Materials: 0.282 $/ m^2

Process No. 3.6.04-01

Form 5
Page 1 of 1
Revision 1 Date 2-81

2.3 Expendable Tooling:

2.3_ Type: ______

______ Quantity Required: ______ ___/___: Unit Cost: ___\$/___ Cost: ___\$/___

2.3_ Type: ______

______ Quantity Required: ______ ___/___: Unit Cost: ___\$/___ Cost: ___\$/___

2.3_ Type: ______

______ Quantity Required: ______ ___/___: Unit Cost: ___\$/___ Cost: ___\$/___

2.3_ Type: ______

______ Quantity Required: ______ ___/___: Unit Cost: ___\$/___ Cost: ___\$/___

2.3	Subtotal Expendable Tooling:	___\$/___

2.4 Energy

2.4 1 Type: DC power: ~ 60 mA/cm^2 and nominal voltage of 6V: ~ 4 kWh/m^2 output. Rectifer efficiency assumed to be 80%.

______ Quantity Required: 5 kWh/m^2 : Unit Cost: 0.05 \$/kWh Cost: 0.250 \$/m^2

2.4_ Type: ______

______ Quantity Required: ______ ______: Unit Cost: ___\$/___ Cost: ___\$/___

Item	Value
2.4 Subtotal Energy Costs:	0.250 \$/m^2
2.5 Subtotal 2.1 to 2.4:	0.727 \$/m^2
2.6 Handling Charge: 5.26 % of item 2.5	0.038 \$/m^2
2.7 Subtotal Materials and Supplies: (2.5 + 2.6)	0.765 \$/m^2

ORIGINAL PAGE IS
OF POOR QUALITY

Process No. 3 . 6 . 0 4 - 0 1

Form 6
Page 1 of 1
Revision 1 Date 1-81

3.1 Direct Labor:

3.1_ Category: Semiconductor Assembler (SAMICS B5464D) Activity: Loading, changing electrodes and monitoring
Amount Required: 1 h/ h ; Rate: $ 5.65 /h; Load 113 %*; Cost: 0.422 $/ m^2

3.1_ Category: ______ Activity: ______
Amount Required: ______ h/ ______ ; Rate: $ ______ /h; Load ______ %; Cost: ______ $/ ______

3.1_ Category: ______ Activity: ______
Amount Required: ______ h/ ______ ; Rate: $ ______ /h; Load ______ %; Cost: ______ $/ ______

3.1 Direct Labor Subtotal: 0.422 $/ m^2

3.2 Indirect Labor: Taken as 25% of direct

3.2_ Category: ______ Activity: ______
Amount Required: ______ h/ ______ ; Rate: $ ______ /h; Load ______ %; Cost: ______ $/ ______

3.2_ Category: ______ Activity: ______
Amount Required: ______ h/ ______ ; Rate: $ ______ /h; Load ______ %; Cost: ______ $/ ______

3.2_ Category: ______ Activity: ______
Amount Required: ______ h/ ______ ; Rate: $ ______ /h; Load ______ %; Cost: ______ $/ ______

3.2 Indirect Labor Subtotal: 0.106 $/ m^2

3.3 Subtotal 3.1 and 3.2 0.528 $/ m^2

3.4 Overhead on Labor: 5.26 % 0.028 $/ m^2

3.5 Subtotal Labor 0.556 $/ m^2

*Includes benefits and replacement labor costs.

Form 7
Page 1 of 1
Revision 1 Date 2-81

Process No. 3 . 6 . 0 4 - 0 1

4.1 Equipment

4.11 Type: Automatic plating machines, complete (2 required for plating 2 sides)

Cost: 400,000 for 2 \$; Installation Cost: 200,000* \$; Throughput: 30 m^2 /h;

Plant Oper'g Time 8280 h/y; Machine Avail'ty: 95 %; Machine Oper'g Time 7866 h/y

Servicing Costs: Labor ______ h/y at ______ \$/h; Parts or Outside Service: ______ \$/y

Useful Life. ______ y; Charge R[illegible]: [illegible] 35 % of Cost/y; Capital Cost: 128,100 \$/y — 0.543 \$/ m^2

*Includes waste treatment and byproduct recovery system.

4.1_ Type: ______

Cost: ______ \$; Installation Cost: ______ \$; Throughput: ______ /h;

Plant Oper'g Time ______ h/y; Machine Avail'ty: ______ %; Machine Oper'g Time ______ h/y

Servicing Costs: Labor ______ h/y at ______ \$/h; Parts or Outside Service: ______ \$/y

Useful Life: ______ y; Charge Rate: ______ % of Cost/y; Capital Cost: ______ \$/y — ______ \$/ ______

4.1_ Type: ______

Cost: ______ \$; Installation Cost: ______ \$; Throughput: ______ /h;

Plant Oper'g Time ______ h/y; Machine Avail'ty: ______ %; Machine Oper'g Time ______ h/y

Servicing Costs: Labor ______ h/y at ______ \$/h; Parts or Outside Service: ______ \$/y

Useful Life: ______ y; Charge Rate: ______ % of Cost/y; Capital Cost: ______ \$/y — ______ \$/ ______

4.1 Subtotal Equipment Cost: 0.543 \$/ m^2

Process No. 3 . 6 . 0 4 - 0 1

Form 8
Page 1 of 1
Revision 1 Date 2-81

4.2 Facilities:

4.21 Type: Ventilated process area Floor Area: 90 m^2; Throughput: 236,000 m^2 /y

Charge Rate: 179.13* $/($m^2$·y);

Energy Use:

Heating ______ /y at ______ $/______

Air Cond'g ______ /y at ______ $/______

Lighting ______ /y at ______ $/______

Maintenance Costs:

Labor: ______ h/y at ______ $/h

Supplies: ______ $/y

Outside Services: ______ $/y

Total Cost: 16 122 $/y — 0.068 $/ m^2

4.2_ Type: ______ Floor Area: ______ m^2; Throughput: ______ /y

Charge Rate: ______ $/($m^2$·y);

Energy Use:

Heating ______ /y at ______ $/______

Air Cond'g ______ /y at ______ $/______

Lighting ______ /y at ______ $/______

Maintenance Costs:

Labor: ______ h/y at ______ $/h

Supplies: ______ $/y

Outside Services: ______ $/y

Total Cost: ______ $/y — ______ $/______

4.2_ Type: ______ Floor Area: ______ m^2; Throughput: ______ /y

Charge Rate: ______ $/($m^2$·y);

Energy Use:

Heating ______ /y at ______ $/______

Air Cond'g ______ /y at ______ $/______

Lighting ______ /y at ______ $/______

Maintenance Costs:

Labor: ______ h/y at ______ $/h

Supplies: ______ $/y

Outside Services: ______ $/y

Total Cost: ______ $/y — ______ $/______

4.2 Subtotal Facilities: 0.068 $/ m^2

4.3 Equipment and Facilities Subtotal: 0.611 $/ m^2

*Includes energy use

Process No. 3 . 6 . 04 — 01

Revision 1 Date 2-81

7. Process Cost Computation

Item	Description	Value
7.11	Manufacturing Add-On Costs (sum of 2.7, 3.5, 4.3, 6.)	1.932 $/ m^2
7.22	Other Indirect Costs: ___ % of 7.11 (0.059 x 4.1 + 0.108 x 4.2)	0.039 $/ m^2
7.21	Total Operating Add-on Costs of Process:	1.971 $/ m^2
7.22	G & A ___ % of 7.21	$/
7.31	Total Gross Add-On Cost of Process	1.971 $/ m^2
7.32	Credit for Salvaged Material (5.8)	- $/
7.33	Cost of Work-in-Process Lost (5.3)	- $/
7.34	Specific Add-On Cost of Process (7.31 + 7.33)-(7.32)	1.971 $/ m^2
7.35	Cost of Input Work-in-Process Contained in Good Output Work-in-Process (5.4)	NA $/
7.36	Loading on Item 7.35 at Rate ___ %	NA $/
7.37	Cost of Output Work-in-Process (7.34 + 7.35 + 7.36)	NA $/

Item	Description	Value
7.41	Theoretical Yield (or Conversion Rate, if output units of work-in-process do not equal input units)	1 m^2 / m^2
7.42	Practical Yield	99.8%
7.43	Effective Yield (7.41 x 7.42)	0.998 m^2 / m^2
7.44	Number of Units of Good Output Work-in-Process per Computation Unit Used up to 7.35	0.998 m^2 / m^2

Item	Description	Value
7.51	Cost of Unit of Good Output Work-in-Process (7.37 ÷ 7.44)	NA $/
7.52	Specific Add-On Cost per Unit of Good Output Work-in-Process (7.34 ÷ 7.44)	1.975 $/ m^2

Process No. 3.6.04-01

Form 13-2
Page 1 of 1

Revision 1 Date 2-81

8.2 Alternate 2 (SAMICS Methodology):

8.21 Profit Computation:

0.9274* 0.543 $/ m^2 from Subtotal 4.1 = 0.504 $/ m^2

1.946* 0.068 $/ m^2 from Subtotal 4.2 = 0.132 $/ m^2

Subtotal = 0.636 $/ m^2

8.22 Costs of Amortization of the One-Time Cost:

0.192* 0.765 $/ m^2 from Subtotal 2.7 = 0.147 $/ m^2

0.192* 0.556 $/ m^2 from Subtotal 3.5 = 0.107 $/ m^2

0.2958* 0.543 $/ m^2 from Subtotal 4.1 = 0.161 $/ m^2

2.77* 0.068 $/ m^2 from Subtotal 4.2 = 0.188 $/ m^2

Subtotal = 0.603 $/ m^2

8.23 Total Net Cost of Equity (8.21 + 8.22): 1.239 $/ m^2.

8.24 Profit and Amortization of Start-up Costs per Unit of Good Output Work-in-Process:
(Divide Subtotal 8.23 by 0.998 m^2 / m^2 from 7.44)

1.241 $/ m^2

8.25 Price of Process (7.52 + 8.24) 3.216 $/ m^2
2.14 ¢/W(peak)

8.26 Price of Work-in-Process (7.51 + 8.24) $/

Process No. 3 . 6 . 0 4 - 0 2

Form 1

University of Pennsylvania

PROCESS CHARACTERIZATION

(UPPC)

Process: Device Fabrication

Subprocess: Contact Metallization (Front and Rear)

Option: Solder Dip

INDEX

Form	Pages	Rev.	Date	Remarks
1		1	2-81	
2	1 to 1		11-78	
3	1 to 1		11-78	
4	1 to 1	1	2-81	
5	1 to 1	1	2-81	
6	1 to 1		11-78	
7	1 to 1		11-78	
8	1 to 1		11-78	
9-1	1 to -			
9-2	1 to -			
9-3	1 to -			
10	1 to -			
11	1 to -			
12	1 to 1	1	2-81	
13-1	1 to -			
13-2	1 to 1	1	2-81	
14	1 to -			
15	1 to -			
16	1 to -			

Form 2

Revision ______ Date 11-78

Process No. 3 . 6 . 04 - 02

0.1 Value Added:	$/

Process Description: Steps include flux application, pre-heating, soldering, cleaning and drying. Surface coverage is 6.2% on front (127 μm line width), and 100% on back. Throughout rates is 3,000 wafers/h, and up-time is 88% for an effective throughput rate of 26.4 m^2/h. Average coating thickness is 55 μm.

1. Input Specification:

Name of Item: n^+pp^+ silicon solar cells with nickel (or other solderable metal) plated, ∿ 0.5 μm thick metallization

Dimensions: 10 cm square

Material:

Other Specifications:

1.1 Quantity Required: ______ ______ / ______ Unit Cost: ______ $/ ______

1.2 Input Value:	$/
1.3 Input Cost:	$/

Note to Item 1.3: Use price, if input produced in own plant.

Process No. 3 . 6 . 0 4 – 0 2

Revision ______ Date 11-78

2.1 Direct Materials:

2.11 Type: Tin Lead Solder (60:40), $\rho = 8.9\ g/cm^3$;

Specification: Solder thickness is 55 μm, area coverage is 106.2%. Coating efficiency is 95%. Cost is $10/kg.;

Quantity Required: 547.4 g / m^2; Unit Cost: 10 $/kg; Cost: 5.474 $/$m^2$

2.1_ Type: ;

Specification: ;

Quantity Required: ___/___; Unit Cost: ___$/___; Cost: ___$/___

2.1_ Type: ;

Specification: ;

Quantity Required: ___/___; Unit Cost: ___$/___; Cost: ___$/___

2.1 Subtotal Direct Materials: 5.474 $/$m^2$

Process No. 3 . 6 . 04 - 02

Form 4

Page 1 of 1

Revision 1 Date 2-81

2.2 Indirect Materials (incl. supplies and non-energy utilities):

2.2.1 Type: Flux, water-soluble ;

Specification: One gallon of flux can coat 18.5 m^2 of cells. When bought in 53 gallon drums, cost is $6.75/gal (1978).

Quantity Required: 0.054 gal / m^2; Unit Cost: 6.75 $/gal ; Cost: 0.363 $/$m^2$

2.2.2 Type: Deionized water

Specification: Used continuously for flux residue removal at flow rate of 1 gal/min.

Cost is $660 for 100 m^3 (SAMICS C1128D)

Quantity Required: 8 l / m^2; Unit Cost: 0.0066 $/l ; Cost: 0.053 $/$m^2$

2.2_ Type:

Specification:

Quantity Required: ___ / ___; Unit Cost: ___ $/ ___; Cost: ___ $/ ___

2.2 Subtotal Indirect Materials: 0.416 $/$m^2$

Process No. 3 . 6 . 0 4 – 0 2

Form 5

Page 1 of 1

Revision 1 Date 2-81

2.3 Expendable Tooling:

2.3_ Type: ______

______ Quantity Required: ______ ____/____: Unit Cost: ____$/____ Cost: ______$/____

2.3_ Type: ______

______ Quantity Required: ______ ____/____: Unit Cost: ____$/____ Cost: ______$/____

2.3_ Type: ______

______ Quantity Required: ______ ____/____: Unit Cost: ____$/____ Cost: ______$/____

2.3_ Type: ______

______ Quantity Required: ______ ____/____: Unit Cost: ____$/____ Cost: ______$/____

2.3 Subtotal Expendable Tooling:	– $/ m^2

2.4 Energy

2.4 1 Type: Electricity, utilization is 95% and name plate rating is 15kW

______ Quantity Required: 0.27 kWh/m^2 : Unit Cost: 0.05 $/ kWh Cost: 0.013 $/ m^2

2.4_ Type: ______

______ Quantity Required: ______ ______: Unit Cost: ____$/____ Cost: ______$/____

2.4 Subtotal Energy Costs:	0.013 $/ m^2
2.5 Subtotal 2.1 to 2.4:	5.903 $/ m^2
2.6 Handling Charge: 5.26 % of item 2.5	0.310 $/ m^2
2.7 Subtotal Materials and Supplies: (2.5 + 2.6)	6.213 $/ m^2

Process No. 3.6.04-02

Form 6
Page 1 of 1
Revision ____ Date 11-78

3.1 Direct Labor:

3.11 Category: Semiconductor Assembler (SAMICS B5464D) Activity: Solder System Operator

Amount Required: 1 h/ h ; Rate: $ 5.65 /h; Load 113 %*; Cost: 0.456 $/ m^2

3.1_ Category: ____ Activity: ____

Amount Required: ____ h/ ____ ; Rate: $ ____ /h; Load ____ %; Cost: ____ $/ ____

3.1_ Category: ____ Activity: ____

Amount Required: ____ h/ ____ ; Rate: $ ____ /h; Load ____ %; Cost: ____ $/ ____

3.1 Direct Labor Subtotal: 0.456 $/ m^2

3.2 Indirect Labor: Taken as 25% of direct

3.2_ Category: ____ Activity: ____

Amount Required: ____ h/ ____ ; Rate: $ ____ /h; Load ____ %; Cost: ____ $/ ____

3.2_ Category: ____ Activity: ____

Amount Required: ____ h/ ____ ; Rate: $ ____ /h; Load ____ %; Cost: ____ $/ ____

3.2_ Category: ____ Activity: ____

Amount Required: ____ h/ ____ ; Rate: $ ____ /h; Load ____ %; Cost: ____ $/ ____

3.2 Indirect Labor Subtotal: 0.114 $/ m^2

3.3 Subtotal 3.1 and 3.2: 0.570 $/ m^2

3.4 Overhead on Labor: ____ %: 0.030 $/ m^2

3.5 Subtotal Labor: 0.600 $/ m^2

*Includes labor replacement costs and benefits.

Process No. 3 . 6 . 0 4 - 0 2

Revision ____ Date 11-78

4.1 Equipment

4.11 Type: Solder system (flux appliction, cell pre-heater, solder dipping, flux removal, drying stations with automatic cell handling)

Cost: 50,000 \$; Installation Cost: - \$; Throughput: 30 m^2 /h;

Plant Oper'g Time 8280 h/y; Machine Avail'ty: 88 %; Machine Oper'g Time 7286 h/y

Servicing Costs: Labor ____ h/y at ____ \$/h; Parts or Outside Service: ____ \$/y

Useful Life: 7 y; Charge Rate: 21.35 % of Cost/y; Capital Cost: 10,675 \$/y — 0.049 \$/m^2

4.1_ Type: ____

Cost: ____ \$; Installation Cost: ____ \$; Throughput: ____ /h;

Plant Oper'g Time ____ h/y; Machine Avail'ty: ____ %; Machine Oper'g Time ____ h/y

Servicing Costs: Labor ____ h/y at ____ \$/h; Parts or Outside Service: ____ \$/y

Useful Life: ____ y; Charge Rate: ____ % of Cost/y; Capital Cost: ____ \$/y — ____ \$/____

4.1_ Type: ____

Cost: ____ \$; Installation Cost: ____ \$; Throughput: ____ /h;

Plant Oper'g Time ____ h/y; Machine Avail'ty: ____ %; Machine Oper'g Time ____ h/y

Servicing Costs: Labor ____ h/y at ____ \$/h; Parts or Outside Service: ____ \$/y

Useful Life: ____ y; Charge Rate: ____ % of Cost/y; Capital Cost: ____ \$/y — ____ \$/____

4.1 Subtotal Equipment Cost: 0.049 \$/m^2

Process No. 3 . 6 . 04 – 02

Form 8
Page 1 of 1
Revision ____ Date 11-78

4.2 Facilities:

4.21 Type: Ventilated process area Floor Area: 9.3 m^2; Throughput: 218,600 m^2/y

Charge Rate: 179.13* $/($m^2$·y);

Energy Use:

Heating ____ ____/y at ____ $/____

Air Cond'g ____ ____/y at ____ $/____

Lighting ____ ____/y at ____ $/____

Maintenance Costs:

Labor: ____ h/y at ____ $/h

Supplies: ____ $/y

Outside Services: ____ $/y

Total Cost: 1665 $/y — 0.022 $/$m^2$

4.2_ Type: ____ Floor Area: ____ m^2; Throughput: ____ ____/y

Charge Rate: ____ $/($m^2$·y);

Energy Use:

Heating ____ ____/y at ____ $/____

Air Cond'g ____ ____/y at ____ $/____

Lighting ____ ____/y at ____ $/____

Maintenance Costs:

Labor: ____ h/y at ____ $/h

Supplies: ____ $/y

Outside Services: ____ $/y

Total Cost: ____ $/y — ____ $/____

4.2_ Type: ____ Floor Area: ____ m^2; Throughput: ____ ____/y

Charge Rate: ____ $/($m^2$·y);

Energy Use:

Heating ____ ____/y at ____ $/____

Air Cond'g ____ ____/y at ____ $/____

Lighting ____ ____/y at ____ $/____

Maintenance Costs:

Labor: ____ h/y at ____ $/h

Supplies: ____ $/y

Outside Services: ____ $/y

Total Cost: ____ $/y — ____ $/____

4.2 Subtotal Facilities:	0.022 $/$m^2$
4.3 Equipment and Facilities Subtotal :	0.071 $/$m^2$

*Includes energy use

ORIGINAL PAGE IS OF POOR QUALITY

Process No. 3 . 6 . 0 4 — 0 2

Revision 1 Date 2-81

7. Process Cost Computation

Item	Description	Value
7.11	Manufacturing Add-On Costs (sum of 2.7, 3.5, 4.3, 6.)	6.883 $/$m^2$
7.22	Other Indirect Costs: (0.059 x 4.1 + ~~0.108 x 4.2~~) % of 7.11	0.006 $/$m^2$
7.21	Total Operating Add-on Costs of Process:	6.889 $/$m^2$
7.22	G & A ______ % of 7.21	- $/
7.31	Total Gross Add-On Cost of Process	6.889 $/$m^2$
7.32	Credit for Salvaged Material (5.8)	- $/
7.33	Cost of Work-in-Process Lost (5.3)	- $/
7.34	Specific Add-On Cost of Process (7.31 + 7.33)-(7.32)	6.889 $/$m^2$
7.35	Cost of Input Work-in-Process Contained in Good Output Work-in-Process (5.4)	NA $/
7.36	Loading on Item 7.35 at Rate ______ %	NA $/
7.37	Cost of Output Work-in-Process (7.34 + 7.35 + 7.36)	$/

Item	Description	Value
7.41	Theoretical Yield (or Conversion Rate, if output units of work-in-process do not equal input units)	1 m^2 / m^2
7.42	Practical Yield	99.8 %
7.43	Effective Yield (7.41 x 7.42)	0.998 /
7.44	Number of Units of Good Output Work-in-Process per Computation Unit Used up to 7.35	0.998 m^2 / m^2

Item	Description	Value
7.51	Cost of Unit of Good Output Work-in-Process (7.37 ÷ 7.44)	$/
7.52	Specific Add-On Cost per Unit of Good Output Work-in-Process (7.34 ÷ 7.44)	6.903 $/$m^2$

Process No. 3.6.04-02

Form 13-2
Page 1 of 1
Revision 1 Date 2-81

8.2 Alternate 2 (SAMICS Methodology):

8.21 Profit Computation:

0.9274* 0.049 $/ m^2 from Subtotal 4.1 = 0.045 $/ m^2

1.946* 0.022 $/ m^2 from Subtotal 4.2 = 0.044 $/ m^2

Subtotal = 0.089 $/ m^2

8.22 Costs of Amortization of the One-Time Cost:

0.192* 6.213 $/ m^2 from Subtotal 2.7 = 1.193 $/ m^2

0.192* 0.599 $/ m^2 from Subtotal 3.5 = 0.115 $/ m^2

0.2958* 0.049 $/ m^2 from Subtotal 4.1 = 0.387 $/ m^2

2.77* 0.022 $/ m^2 from Subtotal 4.2 = 0.062 $/ m^2

Subtotal = 1.757 $/ m^2

8.23 Total Net Cost of Equity (8.21 + 8.22): 1.846 $/ m^2

8.24 Profit and Amortization of Start-up Costs per Unit of Good Output Work-in-Process:
(Divide Subtotal 8.23 by 0.998 m^2 / m^2 from 7.44)

1.850 $/ m^2

8.25 Price of Process (7.52 + 8.24) 8.753 $/ m^2 or 5.84 ¢/W (peak)

8.26 Price of Work-in-Process (7.51 + 8.24) $/

Process No. 3 . 6 . 04 - 03

Form 1

University of Pennsylvania

PROCESS CHARACTERIZATION

(UPPC)

Process: Devices Fabrication

Subprocess: Contact Formation (front and rear)

Option: Sputter Deposition of Copper conductor layer (projected process)

INDEX

Form	Pages	Rev.	Date	Remarks
1		1	2-81	
2	1 to 1	1	2-81	
3	1 to 2	1	2-81	
4	1 to 1	1	2-81	
5	1 to 1	1	2-81	
6	1 to 1	1	2-81	
7	1 to 1	1	2-81	
8	1 to 1	1	2-81	
9-1	1 to -			
9-2	1 to -			
9-3	1 to -			
10	1 to -			
11	1 to -			
12	1 to 1	1	2-81	
13-1	1 to -			
13-2	1 to 1	1	2-81	
14	1 to -			
15	1 to -			
16	1 to 1		2-81	

Form 2

Revision 1 Date 2-81

Process No. 3.6.04-03

0.1 Value Added:	$/

Process Description: Copper is sputtered from target by Argon ions. Voltage between cathode and copper target is about 500 volts. Distance between target and solar cell is 5-8 cm. This is a continuous process but machine has to be shut down 1.5 hour every two shifts for replacement of copper and cleaning. The cells move past the target at a rate of 0.833 m/min. Gross output rate is 30 m^2/h. Since uptime fraction is 90%, net output rate is 27 m^2/h. The area coverage is 3.4% front, 100% rear; metal thickness is 10 μm. Deposition rate is 2-3 μm/min. Shadow mask used for pattern definition.

1. Input Specification:

Name of Item: n^+pp^+ silicon solar cells with barrier metal layer.

Dimensions: 10 cm square.

Material:

Other Specifications:

1.1 Quantity Required: / Unit Cost: $/

1.2 Input Value:	$/
1.3 Input Cost:	$/

Note to Item 1.3: Use price, if input produced in own plant.

Process No. 3 . 6 . 04 - 03

Form 3

Page 1 of 2

2.1 Direct Materials:

Revision 1 Date 2-81

2.11 Type: Copper sputter targets-electronic grade (virgin material);

Specification: Size is 90 cm x 45 x 2.5 cm (90.7 kg). Need 6 targets/machine, change every 2160 m^2 of cells, or 72 h. Efficiency of deposition on holder plus masks is 65%, mask area is 71% of holder and mask area. 75% of wall (Continued on Form 3, page 2)

Quantity Required: 188 g/ m^2; Unit Cost: 3.30 $/ kg; Cost: 0.620 $/ m^2

2.12 Type: Copper sputter targets-electronic grade (recycled material);

Specification: same as 2.11;

200 g/m^2 of wall, holder, and mask deposits recycled, $\frac{188}{3}$ g/m^2 = 63 g/m^2 of target material recycled.

Quantity Required: 263 g/ m^2; Unit Cost: 1.50 $/ kg; Cost: 0.395 $/ m^2

2.1_ Type: ;

Specification: ;

Quantity Required: /; Unit Cost: $/; Cost: $/

2.1 Subtotal Direct Materials: 1.015 $/ m^2

Process No. 3 . 6 . 0 4 - 0 3

Form 3

Revision 1 Date 2-81

2.1 Direct Materials:

2.1 1 Type: ;

Specification: and holder deposits can be recycled, 50% of deposit on mask. Only 75% of target material can be used, but remainder can be recycled.

;

Quantity Required: ___/___; Unit Cost: ___$/___; Cost: ___$/___

2.1_ Type: ;

Specification: ;

Quantity Required: ___/___; Unit Cost: ___$/___; Cost: ___$/___

2.1_ Type: ;

Specification:

;

Quantity Required: ___/___; Unit Cost: ___$/___; Cost: ___$/___

2.1 Subtotal Direct Materials: ___$/___

Process No. 3 . 6 . 04 - 03

Form 4

Revision 1 Date 2-81

2.2 Indirect Materials (incl. supplies and non-energy utilities):

2.21 Type: Argon gas;

Specification: Gas is used to maintain chamber pressure at 5 Torr for sputtering copper off the target. Flow rate is 1 ℓ/min. Cost of T-size cylinder (332 ft^3) is $100.00 (Linde, 3/79)

Quantity Required: 4.44 ℓ/m^2; Unit Cost: 0.011 $/ℓ; Cost: 0.049 $/$m^2$

2.22 Type: Pump Oil

Specification:

Quantity Required: ___/___; Unit Cost: ___$/___; Cost: 0.017 $/$m^2$

2.2_ Type:

Specification:

Quantity Required: ___/___; Unit Cost: ___$/___; Cost: ___$/___

2.2 Subtotal Indirect Materials: 0.066 $/$m^2$

Process No. 3.6.04-03

Form 5

Revision 1 Date 2-81

2.3 Expendable Tooling:

2.3_ Type: ______

______ Quantity Required: ______ ____/____: Unit Cost: ____$/____ Cost: ______$/____

2.3_ Type: ______

______ Quantity Required: ______ ____/____: Unit Cost: ____$/____ Cost: ______$/____

2.3_ Type: ______

______ Quantity Required: ______ ____/____: Unit Cost: ____$/____ Cost: ______$/____

2.3_ Type: ______

______ Quantity Required: ______ ____/____: Unit Cost: ____$/____ Cost: ______$/____

2.3 Subtotal Expendable Tooling:	______$/____

2.4 Energy

2.41 Type: Electricity, name plate rating is 20 kW for sputter units, (75% duty cycle) 45 kW for pumps (30% duty cycle)

______ Quantity Required: 1.06 kWh/m^2: Unit Cost: 0.05 $/kWh Cost: 0.053 $\$/m^2$

2.4_ Type: ______

______ Quantity Required: ______ ______: Unit Cost: ____$/____ Cost: ______ $\$/m^2$

2.4 Subtotal Energy Costs:	0.053 $\$/m^2$
2.5 Subtotal 2.1 to 2.4:	1.134 $\$/m^2$
2.6 Handling Charge: 5.26 % of item 2.5	0.060 $\$/m^2$
2.7 Subtotal Materials and Supplies: (2.5 + 2.6)	1.194 $\$/m^2$

Process No. 3.6.04-03

Form 6
Page 1 of 1
Revision 1 Date 2-81

3.1 Direct Labor:

3.11 Category: Semiconductor Assembler (SAMICS B5464D) Activity: loading, unloading, & monitoring
Amount Required: 1.0 h/ h ; Rate: $ 5.65 /h; Load 113 %;* Cost: 0.446 $/ m^2

3.12 Category: Maintenance Mechanic (SAMICS B5224D) Activity: Service and repair
Amount Required: 0.1 h/ h ; Rate: $ 7.95 /h; Load 113 %;* Cost: 0.063 $/ m^2

3.13 Category: Electronics Technician (SAMICS B5176D) Activity: Electronics repair
Amount Required: 0.1 h/ h ; Rate: $ 7.40 /h; Load 113 %;* Cost: 0.058 $/ m^2

3.1 Direct Labor Subtotal: 0.567 $/ m^2

3.2 Indirect Labor: Taken as 25% of direct

3.2_ Category: ______ Activity: ______
Amount Required: ______ h/ ______ ; Rate: $ ______ /h; Load ______ %; Cost: ______ $/ ______

3.2_ Category: ______ Activity: ______
Amount Required: ______ h/ ______ ; Rate: $ ______ /h; Load ______ %; Cost: ______ $/ ______

3.2_ Category: ______ Activity: ______
Amount Required: ______ h/ ______ ; Rate: $ ______ /h; Load ______ %; Cost: ______ $/ ______

3.2 Indirect Labor Subtotal: 0.142 $/ m^2

3.3 Subtotal 3.1 and 3.2: 0.709 $/ m^2

3.4 Overhead on Labor: 5.26 %: 0.037 $/ m^2

3.5 Subtotal Labor: 0.746 $/ m^2

*Includes benefits and replacement personnel costs.

Form 7
Page 1 of 1
Revision 1 Date 2-81

Process No. 3.6.04-03

4.1 Equipment

4.11 Type: Vacuum sputtering machine; 2 to 6 targets: 60-cm workpiece width

Cost: 2,500,000 \$; Installation Cost: 500,000 \$; Throughput: 30 m^2 /h;

Plant Oper'g Time 8280 h/y; Machine Avail'ty: 90 %; Machine Oper'g Time 7452 h/y

Servicing Costs: Labor ______ h/y at ______ \$/h; Parts or Outside Service: ______ \$/y

Useful Life: 7 y; Charge Rate: 21.35 % of Cost/y; Capital Cost: 640,500 \$/y — 2,865 \$/m^2

4.1_ Type: ______

Cost: ______ \$; Installation Cost: ______ \$; Throughput: ______ /h;

Plant Oper'g Time ______ h/y; Machine Avail'ty: ______ %; Machine Oper'g Time ______ h/y

Servicing Costs: Labor ______ h/y at ______ \$/h; Parts or Outside Service: ______ \$/y

Useful Life: ______ y; Charge Rate: ______ % of Cost/y; Capital Cost: ______ \$/y — ______ \$/______

4.1_ Type: ______

Cost: ______ \$; Installation Cost: ______ \$; Throughput: ______ /h;

Plant Oper'g Time ______ h/y; Machine Avail'ty: ______ %; Machine Oper'g Time ______ h/y

Servicing Costs: Labor ______ h/y at ______ \$/h; Parts or Outside Service: ______ \$/y

Useful Life: ______ y; Charge Rate: ______ % of Cost/y; Capital Cost: ______ \$/y — ______ \$/______

4.1 Subtotal Equipment Cost:	2,865. \$/m^2

Process No. 3 . 6 . 04 – 03

Form 8
Page 1 of 1
Revision 1 Date 2-81

4.2 Facilities:

4.2.1 Type: Equipment Area Floor Area: 60 m^2; Throughput: 223,560 m^2/y

Charge Rate: 179.13* \$/(m^2·y);

Energy Use:

Heating ______ /y at ______ \$/______

Air Cond'g ______ /y at ______ \$/______

Lighting ______ /y at ______ \$/______

Maintenance Costs:

Labor: ______ h/y at ______ \$/h

Supplies: ______ \$/y

Outside Services: ______ \$/y

Total Cost: 10,750 \$/y — 0.048 \$/m^2

4.2._ Type: ______ Floor Area: ______ m^2; Throughput: ______ /y

Charge Rate: ______ \$/(m^2·y);

Energy Use:

Heating ______ /y at ______ \$/______

Air Cond'g ______ /y at ______ \$/______

Lighting ______ /y at ______ \$/______

Maintenance Costs:

Labor: ______ h/y at ______ \$/h

Supplies: ______ \$/y

Outside Services: ______ \$/y

Total Cost: ______ \$/y — ______ \$/______

4.2._ Type: ______ Floor Area: ______ m^2; Throughput: ______ /y

Charge Rate: ______ \$/(m^2·y);

Energy Use:

Heating ______ /y at ______ \$/______

Air Cond'g ______ /y at ______ \$/______

Lighting ______ /y at ______ \$/______

Maintenance Costs:

Labor: ______ h/y at ______ \$/h

Supplies: ______ \$/y

Outside Services: ______ \$/y

Total Cost: ______ \$/y — ______ \$/______

4.2 Subtotal Facilities: 0.048 \$/m^2

4.3 Equipment and Facilities Subtotal : 2.913 \$/m^2

*Includes energy use

Form 12
Page 1 of 1

Process No. 3 . 6 . 0 4 — 0 3 Revision 1 Date 2-81

7. Process Cost Computation

Item		Value
7.11	Manufacturing Add-On Costs (sum of 2.7, 3.5, 4.3, 6.)	4.852 $/$m^2$
7.22	Other Indirect Costs: (0.059 x 4.1 + 0.108 x 4.2) % of 7.11	0.174 $/$m^2$
7.21	Total Operating Add-on Costs of Process:	5.026 $/$m^2$
7.22	G & A ____ % of 7.21	- $/
7.31	Total Gross Add-On Cost of Process	5.026 $/$m^2$
7.32	Credit for Salvaged Material (5.8)	incl'd $/
7.33	Cost of Work-in-Process Lost (5.3)	- $/
7.34	Specific Add-On Cost of Process (7.31 + 7.33)-(7.32)	5.026 $/$m^2$
7.35	Cost of Input Work-in-Process Contained in Good Output Work-in-Process (5.4)	NA $/
7.36	Loading on Item 7.35 at Rate ____ %	NA $/
7.37	Cost of Output Work-in-Process (7.34 + 7.35 + 7.36)	NA $/

Item		Value
7.41	Theoretical Yield (or Conversion Rate, if output units of work-in-process do not equal input units)	1 m^2 / m^2
7.42	Practical Yield	99 %
7.43	Effective Yield (7.41 x 7.42)	0.99 /
7.44	Number of Units of Good Output Work-in-Process per Computation Unit Used up to 7.35	0.99 m^2 / m^2

Item		Value
7.51	Cost of Unit of Good Output Work-in-Process (7.37 ÷ 7.44)	$/
7.52	Specific Add-On Cost per Unit of Good Output Work-in-Process (7.34 ÷ 7.44)	5.077 $/ m^2

ORIGINAL PAGE IS OF POOR QUALITY

Process No. 3.6.04-03

Form 13-2
Page 1 of 1

Revision 1 Date 2-81

8.2 Alternate 2 (SAMICS Methodology):

8.21 Profit Computation:

0.9274* 2.865 $/ m^2 from Subtotal 4.1 = 2.657 $/ m^2

1.946* 0.048 $/ m^2 from Subtotal 4.2 = 0.093 $/ m^2

Subtotal = 2.750 $/ m^2

8.22 Costs of Amortization of the One-Time Cost:

0.192* 1.194 $/ m^2 from Subtotal 2.7 = 0.229 $/ m^2

0.192* 0.745 $/ m^2 from Subtotal 3.5 = 0.143 $/ m^2

0.2958* 2.865 $/ m^2 from Subtotal 4.1 = 0.847 $/ m^2

2.77* 0.048 $/ m^2 from Subtotal 4.2 = 0.133 $/ m^2

Subtotal = 1.352 $/ m^2

8.23 Total Net Cost of Equity (8.21 + 8.22): 4.102 $/ m^2

8.24 Profit and Amortization of Start-up Costs per Unit of Good Output Work-in-Process:
(Divide Subtotal 8.23 by 0.99 m^2 / m^2 from 7.44)

4.144 $/ m^2

8.25 Price of Process (7.52 + 8.24) 9.221 $/ m^2

6.15 ¢/W(peak)

8.26 Price of Work-in-Process (7.51 + 8.24) $/

Process No. 3 . 6 . 0 4 - 0 3

Form 16
Page 1 of 1
Revision - Date 2-81

WORKSHEET TO ITEM ____________, FORM 3 PAGE 1

Mass evaporated from target:

$$M_{evap} = \frac{1.10^4\ cm^2/0.71}{0.65} \cdot 2\cdot 10^{-3}\cdot 8.96\ g/cm^3 = 388.3\ g/m^2$$

Mass on cell: As in 3.6-01-05: $M_{subs} = 92.6\ g/cm^3$

Net metal used:

$$M_{net} = \frac{1\cdot 10^4\ cm^2}{0.71} \cdot 8.96\ g/cm^3 \left\{\left[\frac{0.35}{0.65} \cdot 0.25 + 0.29\cdot 0.25\right] 2\cdot 10^{-3}\ cm + 0.71\ \left[0.96\cdot 1\cdot 10^{-3}\ cm\cdot 0.5\right]\right\} + 92.6\ g/cm^3;$$

$$= 188.2\ g/m^2$$

$\eta_{dep} = 0.65$; all other data as in 3.6-01-05.

Metal recycled:

$$M_{recl} = \frac{1\cdot 10^4\ cm^2}{0.71} \cdot 8.9\ g/cm^3 \left\{\left[\frac{0.35}{0.65}\ 0.75 + 0.29\cdot 0.75\right] \cdot 2\cdot 10^{-3}\ cm + 0.71\left[0.966\cdot 1\cdot 10^{-3}\ cm\cdot 0.5\right]\right\}$$

$$= 200.1\ g/m^2$$

APPENDIX II

SAMIC FORMAT A

FOR THE

SIX GENERIC METALLIZATION PROCESSES

SOLAR ARRAY MANUFACTURING INDUSTRY COSTING STANDARDS

FORMAT A

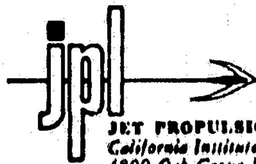

JET PROPULSION LABORATORY
California Institute of Technology
4800 Oak Grove Dr. / Pasadena, Calif. 91103

PROCESS DESCRIPTION

Note: Names given in brackets [ ] are the names of process attributes requested by the SAMICS III computer program.

A1 Process [Referent] METTFAG

A2 [Descriptive Name] Metallization, front only, by thick film screen printing of silver

PART 1 – PRODUCT DESCRIPTION

A3 [Product Referent] METCEL 3

A4 Descriptive Name [Product Name] Metallized solar cell

A5 Unit Of Measure [Product Units] 1 m^2 (100 cells)

PART 2 – PROCESS CHARACTERISTICS

A6 [Output Rate] (Not Thruput) 0.198 Units (given on line A5) Per Operating Minute

A7 Average Time at Station [Processing Time] ______ Calendar Minutes (Used only to compute in-process inventory)

A8 Machine "Up" Time Fraction [Usage Fraction] 0.95 Operating Minutes Per Minute

PART 3 – EQUIPMENT COST FACTORS [Machine Description]

A9	Component [Referent]			
A9a	Component [Descriptive Name] (Optional)	Screen printer	Ink drier	Belt Furnace
A10	Base Year For Equipment Prices [Price Year]	1979	1979	1979
A11	Purchase Price ($ Per Component) [Purchase Cost]	50,000	20,000	35,000
A12	Anticipated Useful Life (Years) [Useful Life]	7	7	7
A13	[Salvage Value] ($ Per Component)	–	–	–
A14	[Removal and Installation Cost] ($/Component)	–	–	–

Note: The SAMICS III computer program also prompts for the [payment float interval], the [inflation rate table], the [equipment tax depreciation method], and the [equipment book depreciation method]. In the LSA SAMICS context, use 0.0, (1975, 4.0), DDB, and SL.

Format A: Process Description (Continued)

A15 Process Referent (From Page 1 Line A1) METTFAG

PART 4 – DIRECT REQUIREMENTS PER MACHINE (Facilities) OR PER MACHINE PER SHIFT (Personnel)
[Facilities and Personnel Requirements]

A16 Catalog Number [Expense Item Referent]	A18 Amount Required Per Machine (Per Shift) [Amount per Machine]	A19 Units	A17 Requirement Description
A 3016D	400	sq ft	Manuf'g Space Type A
B 5464D	0.25	persons/shift	Semicond. Assembler
B 5176D	0.25	dto	Maintenance Person

PART 5 – DIRECT REQUIREMENTS PER MACHINE PER MINUTE
[Byproduct Outputs] and [Utilities and Commodities Requirements]

A20 Catalog Number [Expense Item Referent]	A22 Amount Required Per Machine Per Minute [Amount per Cycle]	A23 Units	A21 Requirement Description
E	2.4	g/min	Ag ink ($0.70/g)
E	5.2	g/min	Xylene ($0.52/lb)
E	0.0022	screens/min	print screen ($25.-/ screen)
E	0.0176	squeegees/ min	squeegee ($0.40/ squeegee)
G 1016B	0.3	kWh/min	Electricity

PART 6 – INTRA-INDUSTRY PRODUCT(S) REQUIRED [Required Products]

A24 [Product Reference]	A26 Usable Output Per Unit of Input Product	A27 Units	A25 Product Name
	0.99	m^2/m^2	Wafer with pn junction

Prepared by M. Wolf Date 3-16-81

SOLAR ARRAY MANUFACTURING INDUSTRY COSTING STANDARDS

FORMAT A

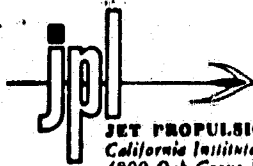

PROCESS DESCRIPTION

JET PROPULSION LABORATORY
California Institute of Technology
4800 Oak Grove Dr. / Pasadena, Calif. 91103

Note: Names given in brackets [ ] are the names of process attributes requested by the SAMICS III computer program.

A1 **Process [Referent]** METEVAP

A2 **[Descriptive Name]** Metallization front and back by Ni and 10 µm Cu by vacuum evaporation

PART 1 – PRODUCT DESCRIPTION

A3 **[Product Referent]** METCEL 1

A4 **Descriptive Name [Product Name]** Metallized solar cell

A5 **Unit Of Measure [Product Units]** 1 m^2 (= 100 cells)

PART 2 – PROCESS CHARACTERISTICS

A6 [Output Rate] (Not Thruput) 0.792 Units (given on line A5) Per Operating Minute

A7 Average Time at Station [Processing Time] 55 Calendar Minutes (Used only to compute in-process inventory)

A8 Machine "Up" Time Fraction [Usage Fraction] 0.85 Operating Minutes Per Minute

PART 3 – EQUIPMENT COST FACTORS [Machine Description]

A9	Component [Referent]			
A9a	Component [Descriptive Name] (Optional)	Automatic Vacuum System		
A10	Base Year For Equipment Prices [Price Year]	1980		
A11	Purchase Price ($ Per Component) [Purchase Cost]	2 Mill		
A12	Anticipated Useful Life (Years) [Useful Life]	7y		
A13	[Salvage Value] ($ Per Component)	0		
A14	[Removal and Installation Cost] ($/Component)	-		

Note: The SAMICS III computer program also prompts for the [payment float interval], the [inflation rate table], the [equipment tax depreciation method], and the [equipment book depreciation method]. In the LSA SAMICS context, use 0.0, (1975, 4.0), DDB, and SL.

Format A: Process Description (Continued)

A15 Process Referent (From Page 1 Line A1) METEVAP

PART 4 – DIRECT REQUIREMENTS PER MACHINE (Facilities) OR PER MACHINE PER SHIFT (Personnel)
[Facilities and Personnel Requirements]

A16 Catalog Number [Expense Item Referent]	A18 Amount Required Per Machine (Per Shift) [Amount per Machine]	A19 Units	A17 Requirement Description
A 3016D	480	sq ft	Manuf'g Space Type A
B 5464D	0.5	persons/shift	Semicond. Assembler
B 5176D	0.2	dto	Maintenance Person

PART 5 – DIRECT REQUIREMENTS PER MACHINE PER MINUTE
[Byproduct Outputs] and [Utilities and Commodities Requirements]

A20 Catalog Number [Expense Item Referent]	A22 Amount Required Per Machine Per Minute [Amount per Cycle]	A23 Units	A21 Requirement Description
E	145.2	g/min	Rod, 99.9% Cu, oxygen free, 1/8" dia. ($3/kg)
E	142.8	g/min	dto., but recycled Cu. ($1.30/kg)
E	1.44	g/min	Wire, 99.9% Ni ($11/kg)
E	$4.64\ 10^{-4}$	qt/min	Vacuum pump oil Convoil 20 ($30/qt)
E	$6.4\ 10^{-4}$	crucible/min	graphite crucible ($1000/cruc.)
C 1016B	1.92	kWh/min	electricity

PART 6 – INTRA-INDUSTRY PRODUCT(S) REQUIRED [Required Products]

A24 [Product Reference]	A26 Usable Output Per Unit of Input Product	A27 Units	A25 Product Name
	0.99	m^2 / m^2	Wafer with pn junction

Prepared by M. Wolf Date 3-16-81

SOLAR ARRAY MANUFACTURING INDUSTRY COSTING STANDARDS

FORMAT A

JET PROPULSION LABORATORY
California Institute of Technology
4800 Oak Grove Dr. / Pasadena, Calif. 91103

PROCESS DESCRIPTION

Note: Names given in brackets [ ] are the names of process attributes requested by the SAMICS III computer program.

A1 Process [Referent] METLESNI

A2 [Descriptive Name] Electroless plating of Ni strike or barrier layer

PART 1 – PRODUCT DESCRIPTION

A3 [Product Referent] METCEL 4

A4 Descriptive Name [Product Name] Cell with Ni strike layer

A5 Unit Of Measure [Product Units] m^2 (100 cells)

PART 2 – PROCESS CHARACTERISTICS

A6 [Output Rate] (Not Thruput) 0.495 Units (given on line A5) Per Operating Minute

A7 Average Time at Station [Processing Time] 20 Calendar Minutes (Used only to compute in-process inventory)

A8 Machine "Up" Time Fraction [Usage Fraction] 0.88 Operating Minutes Per Minute

PART 3 – EQUIPMENT COST FACTORS [Machine Description]

A9	Component [Referent]			
A9a	Component [Descriptive Name] (Optional)	2 Laminar Flow hoods	2 chemical recirculating systems	Drying station
A10	Base Year For Equipment Prices [Price Year]	1979	1979	1979
A11	Purchase Price ($ Per Component) [Purchase Cost]	9,000	15,000	20,000
A12	Anticipated Useful Life (Years) [Useful Life]	7	7	7
A13	[Salvage Value] ($ Per Component)	-	-	-
A14	[Removal and Installation Cost] ($/Component)	-	-	10,000

Note: The SAMICS III computer program also prompts for the [payment float interval], the [inflation rate table], the [equipment tax depreciation method], and the [equipment book depreciation method]. In the LSA SAMICS context, use 0.0, (1975, 4.0), DDB, and SL.

Format A: Process Description (Continued)

A15 Process Referent (From Page 1 Line A1) METLESNI

PART 4 – DIRECT REQUIREMENTS PER MACHINE (Facilities) OR PER MACHINE PER SHIFT (Personnel)
[Facilities and Personnel Requirements]

A16 Catalog Number [Expense Item Referent]	A18 Amount Required Per Machine (Per Shift) [Amount per Machine]	A19 Units	A17 Requirement Description
A 3016D	84	sq ft	Manuf'g Space Type A
B 5464D	1	person/shift	Semicond. Assembler

PART 5 – DIRECT REQUIREMENTS PER MACHINE PER MINUTE
[Byproduct Outputs] and [Utilities and Commodities Requirements]

A20 Catalog Number [Expense Item Referent]	A22 Amount Required Per Machine Per Minute [Amount per Cycle]	A23 Units	A21 Requirement Description
E	9	g/min	$NiCl_2 \cdot 6H_2O$, reagent gr. ($16.07/kg)
E	17.5	g/min	Ammonium chloride, reagent ($2.535/kg)
E 4416D	31	g/min	Sodium Citrate, reagent
E 4432D	3.6	g/min	Sodium Hypophosphite, reagent
E	45.	mℓ/min	Ammonium Hydroxide, reagent 58% ($0.8[illegible]/ℓ)
C 1128D	310	mℓ/min	DI Water
C 1016B	0.25	kWh/min	Electricity

PART 6 – INTRA-INDUSTRY PRODUCT(S) REQUIRED [Required Products]

A24 [Product Reference]	A26 Usable Output Per Unit of Input Product	A27 Units	A25 Product Name
	0.99	m^2 / m^2	cells with contact mask
		/	
		/	

Prepared by M. Wolf Date 3-16-81

ORIGINAL PAGE IS OF POOR QUALITY

SOLAR ARRAY MANUFACTURING INDUSTRY COSTING STANDARDS

FORMAT A

JET PROPULSION LABORATORY
California Institute of Technology
4800 Oak Grove Dr. / Pasadena, Calif. 91103

PROCESS DESCRIPTION

Note: Names given in brackets [ ] are the names of process attributes requested by the SAMICS III computer program.

A1 Process [Referent] METSOLD

A2 [Descriptive Name] Solder dipping of solar cell with plated metal

PART 1 – PRODUCT DESCRIPTION

A3 [Product Referent] METCEL 2

A4 Descriptive Name [Product Name] Solder dipped solar cell

A5 Unit Of Measure [Product Units] m^2 (100 cells)

PART 2 – PROCESS CHARACTERISTICS

A6 [Output Rate] (Not Thruput) 29.94 Units (given on line A5) Per Operating Minute

A7 Average Time at Station [Processing Time] ______ Calendar Minutes (Used only to compute in-process inventory)

A8 Machine "Up" Time Fraction [Usage Fraction] 0.88 Operating Minutes Per Minute

PART 3 – EQUIPMENT COST FACTORS [Machine Description]

A9	Component [Referent]			
A9a	Component [Descriptive Name] (Optional)	Solder Dip System		
A10	Base Year For Equipment Prices [Price Year]	1978		
A11	Purchase Price ($ Per Component) [Purchase Cost]	50,000		
A12	Anticipated Useful Life (Years) [Useful Life]	7		
A13	[Salvage Value] ($ Per Component)	-		
A14	[Removal and Installation Cost] ($/Component)	-		

Note: The SAMICS III computer program also prompts for the [payment float interval], the [inflation rate table], the [equipment tax depreciation method], and the [equipment book depreciation method]. In the LSA SAMICS context, use 0.0, (1975, 4.0), DDB, and SL.

Format A: Process Description (Continued)

A15 Process Referent (From Page 1 Line A1) METSOLD

PART 4 – DIRECT REQUIREMENTS PER MACHINE (Facilities) OR PER MACHINE PER SHIFT (Personnel)
[Facilities and Personnel Requirements]

A16 Catalog Number [Expense Item Referent]	A18 Amount Required Per Machine (Per Shift) [Amount per Machine]	A19 Units	A17 Requirement Description
A 3016D	93	sq ft.	Manuf'g Space Type A
B 5464D	1	person/shift	Semiconductor Assembler

PART 5 – DIRECT REQUIREMENTS PER MACHINE PER MINUTE
[Byproduct Outputs] and [Utilities and Commodities Requirements]

A20 Catalog Number [Expense Item Referent]	A22 Amount Required Per Machine Per Minute [Amount per Cycle]	A23 Units	A21 Requirement Description
E	113	g/min	60/40 Sn/Pb Solder
			(10.-/kg)
E	0.027	gal/min	Flux, water soluble
			(6.75/gal)
C 1128D	4	ℓ/min	DI Water
C 1016B	0.135	kWh/min	Electricity

PART 6 – INTRA-INDUSTRY PRODUCT(S) REQUIRED [Required Products]

A24 [Product Reference]	A26 Usable Output Per Unit of Input Product	A27 Units	A25 Product Name
	0.998	m^2 / m^2	metallized cell

Prepared by M. Wolf Date 3-16-81

SOLAR ARRAY MANUFACTURING INDUSTRY COSTING STANDARDS

FORMAT A

PROCESS DESCRIPTION

Note: Names given in brackets [ ] are the names of process attributes requested by the SAMICS III computer program.

A1 Process [Referent] METLYTCU

A2 [Descriptive Name] Electrolytic plating of copper over a Ni strike layer, front and rear.

PART 1 – PRODUCT DESCRIPTION

A3 [Product Referent] METCEL 1

A4 Descriptive Name [Product Name] Metallized solar cell, possibly having a contact mask attached.

A5 Unit Of Measure [Product Units] m^2 (100 cells)

PART 2 – PROCESS CHARACTERISTICS

A6 [Output Rate] (Not Thruput) 29.94 Units (given on line A5) Per Operating Minute

A7 Average Time at Station [Processing Time] 15 Calendar Minutes (Used only to compute in-process inventory)

A8 Machine "Up" Time Fraction [Usage Fraction] 0.95 Operating Minutes Per Minute

PART 3 – EQUIPMENT COST FACTORS [Machine Description]

A9	Component [Referent]			
A9a	Component [Descriptive Name] (Optional)	2 automatic plating machines		
A10	Base Year For Equipment Prices [Price Year]	1979		
A11	Purchase Price ($ Per Component) [Purchase Cost]	400,000		
A12	Anticipated Useful Life (Years) [Useful Life]	7		
A13	[Salvage Value] ($ Per Component)	-		
A14	[Removal and Installation Cost] ($/Component)	200,000		

Note: The SAMICS III computer program also prompts for the [payment float interval], the [inflation rate table], the [equipment tax depreciation method], and the [equipment book depreciation method]. In the LSA SAMICS context, use 0.0, (1975, 4.0), DDB, and SL.

Format A: Process Description (Continued)

A15 Process Referent (From Page 1 Line A1) METLYTCU

PART 4 – DIRECT REQUIREMENTS PER MACHINE (Facilities) OR PER MACHINE PER SHIFT (Personnel)
[Facilities and Personnel Requirements]

A16 Catalog Number [Expense Item Referent]	A18 Amount Required Per Machine (Per Shift) [Amount per Machine]	A19 Units	A17 Requirement Description
A 3016D	900	sq ft	Manuf'g Space Type A
B 5464D	1	person/shift	Semiconductor Assembler

PART 5 – DIRECT REQUIREMENTS PER MACHINE PER MINUTE
[Byproduct Outputs] and [Utilities and Commodities Requirements]

A20 Catalog Number [Expense Item Referent]	A22 Amount Required Per Machine Per Minute [Amount per Cycle]	A23 Units	A21 Requirement Description
E	48.37	g/min	Cu anodes ($2.00/kg)
E	41.	mℓ/min	Replenisher solut'n ($3.43/ℓ)
C 1016B	2.5	kWh/min	Electricity

PART 6 – INTRA-INDUSTRY PRODUCT(S) REQUIRED [Required Products]

A24 [Product Reference]	A26 Usable Output Per Unit of Input Product	A27 Units	A25 Product Name
	0.998	m^2 / m^2	Cell with strike metal

Prepared by M. Wolf Date 3-16-81

SOLAR ARRAY MANUFACTURING INDUSTRY COSTING STANDARDS

FORMAT A

JET PROPULSION LABORATORY
California Institute of Technology
4800 Oak Grove Dr. / Pasadena, Calif. 91103

PROCESS DESCRIPTION

Note: Names given in brackets [ ] are the names of process attributes requested by the SAMICS III computer program.

A1	Process [Referent]	METSPUT
A2	[Descriptive Name]	Sputter deposition of Cu (front and rear)

PART 1 – PRODUCT DESCRIPTION

A3	[Product Referent]	METCEL 1
A4	Descriptive Name [Product Name]	Metallized solar cell
A5	Unit Of Measure [Product Units]	m^2 (100 cells)

PART 2 – PROCESS CHARACTERISTICS

A6	[Output Rate] (Not Thruput)	0.495	Units (given on line A5) Per Operating Minute
A7	Average Time at Station [Processing Time]		Calendar Minutes (Used only to compute in-process inventory)
A8	Machine "Up" Time Fraction [Usage Fraction]	0.875	Operating Minutes Per Minute

PART 3 – EQUIPMENT COST FACTORS [Machine Description]

A9	Component [Referent]			
A9a	Component [Descriptive Name] (Optional)	Vacuum Sputtering System		
A10	Base Year For Equipment Prices [Price Year]	1979		
A11	Purchase Price ($ Per Component) [Purchase Cost]	2.5 Mill		
A12	Anticipated Useful Life (Years) [Useful Life]	7		
A13	[Salvage Value] ($ Per Component)	-		
A14	[Removal and Installation Cost] ($/Component)	0.5 Mill		

Note: The SAMICS III computer program also prompts for the [payment float interval], the [inflation rate table], the [equipment tax depreciation method], and the [equipment book depreciation method]. In the LSA SAMICS context, use 0.0, (1975, 4.0), DDB, and SL.

Format A: Process Description (Continued)

A15 Process Referent (From Page 1 Line A1) METSPUT

PART 4 – DIRECT REQUIREMENTS PER MACHINE (Facilities) OR PER MACHINE PER SHIFT (Personnel)
[Facilities and Personnel Requirements]

A16 Catalog Number [Expense Item Referent]	A18 Amount Required Per Machine (Per Shift) [Amount per Machine]	A19 Units	A17 Requirement Description
B 5464D	1	pers/stat'n	Semiconductor Assembler
B 5224D	0.1	dto	Maintenance Mechanic
B 5176D	0.1	dto	Electronics Technician
A 3016D	600	squ. ft.	Manuf'g Space Type A

PART 5 – DIRECT REQUIREMENTS PER MACHINE PER MINUTE
[Byproduct Outputs] and [Utilities and Commodities Requirements]

A20 Catalog Number [Expense Item Referent]	A22 Amount Required Per Machine Per Minute [Amount per Cycle]	A23 Units	A21 Requirement Description
E	93	g/min	Copper sputter targets

PART 6 – INTRA-INDUSTRY PRODUCT(S) REQUIRED [Required Products]

A24 [Product Reference]	A26 Usable Output Per Unit of Input Product	A27 Units	A25 Product Name
		/	Wafer with pn junction
		/	
		/	

Prepared by M. Wolf Date 3-16-81

ORIGINAL PAGE IS
OF POOR QUALITY

APPENDIX III

SAMPLE SET OF FORMS

FOR THE

UNIVERSITY OF PENNSYLVANIA PROCESS CHARACTERIZATION (UPPC)

Process No. [ ].[ ].[ ][ ]-[ ][ ]

Form 1

University of Pennsylvania

PROCESS CHARACTERIZATION

(UPPC)

Process: ______________________

Subprocess: ______________________

Option: ______________________

____

INDEX

Form	Pages	Rev.	Date	Remarks
1				
2	1 to			
3	1 to			
4	1 to			
5	1 to			
6	1 to			
7	1 to			
8	1 to			
9-1	1 to			
9-2	1 to			
9-3	1 to			
10	1 to			
11	1 to			
12	1 to			
13-1	1 to			
13-2	1 to			
14	1 to			
15	1 to			
16	1 to			

Form 2

Page ____ of ____

Revision _____ Date _______

Process No. ☐.☐.☐☐-☐☐

0.1 Value Added:	_______ $/ _____

Process Description: ______________________________

1. Input Specification:

Name of Item: ______________________________

Dimensions: ______________________________

Material: ______________________________

Other Specifications: ______________________________

______________ 1.1 Quantity Required: _____ ____ / _____ Unit Cost: _____ $/ _____

1.2 Input Value:	_______ $/ ____
1.3 Input Cost:	_______ $/ ____

Note to Item 1.3: Use price, if input produced in own plant.

Process No. ☐.☐.☐☐-☐☐

Form 3

Page __ of __

Revision ______ Date ______

2.1 Direct Materials:

2.1_ Type: ______________________________;

Specification: ______________________________

____

______________________________;

Quantity Required: ____________ ___/___; Unit Cost: ______$/______; Cost: ______$/______

2.1_ Type: ______________________________;

Specification: ______________________________;

____

____

Quantity Required: ____________ ___/___; Unit Cost: ______$/______; Cost: ______$/______

2.1_ Type: ______________________________;

Specification: ______________________________

____

______________________________;

Quantity Required: ____________ ___/___; Unit Cost: ______$/______; Cost: ______$/______

2.1 Subtotal Direct Materials: ______$/______

Process No. ☐.☐.☐☐-☐☐

Form 4

Page __ of __

Revision______ Date______

2.2 Indirect Materials (incl. supplies and non-energy utilities):

2.2_ Type:______________________________;

Specification:______________________________

____

____

Quantity Required:______________ ___/___; Unit Cost: ______$/______; Cost: ______$/____

2.2_ Type: ______________________________

Specification: ______________________________

____

____

Quantity Required: ______________ ___/___; Unit Cost: ______$/______; Cost: ______$/____

2.2_ Type: ______________________________

Specification: ______________________________

____

____

Quantity Required: ______________ ___/___; Unit Cost: ______$/______; Cost: ______$/____

2.2 Subtotal Indirect Materials: ______$/____

Process No. ☐.☐.☐☐-☐☐

Form 5

Page __ of __

Revision_____ Date______

2.3 Expendable Tooling:

2.3_ Type: ________________

________ Quantity Required: ________ ____/____: Unit Cost: _____$/____ Cost: ________$/_____

2.3_ Type: ________________

________ Quantity Required: ________ ____/____: Unit Cost: _____$/____ Cost: ________$/_____

2.3_ Type: ________________

________ Quantity Required: ________ ____/____: Unit Cost: _____$/____ Cost: ________$/_____

2.3_ Type: ________________

________ Quantity Required: ________ ____/____: Unit Cost: _____$/____ Cost: ________$/_____

2.3 Subtotal Expendable Tooling: ________$/_____

2.4 Energy

2.4_ Type: ________________

________ Quantity Required: ________ ________: Unit Cost: _____$/____ Cost: ________$/_____

2.4_ Type: ________________

________ Quantity Required: ________ ________: Unit Cost: _____$/____ Cost: ________$/_____

2.4 Subtotal Energy Costs: ________$/_____

2.5 Subtotal 2.1 to 2.4: ________$/_____

2.6 Handling Charge: _____% of item 2.5 ________$/_____

2.7 Subtotal Materials and Supplies: (2.5 + 2.6) ________$/_____

Process No. □.□.□□-□□

Form 6
Page ___ of ___

Revision ______ Date ________

3.1 Direct Labor:

3.1_ Category: ______________________ Activity: ______________________

Amount Required: ________ h/ ________ ; Rate: $ ________ /h; Load ________ %; Cost: ________ $/ ______

3.1_ Category: ______________________ Activity: ______________________

Amount Required: ________ h/ ________ ; Rate: $ ________ /h; Load ________ %; Cost: ________ $/ ______

3.1_ Category: ______________________ Activity: ______________________

Amount Required: ________ h/ ________ ; Rate: $ ________ /h; Load ________ %; Cost: ________ $/ ______

3.1 Direct Labor Subtotal: ________ $/ ______

3.2 Indirect Labor:

3.2_ Category: ______________________ Activity: ______________________

Amount Required: ________ h/ ________ ; Rate: $ ________ /h; Load ________ %; Cost: ________ $/ ______

3.2_ Category: ______________________ Activity: ______________________

Amount Required: ________ h/ ________ ; Rate: $ ________ /h; Load ________ %; Cost: ________ $/ ______

3.2_ Category: ______________________ Activity: ______________________

Amount Required: ________ h/ ________ ; Rate: $ ________ /h; Load ________ %; Cost: ________ $/ ______

3.2 Indirect Labor Subtotal: ________ $/ ______

3.3 Subtotal 3.1 and 3.2 ________ $/ ______

3.4 Overhead on Labor: ______ % ________ $/ ______

3.5 Subtotal Labor ________ $/ ______

Process No. ☐.☐.☐☐-☐☐

Form 7
Page ___ of __

Revision____ Date ______

4.1 Equipment

4.1_ Type: ______

Cost: ______ $; Installation Cost: ______ $; Throughput: ______ /h;

Plant Oper'g Time ______ h/y; Machine Avail'ty: ____ %; Machine Oper'g Time ______ h/y

Servicing Costs: Labor ______ h/y at ______ $/h;Parts or Outside Service: ______ $/y

Useful Life: ______ y; Charge Rate: ______ % of Cost/y; Capital Cost: ______ $/y ______ $/___

4.1_ Type: ______

Cost: ______ $; Installation Cost: ______ $; Throughput: ______ /h;

Plant Oper'g Time ______ h/y; Machine Avail'ty: ____ %; Machine Oper'g Time ______ h/y

Servicing Costs: Labor ______ h/y at ______ $/h;Parts or Outside Service: ______ $/y

Useful Life: ______ y; Charge Rate: ______ % of Cost/y; Capital Cost: ______ $/y ______ $/___

4.1_ Type: ______

Cost: ______ $; Installation Cost: ______ $; Throughput: ______ /h;

Plant Oper'g Time ______ h/y; Machine Avail'ty: ____ %; Machine Oper'g Time ______ h/y

Servicing Costs: Labor ______ h/y at ______ $/h;Parts or Outside Service: ______ $/y

Useful Life: ______ y; Charge Rate: ______ % of Cost/y; Capital Cost: ______ $/y ______ $/___

4.1 Subtotal Equipment Cost:	______ $/___

Process No. □.□.□□-□□

Form 8
Page ___ of ___
Revision ___ Date ___

4.2 Facilities:

4.2_ Type: ________________ Floor Area: ________ m^2; Throughput: ________ ________/y

Charge Rate: ________ $/($m^2$·y);

Energy Use:

Heating ________ ______/y at ______$/______

Air Cond'g ________ ______/y at ______$/______

Lighting ________ ______/y at ______$/______

Maintenance Costs:

Labor: ________h/y at ________$/h

Supplies: ________$/y

Outside Services: ________$/y

Total Cost: ________$/y ________$/______

4.2_ Type: ________________ Floor Area: ________ m^2; Throughput: ________ ________/y

Charge Rate: ________ $/($m^2$·y);

Energy Use:

Heating ________ ______/y at ______$/______

Air Cond'g ________ ______/y at ______$/______

Lighting ________ ______/y at ______$/______

Maintenance Costs:

Labor: ________h/y at ________$/h

Supplies: ________$/y

Outside Services: ________$/y

Total Cost: ________$/y ________$/______

4.2_ Type: ________________ Floor Area: ________ m^2; Throughput: ________ ________/y

Charge Rate: ________ $/($m^2$·y);

Energy Use:

Heating ________ ______/y at ______$/______

Air Cond'g ________ ______/y at ______$/______

Lighting ________ ______/y at ______$/______

Maintenance Costs:

Labor: ________h/y at ________$/h

Supplies: ________$/y

Outside Services: ________$/y

Total Cost: ________$/y ________$/______

4.2 Subtotal Facilities:	________$/______
4.3 Equipment and Facilities Subtotal :	________$/______

ORIGINAL PAGE IS OF POOR QUALITY

Form 9-1

Page ___ of ___

Revision _______ Date _______

Process No. ☐.☐.☐☐-☐☐

5. Salvaged Material (Work-in-process)

5.1	Quantity of Work-in-Process 1. Contained in Good Output Work-in-Process (per Computation Unit)	_____ _____/_____	
5.21	Input Work-in-process 1. Not Contained in Good Output Work-in-Process ("Amount Required" from 1.1 minus 5.1)	_____ _____/_____	
5.22	Net Amount of 5.21 which is sold for Credit As-Is or After Applying Re-Process ☐.☐.☐☐-☐☐	_____ _____/_____	
5.23	Credit for 5.22 at the Market Value of _____$/_____:	_____$/_____	
5.24	Cost of Reprocessing Material of 5.22 at the Average Reprocessing Cost of _____$/_____:	_____$/_____	
5.25	Net Credit for 5.22 (5.23 minus 5.24):		_____$/_____
5.26	Material of Type 1. Lost in Process (5.21 minus 5.22)	_____ _____/_____	
5.3	Cost of Work-in-Process Not Contained in Good Output Work-in-Process (Amount 5.21 Times Unit Cost 1.1)		_____$/_____
5.4	Cost of Work-in-Process Contained in Good Output Work-in-Process (Amount 5.1 Times Unit Cost from 1.1)		_____$/_____

Salvaged Materials Summary:

5.8	Total Net Credits for All Salvaged Materials (5.25 + 5.67 + 5.76)	_____$/_____

Process No. ☐.☐.☐☐-☐☐

5. Salvaged Material (Direct)

5.5	Quantity of Direct Material 2.1_ Contained in Good Output Work-in Process (per Computation Unit)	_____ ____/_____
5.61_	Input Material of Type 2.1_ Not Contained in Good Work-in-Process ("Amount Required" from 2.1_ minus 5.5_)	_____ ____/_____
5.62_1	Net Amount of 5.61_ which is sold for Credit As-Is or After Applying Re-Process ☐.☐.☐☐-☐☐	_____ ____/_____
5.63_1	Credit for 5.62_1 at the Market Value of ____\$/____:	________\$/_____
5.64_1	Cost of Reprocessing Material of 5.62_1 at the Average Reprocessing Cost of ____\$/____:	________\$/_____
5.65_1	Net Credit for 5.62_1 (5.63_1 minus 5.64_1):	________\$/_____
5.62_2	Net Amount of 5.61_ which is sold for Credit As-Is or After Applying Re-Process ☐.☐.☐☐-☐☐	_____ ____/_____
5.63_2	Credit for 5.62_2 at the Market Value of ____\$/____:	________\$/_____
5.64_2	Cost of Reprocessing Material of 5.62_2 at the Average Reprocessing Cost of ____\$/____:	________\$/_____
5.65_2	Net Credit for 5.62_2 (5.63_2 minus 5.64_2):	________\$/_____
5.66_	Total Net Amount of Material of Type 2.1_ Salvaged (Σ 5.62_i)	_____ ____/_____
5.67_	Total Net Credits for Salvaged Material of Type 2.1_ (Σ 5.45_i)	________\$/_____

Form 9-3

Page ___ of ___

Revision ______ Date ___________

Process No. ☐.☐.☐☐-☐☐

5. Salvaged Material (Indirect)

5.7_	Quantity of Indirect Material 2.2_ Entered into Process (per Computation Unit)	______ ______/______
5.71_1	Net Amount of 5.71_ which is sold for Credit As-Is or After Applying Re-Process ☐.☐.☐☐-☐☐	______ ______/______
5.72_1	Credit for 5.71_1 at the Market Value of ______$/______:	
5.73_1	Cost of Reprocessing Material of 5.71_1 at the Average Reprocessing Cost of ______$/______:	______$/______
5.74_1	Net Credit for 5.71_1 (5.72_1 minus 5.73_1):	______$/______
5.71_2	Net Amount of 5.71_ which is sold for Credit As-Is or After Applying Re-Process ☐.☐.☐☐-☐☐	______ ______/______
5.72_2	Credit for 5.71_2 at the Market Value of ______$/______:	______$/______
5.73_2	Cost of Reprocessing Material of 5.71_2 at the Average Reprocessing Cost of ______$/______:	______$/______
5.74_2	Net Credit for 5.71_2 (5.72_2 minus 5.73_2)"	______$/______
5.75_	Total Net Amount of Material of Type 2.2_ Salvaged (Σ 5.71_i)	______$/______

Process No. ☐.☐.☐☐-☐☐

Revision ________ Date ________

6. Byproducts and Wastes

6.1 Solid Byproducts/Wastes

6.1_ Type (Composition): ____________ Quantity Produced: ______/______

Physical Shape/Size: ____________ Energy Content: ______ kWh/______

Density: ______ g/cm^3; Water Solubility: ______ g/l at ______ ^oC; pH: ______

Toxicity: ______ Biodegradable: ______ Other Remarks: ______

____

Type of Disposal: ____

Input Material for: ____________ Cost/(Credit) ______ $/______; Cost: ______$/______

6.2 Liquid Byproducts/Wastes (inorganic):

6.2_ Type (Composition): ____________ Quantity Produced: ______/______

Density: ____ g/cm^3; Suspended Solids: ______ Amount: ______ mg/l pH: ______

Toxicity: ______ Heavy Metal Content: ____ mg/l Other Remarks: ______

____

Type of Disposal: ____

Input Material for: ____________ Cost/(Credit) ______ $/______ Cost: ______$/______

Carry: ______$/______

ORIGINAL PAGE IS
OF POOR QUALITY

Form 11
Page ___ of ___

Process No. [ ].[ ].[ ][ ]-[ ][ ]

Revision ____ Date ______

6.3 Liquid Byproducts/Wastes (organic)

Carry from Form 10	______ $/ ______

6.3_ Type (Composition): ______________________ Quantity Produced: ______ / ______

Density: ________ g/cm^3; Toxicity: __________ COD: __________ mg/l; BOD: ________ mg/l

Ignition Point: _____ °C; Explosive Mixture in Air: ___ % to ___ %; Other Remarks: ______

____

Type of Disposal: ____

Input Material for: ______________________ Cost(Credit) ____ $/ _____ ; Cost: ______ $/ ______

6.4 Fumes, Gaseous Byproducts/Wastes

6.4_ Type (Composition): ______________________ Quantity Produced: ______ / ______

Energy Content (Combustion): ______ kWh/ ______ ; Explosive Mixture in Air ___ % to ___ %.

Ignition Point: ______ °C; Aerosol [ ] Precipitates in _____ minutes pH ______

Toxicity ____________ Requires Scrubbing [ ] Type of Scrubber: ____________

(enter scrubber under 4.1, 4.2, scrubber effluent under 6.1 to 6.3)

Other remarks: ____

____

Type of Disposal: ____

Operating Costs: __________ $/ _________ ; Cost: ______ $/ ______

6. Subtotal: Byproduct/Waste Disposal Cost:	

Form 12
Page ___ of ___

Process No. ☐.☐.☐☐-☐☐ Revision ______ Date ______

7. Process Cost Computation

7.11 Manufacturing Add-On Costs (sum of 2.7, 3.5, 4.3, 6.)	______$/______
7.22 Other Indirect Costs: ______% of 7.11	______$/______
7.21 Total Operating Add-on Costs of Process:	______$/______
7.22 G & A ______% of 7.21	______$/______
7.31 Total Gross Add-On Cost of Process	______$/______
7.3[illegible] [illegible] for Salvaged Material (5.8)	______$/______
7.33 Cost of Work-in-Process Lost (5.3)	______$/______
7.34 Specific Add-On Cost of Process (7.31 + 7.33)-(7.32)	______$/______
7.35 Cost of Input Work-in-Process Contained in Good Output Work-in-Process (5.4)	______$/______
7.36 Loading on Item 7.35 at Rate ______%	______$/______
7.37 Cost of Output Work-in-Process (7.34 + 7.35 + 7.36)	______$/______

7.41 Theoretical Yield (or Conversion Rate, if output units of work-in-process do not equal input units) ______ ______/______

7.42 Practical Yield ______%

7.43 Effective Yield (7.41 x 7.42) ______/______

7.44 Number of Units of Good Output Work-in-Process per Computation Unit Used up to 7.35 ______/______

7.51 Cost [illegible] Unit of Good Output Work-in-Process (7.37 ÷ 7.44)	______$/______
7.52 Specific Add-On Cost per Unit of Good Output Work-in-Process (7.34 ÷ 7.44)	______$/______

Process No. ☐.☐.☐☐-☐☐

Form 13-1
Page ___ of ___

Revision_____ Date_____

8. Price Computation

8.1 Alternate 1

8.11 Profit at Expected Rate of _____%: _________$/_________
(Profit before income taxes; applied to 7.52)

8.12 Price of Process (7.52 + 8.11) _________$/_________

8.13 Price of Work-in-Process (7.51 + 8.11) _________$/_________

Process No. □.□.□□-□□

Form 13-2
Page ___ of ___

Revision ________ Date ____________

8.2 Alternate 2 (SAMICS Methodology):

8.21 Profit Computation:

0.9274* ________ $/ ____________ from Subtotal 4.1 = ________ $/ __________

1.946* ________ $/ ____________ from Subtotal 4.2 = ________ $/ __________

Subtotal = ________ $/ __________

8.22 Costs of Amortization of the One-Time Cost:

0.192* ________ $/ ____________ from Subtotal 2.7 = ________ $/ __________

0.192* ________ $/ ____________ from Subtotal 3.5 = ________ $/ __________

0.2958* ________ $/ ____________ from Subtotal 4.1 = ________ $/ __________

2.77* ________ $/ ____________ from Subtotal 4.2 = ________ $/ __________

Subtotal = ________ $/ __________

8.23 Total Net Cost of Equity (8.21 + 8.22): ________ $/ ________

8.24 Profit and Amortization of Start-up Costs per Unit of Good Output Work-in-Process:
(Divide Subtotal 8.23 by __________ ________ / ______ from 7.44)

________ $/ __________

8.25 Price of Process (7.52 + 8.24) ________ $/ ________

8.26 Price of Work-in-Process (7.51 + 8.24) ________ $/ ________

Process No. ☐.☐.☐☐-☐☐

Form 14
Page ___ of ___

Revision_____ Date________

9. Process Economic Evaluation:

9.1	Process Cost Balance (7.52 - 0.1)	________$/________
9.2	Relative Process Performance (9.1 ÷ 0.1)	____________
9.3	Output Cost (7.51)	________$/________
9.4	Output Value (0.2 + 0.1)	________$/________
9.5	Relative Excess Cost [(9.3 - 9.4) ÷ 9.4]	____________

ORIGINAL PAGE IS
OF POOR QUALITY

Process No. [ ].[ ].[ ][ ]-[ ][ ]

Form 15
Page ___ of ___

Revision _____ Date _________

0. Output Specification:

Name of item: ______________________________

Dimensions: ______________________________

Material: ______________________________

Other Specifications: ______________________________

Process No. ☐ . ☐ . ☐☐ - ☐☐

Form 16

Page ____ of ____

WORKSHEET TO ITEM ____________________, FORM __________ PAGE ______